ADVANCED PLANETARY PROBE

FINAL TECHNICAL REPORT

TO THE JET PROPULSION LABORATORY

VOLUME 4
APPENDIXES

TRW SYSTEMS

RJ 4/12/67

4547-6007-R0000

ADVANCED PLANETARY PROBE STUDY

FINAL TECHNICAL REPORT

27 July 1966

Prepared for the Jet Propulsion Laboratory
under Contract 951311

Volume 4

Appendixes

This work was performed for the Jet Propulsion Laboratory, California Institute of Technology, sponsored by the National Aeronautics and Space Administration under Contract NAS7-100.

TRW SYSTEMS
1 Space Park
Redondo Beach, California

CONTENTS

CONTENTS (Continued)

ILLUSTRATIONS (Continued)

ILLUSTRATIONS

APPENDIX A

MAINTENANCE OF EARTH-POINTING ATTITUDE

1. INTRODUCTION

The object of this appendix is to summarize the basic concepts of the conical scanning system proposed for the Advanced Planetary Probe and to derive some of the expressions used in Section 4.4 of Volume 2. The concept incorporates an earth-based transmitting station, which generates a constant carrier signal, and a receiver on the spacecraft, with the antenna rotating about the axis of symmetry. When the signal coming from the earth is a constant carrier, an amplitude-modulated signal results when the angle between the spin axis and the spacecraft-to-earth line is not zero.

The conical scanning system thus incorporates a paraboloidal antenna with an offset feed, a frequency conversion stage, an intermediate frequency amplifier, and a linear demodulator. A simplified block diagram of the system is given in Figure A-1. The lateral offset of the antenna feed causes a deviation of the beam center line from the symmetry axis z-z, which is the spin axis of the spacecraft. Therefore, the center line of the antenna beam pattern will carry out a conical scanning motion about the spin axis with an angular velocity equal to the spin rate ω_s. The half-angle of this cone (squint angle) is determined by the offset distance of the antenna feed.

2. RADIATION PATTERN

In the following analysis the antenna dimensions are assumed very large as compared to the wave length of the incoming signal. Thus electromagnetic wave propagation can be approximately analyzed by means of geometrical optics.

Paraboloidal reflectors with uniform illumination have the property of producing a constant phase field on a plane perpendicular to the symmetry axis containing the focal point. In Figure A-2 it is shown that, for a parabola,

$$\overline{FM} + \overline{MP} = 2f = \text{constant}$$

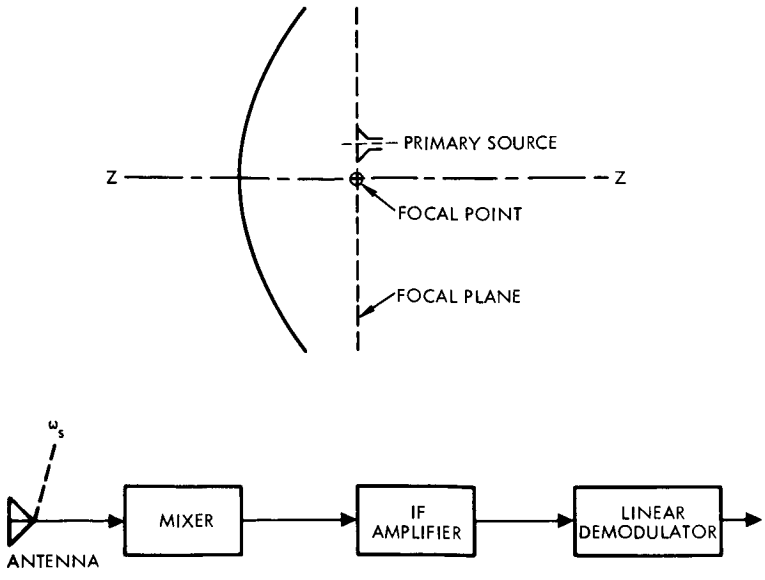

Figure A-1. Conical Scanning System

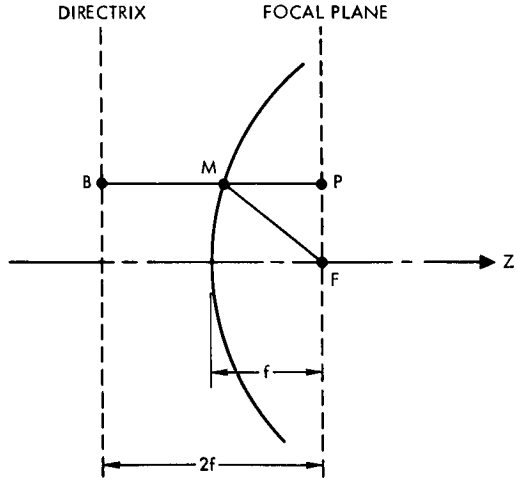

BY DEFINITION OF PARABOLA

$$\overline{FM} = \overline{BM}$$

$$\overline{BM} + \overline{MP} = 2f$$

HENCE

$$\overline{FM} + \overline{MP} = 2f$$

Figure A-2. Geometrical Relations on Parabola

Therefore a wave originating from a source placed at F will give fields at any point on the focal plane lagging the "current" in the source by

$$2f \times \frac{2\pi}{\lambda}$$

For an ideal point source, then, the amplitude and phase of the field on the focal plane are constant. Under these assumptions, the radiation pattern of an ideal paraboloidal antenna will be equal to that of a circular aperture with constant amplitude and phase. The field pattern of the circular aperture with uniform illumination is given in normalized form by*

$$R(u) = A_1(u)$$

where

$A_p(u)$ = lamda function of the p^{th} order and argument u

$u = \frac{2\pi x_o}{\lambda} \sin\theta$

θ = angle measured from the beam axis

x_o = radius of the aperture

λ = wave length

If the illumination is tapered down toward the edge of the aperture there will be a decrease in gain and in increase in beamwidth, but the amplitude of the side lobes will be reduced, which in some cases may be a desirable feature. For the particular cases in which the aperture field distribution is of the form

$$(1 - r^2)^p; \qquad p = 1, 2, \ldots$$

where

$r = \frac{\rho}{x_o}$

ρ = radius vector from the center of the aperture

*S. Silver, "Microwave Antenna Theory and Design," MIT Radiation Laboratory Series, Vol. 12, 1949, pp 192-95.

the radiation pattern is given by

$$R_p(u) = \frac{1}{p+1} A_{p+1}(u)$$

Pattern characteristics as functions of p are given in Table A-1, where the gain factor is a relative measure of antenna gain with respect to the maximum theoretical gain of a circular aperture of the same dimensions with uniform illumination. The half-power beamwidth is defined as the angle between half-power points in the antenna pattern.

Table A-1. Pattern Characteristics as a Function of p

p	Gain Factor	Half-Power Beamwidth	Position of First Zero	First Side Lobe, db below Peak Intensity
0	1.00	$1.02 \frac{\lambda}{2x_o}$	$\sin^{-1} \frac{1.22\lambda}{2x_o}$	17.6
1	0.75	$1.27 \frac{\lambda}{2x_o}$	$\sin^{-1} \frac{1.63\lambda}{2x_o}$	24.6
2	0.56	$1.47 \frac{\lambda}{2x_o}$	$\sin^{-1} \frac{2.03\lambda}{2x_o}$	30.6
3	0.44	$1.65 \frac{\lambda}{2x_o}$	$\sin^{-1} \frac{2.42\lambda}{2x_o}$	--
4	0.36	$1.81 \frac{\lambda}{2x_o}$	$\sin^{-1} \frac{2.79\lambda}{2x_o}$	--

Assuming p = 1, the radiation pattern is

$$R_1(u) = \frac{1}{2} A_2(u)$$

For small values of u, the function $A_2(u)$ can be approximated by a gaussian function of the form

$$e^{-\eta^2 u^2}$$

as shown in Figure A-3, where $\eta = 0.305$; the error is of the order of ± 2 percent in the range $0 \leq u \leq 3.75$.

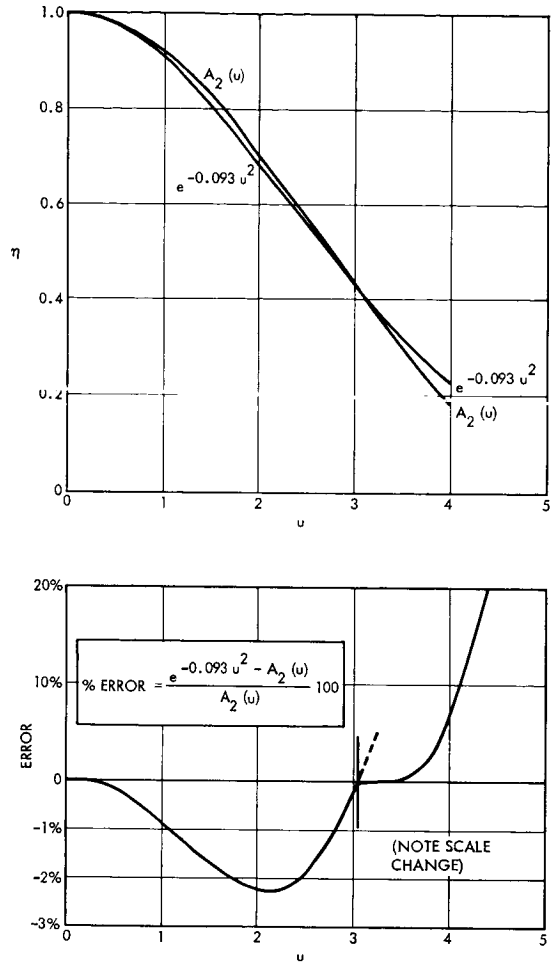

Figure A-3. Gaussian Approximation

The half-power beamwidth will be approximately

$$BW = 0.635 \frac{\lambda}{x_o} \text{ (rad)} = 36.4 \frac{\lambda}{x_o} \text{ (deg)}$$

Therefore, in the interval discussed above

$$R_1(u) \simeq \frac{1}{2} e^{-(0.305u)^2}$$

Substitution of the definition of u into this equation yields

$$R_1(\theta) \simeq \frac{1}{2} e^{\nu^2 \theta^2}$$

where

$$\nu = \frac{70}{BW\ (deg)}$$

and θ has been assumed to be small.

3. THE CONICAL SCAN PROCESS

The geometry of the conical scan process is illustrated in Figure A-4, where the z axis is assumed to coincide with the spin axis of the spacecraft. The ζ axis, or beam axis, is the symmetry axis of

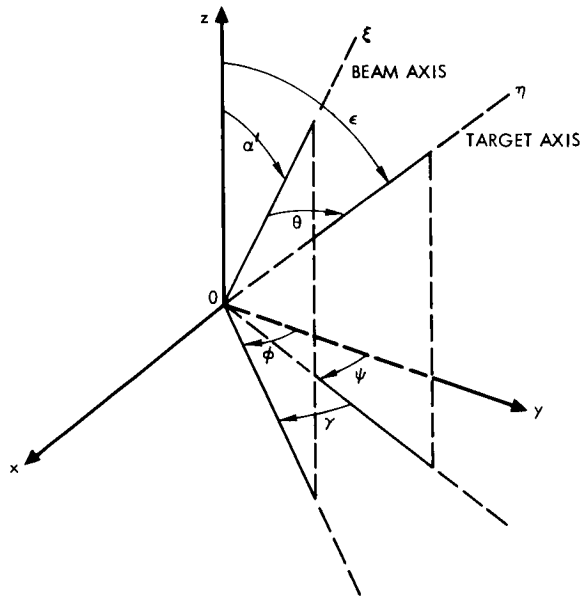

Figure A-4. Geometry of the Conical Scan Process

the antenna radiation pattern and is assumed to be at an angle α from the spin axis. The spacecraft-to-earth line η is denominated "target axis," and its angle ϵ with respect to the spin axis is the attitude error angle.

In a sphere of unity radius, the three planes determined by the z, ζ, and η axes form a spherical triangle as shown in Figure A-5. An approximate expression for θ in terms of α, β, and γ can be obtained from the cosine law

$$\cos a = \cos b \cos c + \sin b \sin c \cos \gamma$$

which, after squaring and substituting, becomes

$$\sin^2 a = \sin^2 b + \sin^2 c - \frac{1}{2} \sin 2b \sin 2c \cos \gamma$$

$$- (1 + \cos^2 \gamma) \sin^2 b \sin^2 c$$

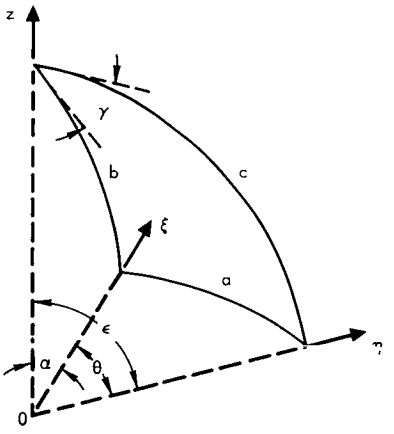

Figure A-5. Spherical Triangle

For small arcs a, b, c (or angles α, β, θ) this expression reduces to

$$\theta^2 = \alpha^2 + \beta^2 - 2 \alpha \beta \cos \gamma$$

which, when substituted into the expression for $R_1(\theta)$ yields

$$R_1(\theta) = e^{-\nu^2(a^2 + \epsilon^2)} e^{2\nu^2 a\epsilon \cos \gamma}$$

Expansion of the right-hand side into a series of modified Bessel functions gives

$$R_1(\theta) = e^{-\nu^2(a^2 + \epsilon^2)} \left[I_o(2\nu^2 a\epsilon) + 2 \sum_{n=1}^{\infty} I_n(2\nu^2 a\epsilon) \cos n \gamma \right]$$

If the following substitutions are made

$$\gamma = \phi - \psi = \omega_s t - \psi$$

where

ω_s = spin angular rate

$$\overline{R}(\epsilon) = e^{-\nu^2(a^2 + \epsilon^2)} I_o(2\nu^2 a\epsilon)$$

$$m_n(\epsilon) = 2 \frac{I_n(2\nu^2 a\epsilon)}{I_o(2\nu^2 a\epsilon)}$$

the radiation pattern function becomes

$$R(\epsilon) = \overline{R}(\epsilon) \left\{ 1 + \sum_{n=1}^{\infty} m_n(\epsilon) \cos \left[n(\omega_s t - \psi) \right] \right\}$$

The voltage at the antenna termination will be then

$$e(t) = k_1 E \, \overline{R}(\epsilon) \left\{ 1 + \sum_{n=1}^{\infty} m_n(\epsilon) \cos \left[n(\omega_s t - \psi) \right] \right\} \cos \omega_c t$$

where ω_c is the carrier angular frequency and k_1 is a proportionality constant.

This expression shows that conical scanning produces an amplitude modulation of the incoming signal which is a function of the error-angle. The carrier amplitude is $kE\,\overline{R}(\epsilon)$, and the modulation index corresponding to the n^{th} harmonic of the sign frequency is $m_n(\epsilon)$.

Values of the modulation index in terms of the parameter $2\nu^2 a\epsilon$ are plotted in Figure A-6 for n up to 6.

The AC component of the demodulator output will be given by

$$e_o(t) = k_2 E \, \overline{R}(\epsilon) \sum_{n=1}^{\infty} m_n(\epsilon) \cos \left[n(\omega_s t - \psi) \right]$$

The peak value occurs when $t = \psi/\omega_s$, which is the instant in which the spin, beam, and target axes are in the same plane and the angle between the beam and target axes is minimum. Thus, from the previous equation,

$$\hat{e}_o = e_o\left(\frac{\psi}{\omega_s}\right) = k_2 E \, \overline{R}(\epsilon) \sum_{n=1}^{\infty} m_n(\epsilon)$$

The peak negative value of $e_o(t)$ occurs when $t = \psi/(\omega_s) + \pi$, and is given by

$$\overset{v}{e}_o = e_o\left(\frac{\psi}{\omega_s} + \pi\right) = k_2 E \, \overline{R}(\epsilon) \sum_{n=1}^{\infty} (-1)^n m_n(\epsilon)$$

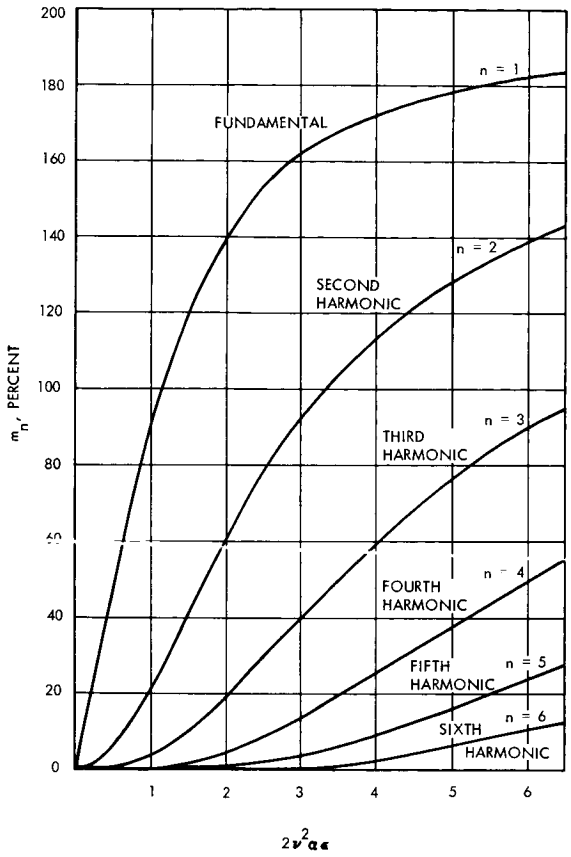

Figure A-6. Modulation Indices Versus $2\nu^2 a\epsilon$

Relative values of positive and negative peaks are plotted in Figure A-7 as functions of the parameter $2\nu^2 a\epsilon$.

For small values of the angular error ϵ, the expression for e_o can be expanded in power series about the point $\epsilon = 0$, and the following approximate expression results when high order terms are dropped:

$$\hat{e}_o(\epsilon) = 2k_2 E\, e^{-\nu^2 a^2}\, \nu^2 a\epsilon$$

which shows that, for values of ϵ in the range of interest (less than 1 degree), the angular error is approximately proportional to the peak value of the demodulator output signal.

In the conical scan system proposed for the Advanced Planetary Probe a measure of the angular error is required only to implement a dead zone. As long as the error is above a specified threshold, the only

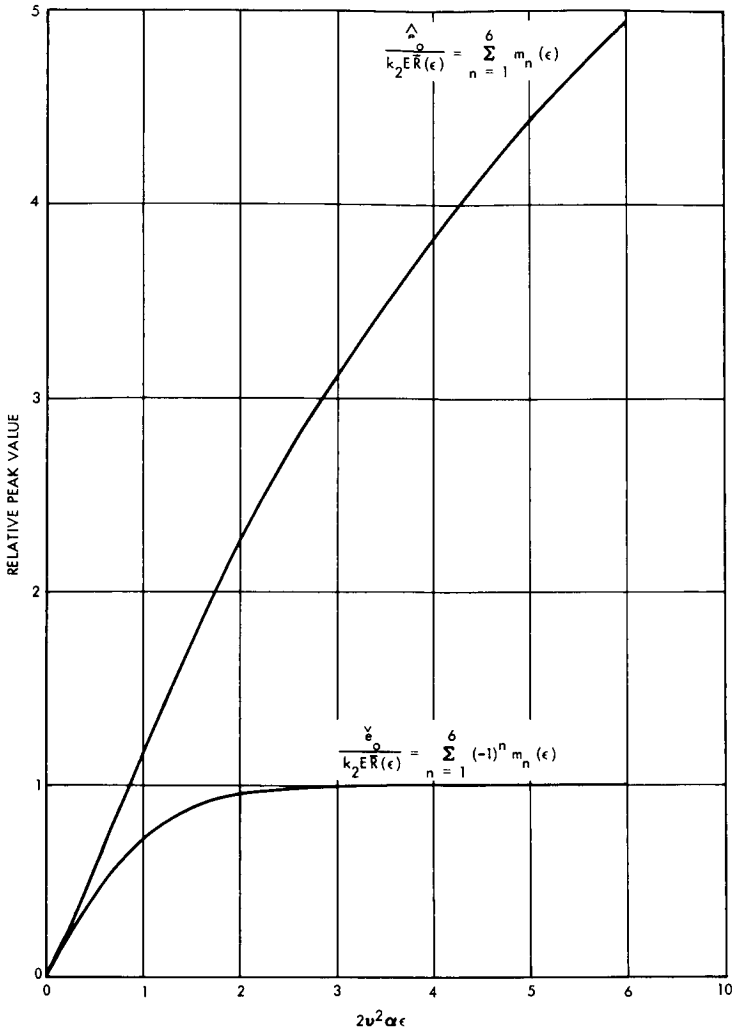

Figure A-7. Relative Value of Positive and Negative Peaks of the Demodulation Output Signal

information required by such a system is the exact time at which the beam axis is closest to the target axis or equivalently to determine the signal zero crossing. The electronic control system logic determines the time at which a rising zero crossing occurs and generates a triggering pulse with a fixed delay.

APPENDIX B

TECHNIQUES FOR CONICAL SCAN SIGNAL PROCESSING

1. INTRODUCTION

This appendix provides general background on conical scan signal processing techniques while Appendix C is a specific study of the use of the medium-gain antenna for fine pointing. This appendix addresses the problem of conical scan signal processing in the presence of significant amounts of noise. The selected solution, using an offsetable feed on the high gain antenna, avoids this problem by providing a large signal to noise margin; however, this choice is based upon sone of the factors covered in these two appendices. In particular, this appendix considers the dead zone limits to be based on noise considerations whereas in the actual implementation, dead zone limits are controlled by the minimum pulse gas jet precession step size and it is necessary that the corresponding dead zone be always larger than the dead zone determined on signal-to-noise ratio considerations. Thus the dead zone region is based upon conical scan signal amplitude independent of noise.

The coherently demodulated conical scan signal, as discussed in Section 4.4 of Volume 2, is approximately a sinusoid with the amplitude proportional to the RF pointing error. The information that has to be extracted from this wideband signal embedded in white gaussian noise is the time when the target axis is closest to the antenna beam center. This corresponds to the point where the value of the conical scan signal reaches the positive maximum and can be determined by measuring the axis crossing time or phase of the sinusoid. No matter how sophisticated a phase estimator is used, for small enough pointing errors, due to the thermal noise, the phase measurement will not be accurate and will result in gas waste. Since the phase estimation accuracy is determined by the SNR, a threshold SNR should be selected below which the attitude correction process is terminated. Of course, this threshold SNR comparator can also be used to initiate attitude correction events automatically. The comparison of RMS signal to RMS noise is preferred over the simpler signal detection scheme because the noise spectral density may not remain constant during

the mission. For instance, there will be short periods of time when the spacecraft antenna is pointed at the sun or at Jupiter, with the resulting increase in the system noise temperature. In summary, the phase of the coherently amplitude demodulated conical scan signal should be estimated and the signal compared to the noise for the purpose of establishing deadzone.

To facilitate tradeoffs involving the signal processing and antenna requirements, it is necessary to investigate several phase measurement techniques. Signal processing methods ranging from optimum maximum likelihood estimators, MLE, to simple minded zero-crossing detectors have been briefly considered. The phase-locked loops, PLL, and the digital tracking filters appeared most promising practical mechanizations and, therefore, have been investigated in more detail.

2. MAXIMUM LIKELIHOOD PHASE ESTIMATOR

One class of optimum estimation procedures (optimum in the sense that the posteriori probability density is maximized) is known as the maximum likelihood. More general techniques based on minimization of average risk (Bayes) are available. However, the MLE are preferred to Bayes systems because the former can be derived more easily and in many cases are efficient and unbiased.

The MLE for the case of a known signal is shown in Figure B-1.* In deriving this mechanization, it is assumed that the phase is fixed, or does not change significantly during time interval T. Such is the case in this application. Note that the conical scan signal frequency has to be externally supplied, presumably by a star sensor. The most serious problem with the MLE is the implementation of the inverse tangent function.

The lower bound on the estimated phase variance, mean square phase error, based on the Cramer-Rao inequality is given by**

---

*D. Slepian, "Estimation of Signal Parameters in the Presence of Noise," Trans. IRE, PGIT-3, 68 (March 1954).

**D. D. Carpenter, "The Problem of Estimating the Unknown Phase of a Sine Wave Signal in Gaussian Noise," TRW 9332.3-347, 8 February 1966.

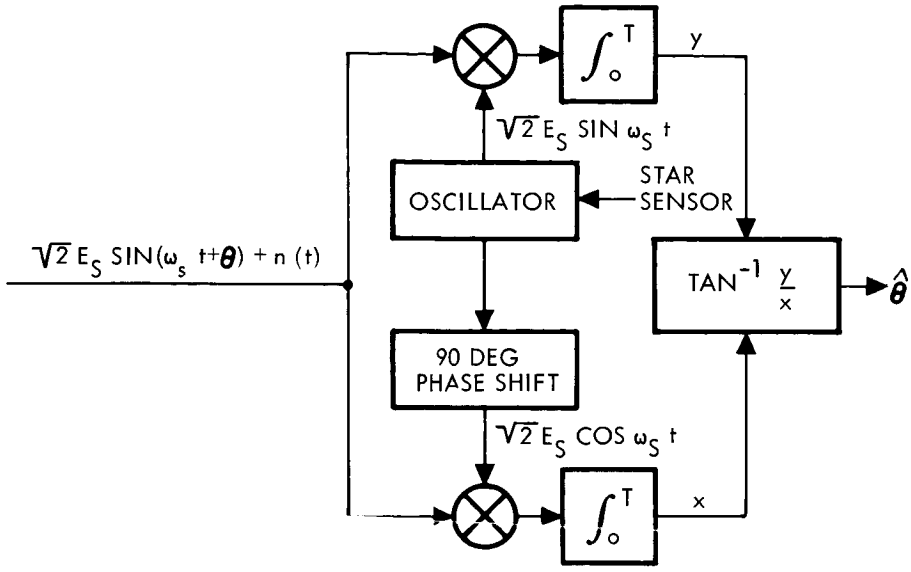

Figure B-1. Maximum Likelihood Phase Estimator

$$\overline{(\theta - \hat{\theta})^2} \geq \text{Var}(\hat{\theta}) \geq \frac{[1 + b'(\theta)]^2}{2\left(\frac{E_s^2 T}{N_o}\right)}$$

where

N_o = one-sided noise spectral density

$b'(\theta) = \frac{2b(\theta)}{2\theta}$

$b(\theta) = \bar{\hat{\theta}} - \theta$ = bias

The probability density function for $\hat{\theta}$, $p(\hat{\theta})$, has also been derived. However, $b'(\theta)$ cannot be expressed in a closed form. For high SNR it can be shown that $b(\theta)$ approaches 0, so that the lower bound further simplifies to

$$\text{Var}(\hat{\theta}) \geq \frac{1}{2\left(\frac{E_s^2 T}{N_o}\right)}.$$

The above bound, for the purpose of comparison with mean square errors derived with suboptimum measurement techniques, can be expressed in terms of power signal-to-noise ration, S/N, as

$$\text{Var}\,(\hat{\theta}) \geq \frac{1}{2\,\frac{S}{N}}$$

where the noise, N, is measured in the equivalent LPF of bandwidth 1/T Hz.

3. SUBOPTIMUM PHASE MEASUREMENT TECHNIQUES

Because of the complexity of the MLE, simpler phase measurement techniques have been investigated. It appears that for high SNR it should be possible to estimate phase accurately with a simple axis crossing detector. Thus, the phase estimation problem reduces to the filtering problem. Since the required bandpass filter bandwidths are of the order of 0.01 Hz and the spinning frequency may vary as much as 0.024 Hz ($\pm$ 20 percent from center frequency of 0.12 Hz), passive filters cannot be used. One possibility is to use a bandpass filter whose frequency is controlled by an auxiliary star sensor. Another possibility is a PLL. The PLL actually accomplishes more than just bandpass filtering.* The remaining problem is to derive mean square phase error variance for high SNR (perhaps above 10) and to compare these with the lower bound for the MLE.

For a PLL it is well known that the mean square phase error for high SNR is given by

$$\text{Var}(\hat{\theta}) = \frac{1}{2\,\frac{S}{N}}$$

where N is measured in the PLL noise bandwidth. Therefore, a PLL with the noise bandwidth of 1/T Hz performs as well as the more complex MLE.

For the digital tracking filter, the output is a sinusoidal signal in noise. In this case, the mean square noise can be computed by assuming ideal axis crossing detector. In practice, axis crossing is usually accomplished by squaring (waveform) the sinusoidal signal.

---

*T. J. Stephens, "Conical Scan RF Angle Tracking Systems," TRW 7331.5147, 22 June 1966.

Thus, it has been demonstrated that if a conical signal-to-noise power ratio of the order of 10 is available or can be achieved with a PLL or digital tracking filters, the RMS phase error for these implementations is equal to the minimum theoretical error possible with the MLE. If the SNR cannot be sufficiently improved with the PLL or digital tracking filter, in principle for individual RMS phase errors less than 90 degrees the measurement accuracy can be further improved by averaging axis crossings over many periods. Unfortunately, simple electronics to perform this averaging could not be devised. If a high-gain antenna is used for RF tracking, even at 10 AU, SNR higher than 10 in 1-Hz bandwidth will be obtained. Therefore, with a high-gain antenna no complex signal processing is required.

4. SIGNAL-TO-NOISE COMPARATORS

As discussed in Section 1, to establish deadzone in an optimum fashion, signal-to-noise powers have to be compared. In case PLL is used, coherent comparator can be mechanized as shown in Figure B-2.

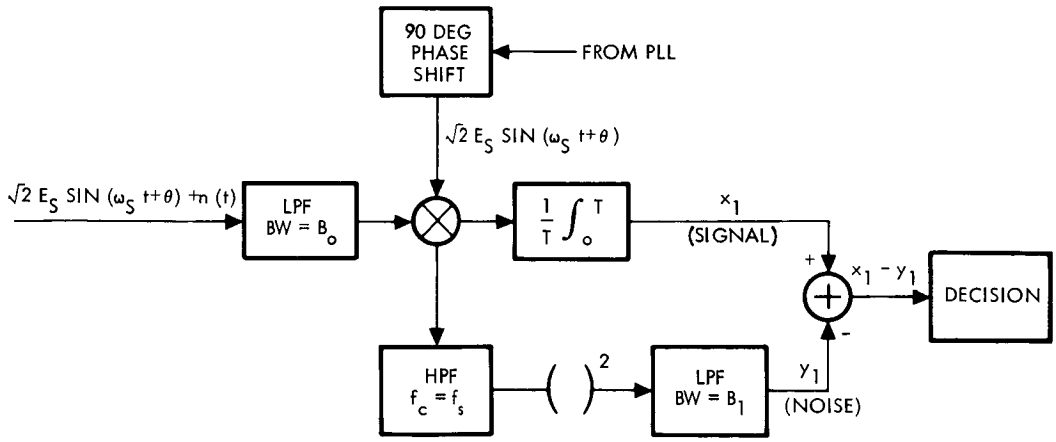

Figure B-2. Coherent Signal-to-Noise Comparator

The output from the signal channel, for sufficiently long T, is the signal power. For the noise channel, since the signal is removed by the high-pass filter, the output is approximately proportional to noise density. Thus, the circuit of Figure B-2 effectively compares signal power to noise spectral density. To show that this is indeed the case, the means and variances for the random variables x_i and y_i (defined in Figure B-2)

have been computed. These parameters, derived under numerous simplifying assumptions, are given by

$$\bar{x}_1 = E_s^2$$

$$\text{Var}\,(x_1) = \frac{N_o E_s^2}{2T}$$

$$\bar{y}_1 = N_o B_o$$

$$\text{Var}\,(y_1) = 2N_o^2 B_o B_1$$

where N_o is the input noise, n(t), density, and the other parameters are defined in Figure B-2. Therefore, for large T the noise from the upper channel is almost completely filtered out, while the lower channel output is proportional to the noise density. When PLL is not available, a noncoherent detector, as illustrated in Figure B-3, can be used. In

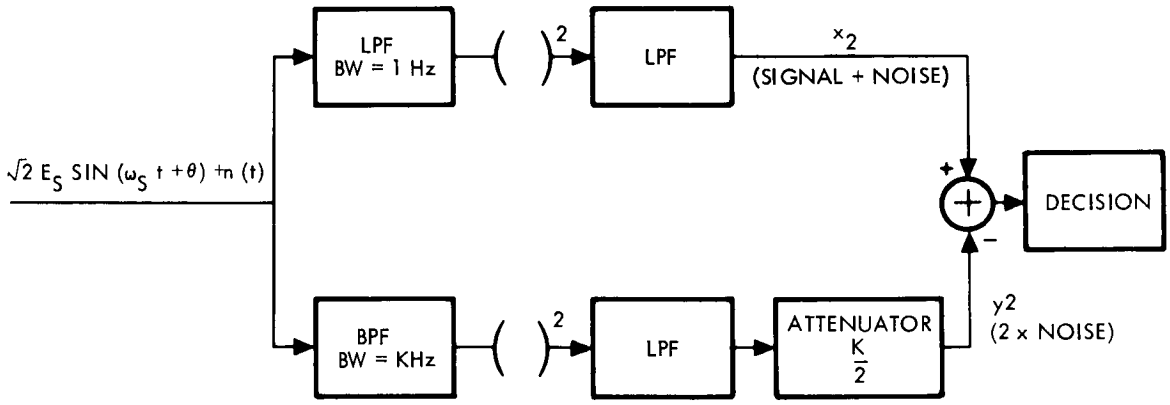

Figure B-3. Noncoherent Signal-to-Noise Comparator

Figure B-3, the upper channel output contains both signal and noise, while the lower channel contains no signal but twice as much noise as the upper channel. To simplify noncoherent comparator implementation, an integrate and dump filter in the noise channel has been replaced by a low-pass filter.

The most appropriate decision strategy, as in the case of conventional radar, is the Neyman-Pearson criterion. In this strategy the

threshold is chosen to provide selected false detection probability, i.e., probability that the SNR is below threshold although a decision is made that it is above threshold. The strategy that minimizes false rejection probability (probability that the SNR is above threshold but a decision is made that it is below threshold) is said to fulfill Neyman-Pearson criterion. The false detection error results in unnecessary use of attitude control system gas, while the false rejection error results in stopping the attitude control process before the pointing error is reduced to the specified value. It appears that the false detection probability is more expensive in this application and, therefore, should be chosen to set the threshold.

Once the false detection probability is chosen, the threshold is determined from the following

$$P_1 = \int_Z^\infty p(z_1)\, dz_1$$

where

P_1 = probability of false detection

Z_1 = threshold

$z_1 = x_1 - y_1$

$p(z_1)$ = probability density function of z

The random variables x_1 and y_1 are defined in Figure B-2. Unfortunately, the random variable y_1 after the square-law detector is not gaussianly distributed. The derivation of the probability density for y_1, therefore, is difficult and cannot be obtained in closed form. For the noncoherent detector neither x_2 nor y_2 is gaussianly distributed. Although it appears that approximate probability densities can be found for y_1, y_2, and x_2, and therefore for z_1 and z_2, the problem is outside the scope of this project.

5. SIGNAL DETECTORS

For sufficiently high input SNR at worst noise condition (at least 10), signal detectors may be sufficient. These signal detectors can be implemented by the upper channels of Figures B-2 and B-3. In the case of the coherent detector, threshold can be easily determined from

$$P_1 = \frac{1}{\sqrt{2\pi}} \int_{\frac{X-\bar{x}}{\sigma_x}}^{\infty} e^{-\frac{u^2}{2}} \, du$$

where

$$\bar{x} = E_S^2$$

$$\sigma_x = [\text{Var}(x)]^{1/2} = \left(\frac{N_o E_S^2}{2T}\right)^{1/2}$$

$$X = \text{threshold setting}$$

For example, to obtain a false detection probability of 0.997, from the error function table it is found that

$$X = E_{STH}^2 + 2.75 \left(\frac{E_{STH}^2 N_{oM}}{2T}\right)^{1/2}$$

where E_{STH} is the RMS signal at threshold and N_{oM} is maximum noise density at the detector input. For threshold SNR, $E_{STH}^2 N_{oM}/2T$, equal to 10, threshold setting reduces to

$$X = 1.87 E_{STH}^2$$

Before the signal can be detected with probability of 0.5, the RMS signal has to increase to

$$E_S = 1.37 E_{STH}$$

This points out a potential problem when the same detector is also used to automatically initiate the attitude correction process. For low false detection probability, there is a region of signal amplitudes for which the

attitude correction process will be continuously started and terminated before complete correction is achieved. One way to avoid this problem is to incorporate a second detector, with substantially higher threshold, for the purpose of initiating attitude correction. Another possibility is to utilize the receiver in-lock signal as the attitude correction event. However, since the ground-to-spacecraft link is also used for command transmission and two-way doppler tracking, this does not appear to be attractive.

Finally, if sufficiently high SNR (at least 10) can be obtained by filtering, a simple level crossing detector can be used for establishing deadzone. To obtain at threshold a detection probability of 0.997, the threshold should be set at

$$V = \sqrt{2}\, E_{STH} \left[1 + \frac{2.75}{\sqrt{2}} \left(\frac{N_{oM} B_o}{E_{STH}^2} \right)^{1/2} \right]$$

where B_o is the bandwidth of the filter preceding the level detector and N_{oM} is the maximum noise density at the filter input. For threshold SNR, $E_{STH}^2/N_{oM}B_o$, of 10, the threshold setting is given by

$$V = 2.3\, E_{STH}$$

For a detection probability of 0.5, RMS signal amplitude has to increase to

$$E_S = 1.63$$

Comparison of the signal amplitude for the level detector and the coherent RMS detector indicates that the latter is superior. The above comparison is based on the assumption that $B_o = 1/2T$. In general, for the RMS detectors since the filtering is done after detection, considerably lower effective bandwidth, $1/2T$, than B_o can be achieved.

6. SUMMARY

It has been demonstrated that a PLL can be mechanized more simply than a maximum likelihood estimator, MLE, for measurement of phase or the time when the signal reaches positive maximum. Futhermore, for the SNR above 10 in the PLL noise bandwidth of 1/T Hz, the RMS phase error with the PLL signal processing is equal to the lower bound on RMS error for the MLE. Similar results hold for the digital filter followed by a simple axis crossing detector. The digital filter, however, requires an auxiliary star sensor to provide the conical scan frequency. For the PLL, on the other hand, the maximum possible frequency deviation that can be tolerated is only about 0.0175 Hz. In addition, some attitude control system disturbance, for instance those occurring during the attitude correction process, may cause the PLL to drop lock.

In general, the MLE can be mechanized to accept considerably lower input signal-to-noise density ratios than the suboptimum phase measurement techniques. For the PLL and digital tracking filters, the filtering is of the bandpass type. For the MLE, filtering following detection is of the low-pass type and appreciably lower bandwidths can be achieved than with the bandpass filters.

For establishment of deadzone, the optimum processing involves signal-to-noise comparison. Two implementations of this comparator, one coherent when PLL is used and a second one noncoherent, have been proposed. Although mechanization of these comparators is simple, for high worst case input SNR (at least 10) they can be further simplified to RMS signal detectors. Finally, the level detectors are considered and it is demonstrated that the coherent RMS detector is superior to the level detector. Although the threshold as a function of false detection probability for the noncoherent detector was not derived, it should also be superior to level detector. For this reason it is recommended that the RMS detector be used for establishing deadzone.

The false detection probability could be related to the threshold setting only for the coherent detector and the level detector. For other cases, due to the nongaussian process, the threshold cannot be easily related to the false detection probability.

APPENDIX C

THE USE OF THE HELIX ANTENNA FOR FINE POINTING

1. INTRODUCTION

This appendix is included to indicate the problems involved in using the helix antenna for fine pointing. These problems justified switching to the offsettable feed on the high-gain antenna, providing high signal-to-noise ratio and allowing simple zero crossing detector for phase information to fire the gas jets for earth (DSIF station) tracking. This relegated the medium-gain antenna to the role of an acquisition antenna.

2. PROCESSING REQUIREMENTS

Use of the helix antenna to generate the conical scan signal results in low signal-to-noise ratios for small angular tracking errors. The signal must be processed by narrow bandpass filtering to achieve the required signal-to-noise ratio. For proper operation of the attitude control electronics, the SNR of the conical scan signal must be at least 10.54 db. The normalized noise power spectral density is

$$\phi = \frac{\frac{N}{B}}{S}$$

where

N/B = noise power spectral density in watts/Hz

S = received signal power

The SNR at the output of a bandpass filter with noise power bandwidth B_N is

$$\left(\frac{S}{N}\right)_o = \frac{1}{\phi B_N}$$

For $\phi = +10.26$ db/Hz, the required noise power bandwidth of the filter is

$$B_N = -20.0 \text{ db Hz} \quad \text{or} \quad 0.01 \text{ Hz}$$

The variation of the spacecraft spin rate is expected to be ±20 percent over the mission time. For a nominal spin rate of 5 rpm, the conical scan signal frequency will lie in the range 0.083 ±0.017 Hz. Since the bandwidth of the filter is 0.01 Hz, the center frequency must change to accommodate the variation in the spin rate.

Center frequency tracking is accomplished automatically if the filter is a phase-lock loop. For the digital filter, a clock signal at a multiple of the spin rate is provided to maintain the center frequency at the spin rate. A DC voltage level proportional to the amplitude of the conical scan signal is required as a measure of the RF angle tracking error.

Since input signal frequency can vary ±20 percent of its nominal value during the mission, the center frequency of the filter must be variable to accommodeate these input signal frequency changes. This aspect precludes the use of a fixed frequency bandpass filter. The required filter is of the frequency tracking type. Two types were studied: a phase lock loop and a digital bandpass filter with variable center frequency.

3. PHASE-LOCK LOOP

A phase-lock loop is a servomechanism type of feedback circuit in which a locally generated waveform tracks an input signal in frequency and phase. A block diagram of the conical scan signal processing system incorporating a phase lock loop is shown in Figure C-1.

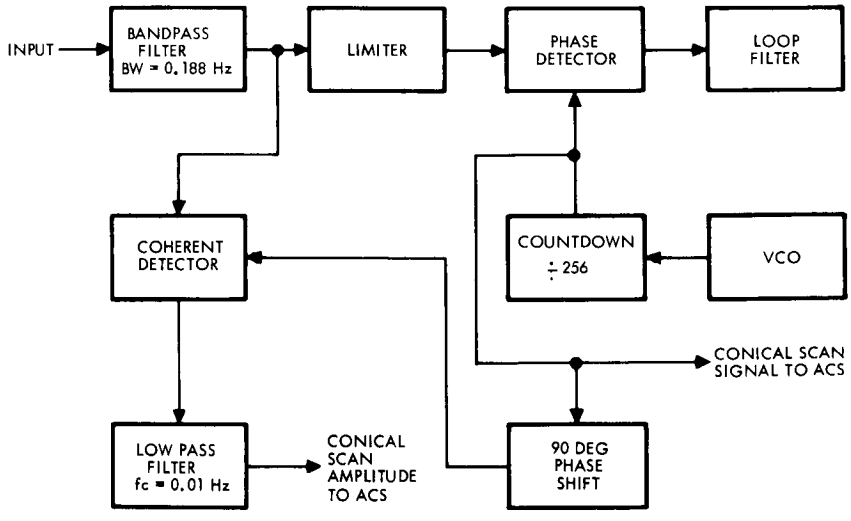

Figure C-1. Conical Scan Processor Using Phase-Lock Loop

The voltage controlled oscillator generates a signal whose frequency is a multiple of the input signal frequency. This frequency is divided by the flip-flop counter chain. The result is a signal whose frequency is near the frequency of the input signal. The phase detector compares the phase of the VCO signal with that of the input signal. An error signal is produced which is filtered by the loop filter, then used to control the frequency of the VCO. The error signal changes the VCO frequency in the direction which reduces the phase error. In the steady state, the phase error is reduced to near zero.

The bandpass filter and limiter preceding the loop fix the amplitude of the loop input signal making the loop insensitive to input signal amplitude changes. The loop output signal is phase shifted 90 degrees and used to coherently detect the conical scan signal. After low pass filtering, a voltage level representing the amplitude of the conical scan signal results at the output. This signal amplitude level and the phase-lock loop output function are used to control the attitude control system.

3.1 Loop Performance Requirement

The noise corruption of the phase-lock loop output is evidenced in the form of phase jitter. The variance of the output phase, σ_P^2, is related to the loop SNR as follows:

$$\sigma_P^2 = \frac{1}{2}\left(\frac{N}{S}\right)_{2B_L} \quad \text{for} \quad \left(\frac{N}{S}\right)_{2B_L} < 0.1$$

where $(N/S)_{2B_L}$ is the noise to signal ratio in the two-sided loop noise bandwidth, $2B_L$. Let

$$\left(\frac{N}{S}\right)_{2B_L} = -10.54 \text{ db}$$

Then $\sigma_P^2 = 0.044$. The RMS phase error is $\sigma_P = 0.21$ radian RMS or $\sigma_P = 12$ deg RMS expressed in degrees.

Thus, the required filter bandwidth, 0.01 Hz, which was determined in Section 2, will produce an output signal having phase jitter of 12 degrees RMS at the assumed input SNR. This value of phase error is sufficiently low for proper attitude control operation.

3.2 Second Order Phase-Lock Loop

The second order phase-lock loop was chosen because it exhibits minimum steady state phase error to a frequency step at the input provided that the open loop gain, G_o, is large. If a first order loop were used, large steady state phase errors would be produced as the spacecraft spin rate varied.

The desired closed loop phase transfer function for the second order loop is

$$H(s) = \frac{\theta_o(s)}{\theta_i(s)} = \frac{1 + \frac{\sqrt{2}}{B_o} S}{1 + \frac{\sqrt{2}}{B_o} S + \frac{S^2}{B_o}\,2}$$

where

$\theta_o(s)$ = phase of loop output

$\theta_i(s)$ = phase of loop input signal

B_o = loop undamped natural frequency

It is readily seen that the above equation describes a second order servomechanism with undamped natural frequency, B_o, and damping factor, $\zeta = \frac{\sqrt{2}}{2}$. The open loop transfer function is

$$H_o(s) = B_o^2 \frac{\left(1 + \frac{\sqrt{2}}{B_o} S\right)}{S^2}$$

The open loop gain, G_o, is the product of the loop component scale factors:

$G_o = 2\pi \alpha K_m K_{VCO}$ $\sec^{-1}$

α = limiter suppression factor

$K_m = K|e_S|$, loop multiplier constant, proportional to the magnitude of the loop input signal.

K_{VCO} = VCO constant, Hz per volt.

The open loop transfer function in terms of the loop components is

$$H_o(S) = G_o F(S) \frac{1}{S}$$

where F(S) is the loop filter transfer function. The 1/S factor results from the fact that the change in phase of the VCO output signal is the integral of the VCO frequency change.

The loop filter transfer function will be:

$$F(S) = \frac{1 + \tau_2 S}{\tau_1 S}$$

and

$$\tau_1 = \frac{G_o}{B_o^2}$$

$$\tau_2 = \frac{\sqrt{2}}{B_o}$$

for realization of the optimum transfer function.

The noise power bandwidth, $2B_{LO}$, of the loop is determined by the integral

$$2B_{LO} = \int_{-\infty}^{\infty} \left| \frac{\theta_o(j\omega)}{\theta_i(j\omega)} \right|^2 df$$

and for the optimum loop is

$$2B_{LO} = \frac{3B_o}{2\sqrt{2}} = 1.06\, B_o \text{ Hz}$$

Under noise conditions, the signal amplitude at the limiter output is suppressed by a factor related to the SNR at the limiter input, $(S/N)_i$. The relationship between the limiter suppression factor, α, and $(S/N)_i$ has been determined by Davenport.*

*W.B. Davenport, Jr., "Signal-to-Noise Ratios in Bandpass Limiters," J. Appl. Phys., 24 (June 1953), 720-27.

For small input signal-to-noise ratios, the relationship can be approximated as follows:

$$\alpha^2 \approx \frac{1}{1 + \frac{4}{\pi}\left(\frac{N}{S}\right)_i}$$

The loop gain, G_o, varies directly as the loop input signal amplitude. Therefore, a knowledge of α is necessary to determine the loop parameters at the design point. The design method is to determine α_o, the suppression factor at the lowest SNR at which the loop must operate. The other loop parameters are then calculated for this condition, resulting in an optimum design at the minimum SNR.

If the loop is initially out of lock, with a frequency difference existing between the VCO and the input signal, the VCO frequency will change in the direction of the input signal frequency until the frequencies are the same and phase acquisition occurs. For a loop with a perfect integrator in the loop filter, the theoretical pull in range is infinite. However, Viterbi* has shown that, for a loop with an imperfect integrator, the pull in range is limited by the time constant of the integrator. In this case, the loop filter transfer function takes the form:

$$F_2(S) = A \frac{(1 + \tau_2 S)}{(1 + \tau_3 S)}$$

where τ_3 is the limiting time constant of the integrator. For the optimum loop having this loop filter characteristic, the approximate pull in frequency range, f_p, is

$$f_p \approx \frac{B_o}{\pi} \sqrt{\frac{B_o \tau_3}{2} + 1} \text{ Hz}$$

*A.J. Viterbi, "Acquisition and Tracking Behavior of Phase-Locked Loops," Proc., Symposium on Active Networks and Feedback Systems, April 1960, Polytechnic Institute of Brooklyn.

An approximate analysis of the time required for frequency acquisition by the loop has been performed by Viterbi. For large initial frequency offset, f_o, the time required for acquisition is

$$t \approx \frac{f_o^2}{4\sqrt{2}\,\pi^2 B_o^3} \quad \text{seconds}$$

for the optimum loop.

For an initial frequency offset of 0.017 Hz, 20 percent of the nominal spin rate, the acquisition time will be on the order of 16 minutes based on the loop noise bandwidth, $2B_{LO}$, being 0.01 Hz.

3.3 Loop Parameters

The noise power bandwidth of the filter was chosen at 0.188 Hz, which provides a satisfactory SNR into the limiter, while causing little phase shift for input signal frequency variation of 20 percent. The SNR at the filter output, $(S/N)_{BW}$, is

$$\left(\frac{S}{N}\right)_{BW} = \frac{BW}{\phi} \text{ db}$$

where

BW = noise power bandwidth of filter

ϕ = normalized noise power spectral density

For BW = 0.188 Hz

$$\left(\frac{S}{N}\right)_{BW} = -3 \text{ db}$$

The limiter suppression factor is calculated at the minimum signal-to-noise ratio.

$$\alpha_o \approx \sqrt{\frac{1}{1 + \frac{4}{\pi}\left(\frac{N}{S}\right)_i}}$$

For

$$\left(\frac{S}{N}\right)_i = -3 \text{ db},$$

$$\alpha_o = 0.54$$

Open loop gain is given by

$$G_o = 2\pi \alpha_o K_m K_{VCO}$$

If the constants have the values

$$\alpha_o = 0.54$$
$$K_m = \frac{5}{\pi} \text{ volts/radian}$$
$$K_{VCO} = 0.005 \text{ Hz/volt}$$

then $G_o = 0.027$ per second.

The loop filter time constants are

$$\tau_1 = \frac{G_o}{B_o^2} = 304 \text{ sec}$$

$$\tau_2 = \frac{\sqrt{2}}{B_o} = 150 \text{ sec}$$

where

$$B_o = \frac{2B_{LO}}{1.06} = 9.43 \times 10^{-3} \text{ rad/sec}$$

The DC gain of the loop filter determines the range of frequencies over which the loop will acquire. As the DC gain is made large the theoretical acquisition range is increased. However, at the same time the initial frequency offset due to errors in the loop circuitry also increases. A maximum value can be found which produces the largest acquisition range:

$$A_{DC_{MAX}} = \frac{\tau_2}{\tau_1}\left[\frac{1}{2\left[\phi_{OFF} + \frac{V_{OFF}}{\alpha K_m}\right]^2} - 1\right]$$

where ϕ_{OFF} and V_{OFF} are the offsets of the loop multiplier and loop filter amplifier. For typically encountered offsets, $A_{DC_{MAX}}$ is on the order of 150. For a normal phase-lock loop this value is easily realizable. However, for the present case, where the bandwidth is very small, the required resistor value would be in the hundreds of megohms. It is felt that the maximum value which could be used successfully, assuming strict humidity control and electrostatic shielding, is on the order of 30 megohms. For this value, $\tau_3 = 4500$ sec, and the pull-in range:

$$f_p \approx \frac{B_o}{\pi}\sqrt{\frac{B_o\tau_3}{\sqrt{2}} + 1} = 0.0175 \text{ Hz}$$

The exact value of τ_3 is not critical. Twenty percent variation in its value would not produce an intolerable effect.

3.4 Phase-Lock Loop Circuitry

The recommended voltage controlled oscillator is an astable multivibrator with a control voltage input. The center frequency is 21.3 Hz. Center frequency stability of 0.5 percent can be realized.

The recommended phase detector is of the switching variety, i.e., it accepts a linear signal at one input and multiplies it by ±1 depending upon the state of a digital signal at the other input.

The loop filter amplifier is a high input impedance operational amplifier. Presently available units can be obtained having:

$$Z \text{ in} > 10^{10} \text{ ohms}$$

$$V_{OFF} < 3 \text{ millivolts}$$

$$I_{OFF} < 1 \text{ nanoamps}$$

These limits are adequate for proper circuit performance.

A circuit diagram of the loop filter is shown in Figure C-2. Because of the high impedances encountered in the implementation, special consideration must be given the choice of capacitors to be used. The DC

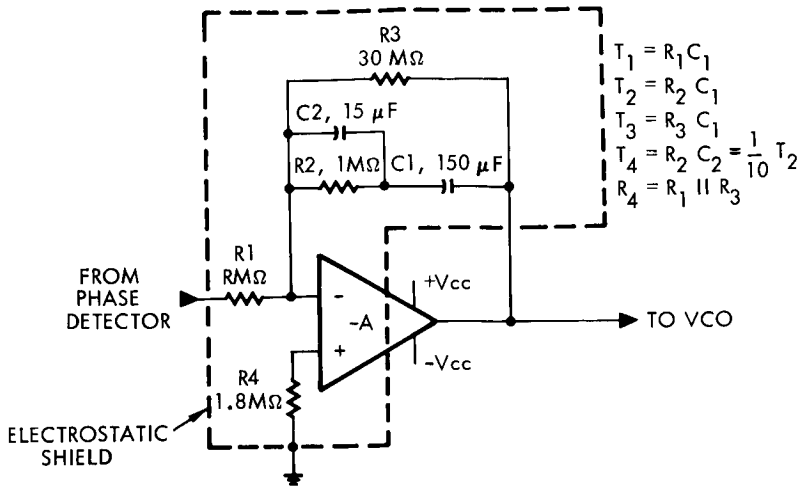

Figure C-2. Loop Filter

resistance of the capacitors must be high compared to the 30 megohms resistor in feedback path. This requirement and size and weight considerations suggests the use of polycarbonate film capacitors. Using polycarbonate capacitors the 150 μf capacitor will have a DC resistance equal to 100 megohms or greater.

Due to the very high impedances involved in the loop filter, special shielding and humidity control must be incorporated into the design. The operational ampoifier summing point must be shielded from external voltages. Power supply voltages, coupled through hundreds of megohms to the summing point, could cause intolerable leakage currents. Using an electrostatic shield connected to ground, this effect can be minimized. The loop filter components should also be enclosed in a hermetically sealed package to prevent surface conduction by moisture.

3.5 Amplitude Detector Circuitry

The coherent detector is a switching type phase detector similar to the circuit used in the phase-lock loop. The low pass filter is a single pole RC filter with cutoff frequency 0.01 Hz.

4. DIGITAL BAND PASS FILTER

A circuit diagram of the system incorporating the digital filter is shown in Figure C-3. The switches in the digital filter section sequentially connect one end of each capacitor to ground. As each capacitor,

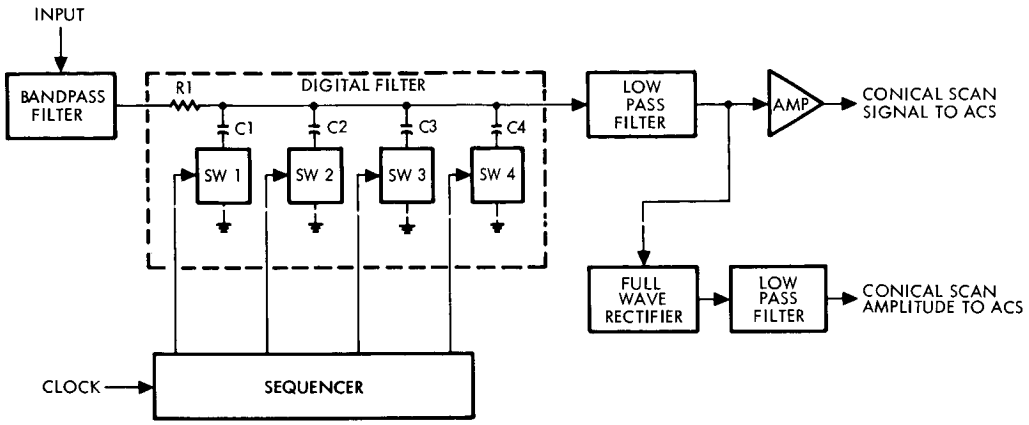

Figure C-3. Conical Scan Processor Using Digital Filter

in turn, is grounded, the input signal is sampled and held as a voltage on the capacitor. Changes in the charge on each capacitor from sample to sample are limited by the cutoff frequency of the RC combination of the input resistor, R, and the sampling capacitor.

Any substantial change in phase of the input signal from sample to sample, that is, a significant frequency difference from the sampling rate, will not be tracked by the RC low pass section. In this manner input voltages whose frequenceis are different from the sampling rate are attenuated, thereby providing a bandpass filter characteristic.*

The sampling filter has the property of providing bandpass filtering in the neighborhood of the sampling rate, but also has responses at frequencies which are multiples of the sampling rate. Because of this factor, a wide bandpass filter must be used preceding the digital filter to

*L. E. Franks and B. I. W. Sandberg, "An Alternate Approach to the Realization of Network Transfer Functions: The N-Path Filter," Bell Sys. Tech. J., Sept. 1960, pp 1321-50; J. Thompson, "RC Digital Filters for Microcircuit Bandpass Amplifiers," Circuit Design Engineering, March 1964, pp 45-49.

suppress input signals at multiples of the desired filter center frequency. Low pass filtering is also required at the output of the digital filter, to remove higher frequency components caused by the discontinuities between sampling intervals. The digital filter waveforms are illustrated in Figure C-4.

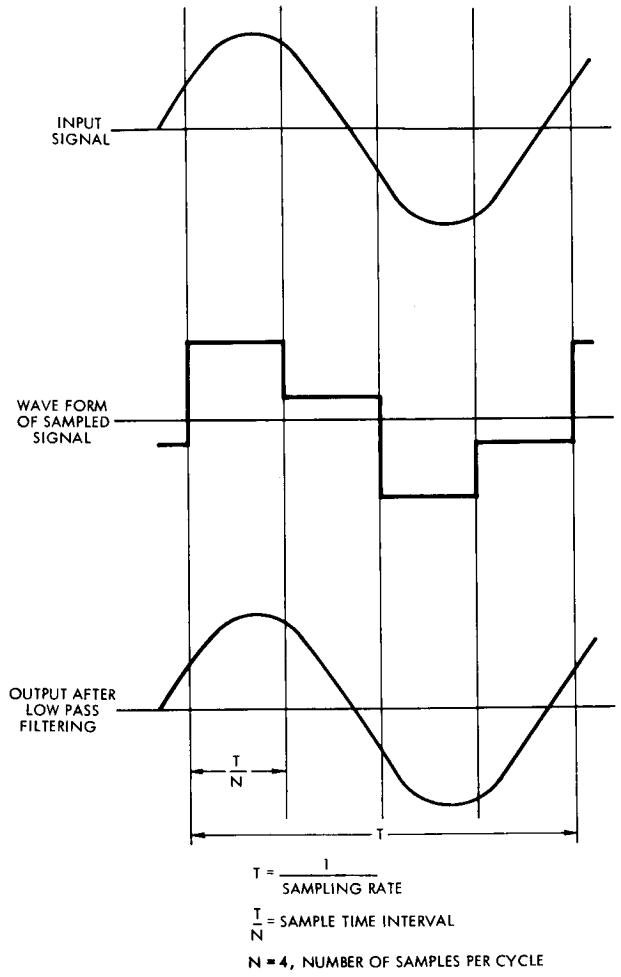

Figure C-4. Digital Filter Wave Forms

4.1 Digital Filter Relationships

Having made the preceding restrictions on the input and output spectra, the transfer function of the digital filter from Viterbi, op. cit. is

$$\frac{E_2(S)}{E_1(S)} = \left(\frac{\sin\frac{\pi}{N}}{\frac{\pi}{N}}\right)^2 \left[\frac{1}{NRC\left(S-j\frac{2\pi}{T}\right)+1} + \frac{1}{NRC\left(S+j\frac{2\pi}{T}\right)+1}\right]$$

where

T = period of the sample sequence

N = number of samples per sampling period

RC = time constant formed by the input resistor and each sampling capacitor

This equation is that of a low pass filter which has been translated in frequency by an amount equal to 1/T, the effective sampling rate. Thus the bandpass characteristic is realized.

The sampling sequence is a commutation process whereby the capacitors sample the input signal in rotation. The effective sampling rate, and thereby the center frequency of the filter, is the rate at which the sequencer rotates, each capacitor providing one sample per cycle. The center frequency is 1/T, the rotation rate of the sequencer. For N sample sections (N sampling capacitors), the stepping rate of the sequencer is N/T. The clock rate of the sequencer is then N times the desired center frequency.

Each capacitor is active during 1/N of each commutator cycle. The effective time constant is, then, NRC. The bandwidth of the digital filter is the two-sided bandwidth of the effective low pass filter section:

$$B_D = \frac{1}{\pi NRC} \text{ Hz}$$

The center frequency, f_c, in terms of the clock rate, C, pulses per second, is:

$$f_c = \frac{C}{N} \text{ Hz}$$

The center frequency of the filter, depending only on the clock rate, will not be affected by variations in the circuit components. It can be changed at will, however, by varying the clock rate.

The bandwidth of the filter is determined by the number of sampling sections and the input RC time constant. It remains constant for shifts in the center frequency.

The application of the digital filter to the conical scan tracking system is as follows: A sun sensor clock, at a multiple of the spin rate is provided aboard the spacecraft. This clock, which is also a multiple of the conical scan signal frequency, can be used as the digital filter clock. The center frequency of the filter would then change automatically as the spin rate varies. The conical scan signal would always be at the center of the filter bandpass.

4.2 Performance Requirement of the Digital Filter

In order to provide an output SNR of +10.74 db, the noise power bandwidth, B_N, of the digital filter is 0.01 Hz. Since the filter is a single pole pair function, the corresponding 3 db bandwidth is:

$$B_f = \frac{2}{\pi} B_N = 0.00636$$

4.3 Circuit Mechanization

The switches used to connect each capacitor to ground are easily implemented as transistors. It is not required that the transistors be choppers, since low offset voltage is not required in this capacitor-coupled circuitry. Switching should be fast, however. Proper measures must be taken to insure that the operating transistor turns off before the next one turns on to prevent charge leakage between capacitors. This phenomenon has the effect of widening the bandwidth of the filter.

The number of switches, N, was chosen as four. The distortion introduced by the sampling process will appear at multiples of twice the center frequency. These components will be removed by the output low pass filter.

For N = 4, the bandwidth is

$$B_f = \frac{1}{4\pi RC} \text{ Hz}$$

For B_f = 0.00636 Hz, RC = 12.5 sec. This time constant can be realized using a 1.25 megohm resistor and a 10 μf polycarbonate capacitor. For N = 4, four capacitors are required.

The input filter is a wide bandpass filter composed of RC elements. The bandwidth is 0.166 Hz or twice the center frequency. There will, then, be little phase shift for variations in the conical scan signal frequency.

The filter at the digital filter output is a low pass filter with a zero at twice the digital filter center frequency. It is required to attenuate the distortion introduced by sampling.

A clock function, a multiple of the spin rate, is to be provided by the attitude control system. This clock, having an accuracy of 0.1 percent is used to drive the digital filter sampling sequencer.

The amplitude of the conical scan signal is detected by a full wave rectifier and filtered by an RC low pass filter.

5. CHOICE OF CAPACITORS

A major difficulty in the implementation of both the phase-lock loop and the digital filter lies in the practical realization of the very long time constants required for filtering at the low frequencies involved. Tantalum capacitors are ruled out because of their high leakage and temperature variation characteristics. Tantalum capacitors, selected on a unit basis and operated at low DC bias voltage, could be used at a reduction in performance. This approach is considered inadequate for proper performance of the system.

For improved leakage characteristics and stable performance over the temperature range, polycarbonate film capacitors are the recommended choice. Presently available units exhibit less than 1 percent change in capacitance with temperature and insulation resistance in excess of 100 megohms for the highest capacitance value required. Although polycarbonate capacitors are considerably larger than tantalum capacitors, the improved performance justifies their choice.

6. COMPARISON OF THE TWO METHODS

Approximately half the weight and volume of each scheme consists of that contributed by the capacitors. Since less capacitance is required in the mechanization of the digital filter, reduced weight and volume result. Also, since the circuitry associated with the digital filter is less complex than that of the phase-lock loop, the digital filter mechanization requires less power. The hardware requirements for the two schemes are summarized in Table C-1.

Table C-1. Hardware Requirements

	Phase Lock Loop	Digital Filter
Weight, lb	1.8	0.9
Volume, in^3	50	25
Power, watts	0.3	0.1
Parts count	140	70

While the phase-lock loop filter performs its function autonomously, the digital filter requires an external clock at a multiple of the spin rate. This is to be provided by the attitude control electronics which uses a sun sensor to detect the spin rate. Under conditions of unfavorable spacecraft orientation, the sun sensor output may be lost, resulting in the disabling of the digital filter.

For a step signal input, the activation time of the digital filter is the filter risetime. The output will attain 85 percent of its final value in approximately one minute, if the noise power bandwidth is 0.01 Hz.

The phase-lock loop, on the other hand, must execute an acquisition procedure. If the conical scan signal frequency differs by 20 percent from the VCO center frequency, the acquisition time will be approximately 16 minutes.

If the spacecraft spin rate is known, it is feasible, by means of an auxiliary VCO input, to maintain the VCO center frequency in the proximity of the spacecraft spin rate. In this case, the phase-lock loop would acquire immediately, without slipping cycles. The transient time during phase acquisition would then be less than one minute.

APPENDIX D

CONICAL SCAN ANGLE TRACKER

1. INTRODUCTION

The receiver block diagram for the spin-stabilized spacecraft using a conical scan angle tracking technique is given in Figure D-1. This is a standard double-conversion superheterodyne receiver employing phase-lock loop (PLL), and conceptually is equivalent to the Mariner IV receiver.

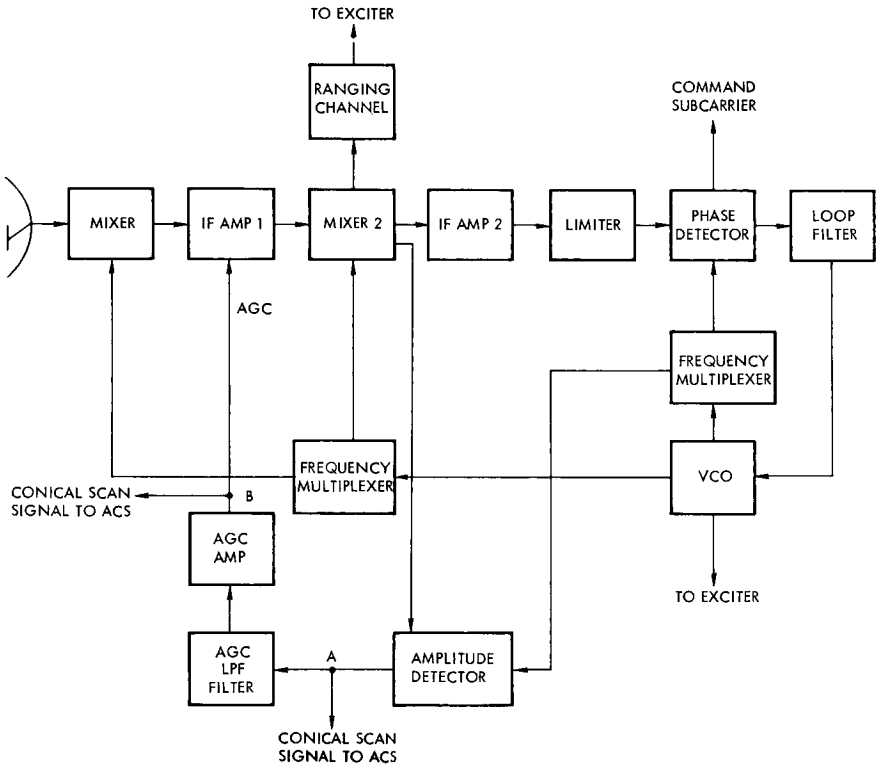

Figure D-1. Receiver Block Diagram for Spin-Stabilized Advanced Planetary Probe

In the case of conventional spacecraft receivers requiring wide dynamic range, the automatic gain control (AGC) is included to maintain signal level at the receiver output constant over the wide communication distances. The AGC loop transfer function minimizing transient and noise errors, when conical scan signal is absent, has been determined.* In our case

*W.K. Victor and M.H. Brockman, "The Application of Linear Servo Theory to the Design of AGC Loops," Proc. IRE, February 1960.

AGC will also be used to derive antenna pointing error signals. These two considerations, which may be in conflict, will determine AGC mechanization.

Depending on the bandwidth of the AGC loop, two types of AGC mechanizations are possible. If the AGC loop passes frequencies only below conical scan frequency f_2, it will be referred to as slow AGC. In this case the amplitude modulation produced by the conical scanning appears at the input to the limiter. It is believed that this amplitude modulation will not affect command or ranging performance. For slow AGC the conical scan signal obtained at the output of amplitude detector, at point A, Figure D-1. Since the conical scan frequency will be of the order of 1/12 Hz, the AGC loop noise bandwidth would have to be much narrower than this. In order to obtain such a low loop bandwidth, the AGC filter may require large size capacitors. The second type of AGC loop has bandwidth much higher than conical scan frequency and sometimes is referred to as fast AGC. The amplitude modulation in this case is almost completely suppressed at the output of the IF amplifier. The error signal can be obtained at the output of the AGC amplifier, at point B in Figure D-1.

2. ANALYSIS

In this section the conical scan SNR at the input to ACS under numerous simplifying assumptions for slow AGC is derived. When fast AGC is used, the analysis is involved and will not be attempted at this time. The open loop SNR is required to determine the closed loop antenna pointing error or accuracy of the altitude control system due to receiver (thermal) noise. It is not implied here that the pointing accuracy will be limited by the receiver noise; it may be that the so-called servo noise or other error sources will dominate.

To simplify analysis, a one-way voltage antenna pattern will be approximated by the gaussian function.*

$$G(\theta) = G_o \exp(-a^2\theta^2)$$

*M.I. Skolnik, Introduction to Radar Systems, Chapter 5, N.Y. McGraw-Hill, 1962.

where θ is defined in Figure D-2(A) and

$$G_o = G(\theta = 0) = \text{on axis antenna gain}$$

$$a^2 = \frac{1.388}{\theta_b^2}$$

θ_b = 3 db antenna beamwidth

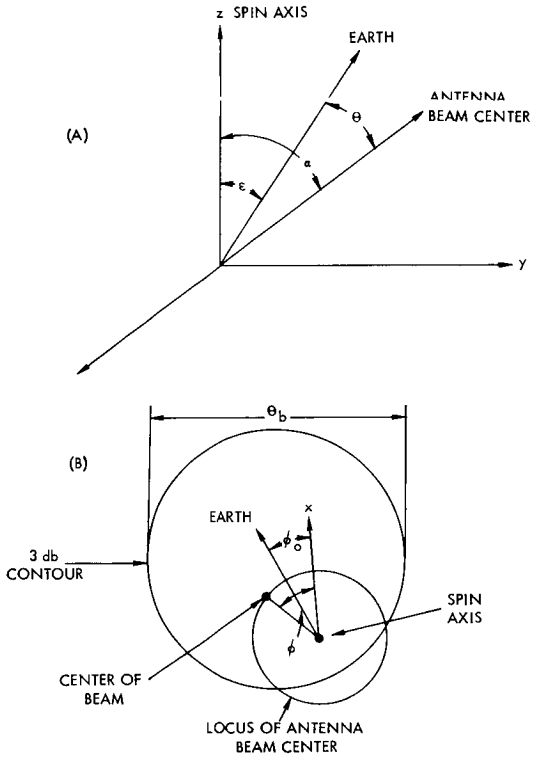

Figure D-2. Geometry of Antenna Beam

Under the assumption that angles θ, α, and ϵ are small, the signal into the receiver can be expressed as

$$x(t) = \sqrt{2}\, A_c\, C \left[1 + \sum_{n=1}^{\infty} K_n \cos\left(n\omega_2 t - n\phi_o\right)\right] \sin \omega_1 t$$

where ϕ_o is defined in Figure D-2(B) and

$G_o = 1$

A_c = received carrier amplitude

$$C = \left\{ \exp\left[-a^2(\alpha^2 + \epsilon^2) \right] \right\} I_o(2a^2 \alpha \epsilon)$$

$$K_n = \frac{2I_n(2a^2 \alpha \epsilon)}{I_o(2a^2 \alpha \epsilon)}$$

ω_1 = carrier frequency

$\omega_2 = \frac{\phi}{t}$ = angular conical scan frequency

For coherent AGC, the receiver can be simplified to the one shown in Figure D-3. Assuming that the amplitude of the AGC amplifier is maintained at constant level L, the receiver gain is L/A_c. The amplitude detector output is given by

$$y(t) = x(t) \cdot \sqrt{2} \sin \omega_1 t$$

$$= L \cdot C \left[1 + \sum_{n=1}^{\infty} K_n \cos (n\omega_s t - n\phi_o) \right]$$

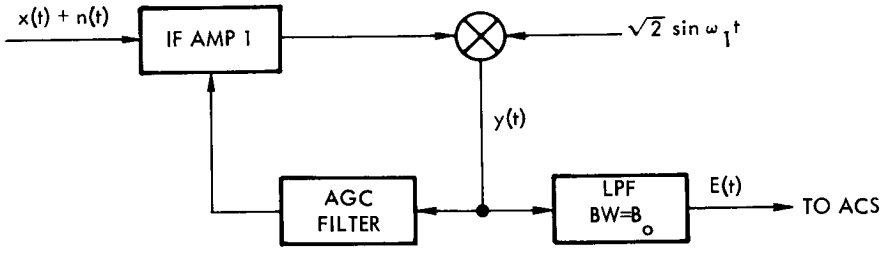

Figure D-3. Equivalent Receiver Block Diagram for Spin-Stabilized Advanced Planetary Probe

If the bandwidth of the LPF, B_o, is chosen to pass only the fundamental of the scan frequency, this equation reduces to

$$2(t) \simeq 2L \exp\left[-a^2(a^2 + \epsilon^2) \right] I_1(2a^2 a \epsilon) \cos(\omega_2 t - \phi_o)$$

Note that the constant DC term is of no interest and has been omitted. For $2a^2 \alpha \epsilon << 1$, the above equation can be approximated by

$$E(t) \simeq C_1 \epsilon \cos(\omega_2 t - \phi_o)$$

where

$$C_1 = 2La^2\alpha \exp(-a^2 \alpha^2)$$

Thus, the amplitude of E(t) is proportional to the error angle and can be used by ACS to point the spacecraft at the earth.

The output noise spectral density, assuming that the input noise is white gaussian with one-sided spectral density N_o, will be $N_o(L/A_c)^2$. The filters were assumed ideal, i.e., they pass all frequencies within the passbands and attenuate completely all other frequencies. The signal power-to-noise ratio at the output of the LP filter will be

$$\frac{S}{N} = \frac{2(A_c a^2 \alpha \epsilon)^2 \exp(-2a^2 \alpha^2)}{N_o B_o} .$$

APPENDIX E

POWER AMPLIFIER SURVEY

1. INTRODUCTION

In this appendix the results of a brief S-band power amplifier survey are presented. In this survey, devices with power outputs from 1 to 100 watts were considered for possible spacecraft launched between 1970 and 1980. As expected, the more distant future cannot be predicted with any confidence so that the emphasis was placed on the 1972 launch date. The following devices are considered: tunnel diodes, transit time devices, transistors, diode multipliers, up-converters, vacuum tube triodes, klystrons, amplitrons, and traveling wave tubes (TWT).

2. TUNNEL AND TRANSIT-TIME DEVICES

Tunnel diode circuits for RF power sources are limited to the low milliwatt range, and it is not foreseeable that much higher levels are possible. Also likely to remain at low power levels are transit time devices (Gunn, Read, and similar diode types) involving avalanche or domain transit phenomena. These are sometimes characterized by high spectral purity, but at powers below 0.1 watt. Therefore, these various devices are ruled out for near-term transmitter applications.

3. TRANSISTORS

For generation of power up to 2 Gc, transistor technology is such that 1 to 2 watts are now or will soon be achievable. Simplicity, high efficiency, and high reliability are all to be expected from direct generation in transistor output stages. In addition there is a gain in weight, efficiency, and reliability associated with the power supply needed because the DC-DC converter can usually be omitted. Extrapolation of failure rate data to low or zero dissipation levels indicates that up to an order-of-magnitude failure rate reduction may be expected during power-off periods, although both cycling and switching reduce the actually attainable improvements.

Above the 2 Gc limit, available output power drops radically, due to device geometry and fabrication problems. Significant improvement is not expected for several years.

4. DIODE MULTIPLIERS AND UP-CONVERTERS

Multiplier circuits utilizing the voltage-variable ("varacter") diode are expected to remain the only significant solid-state RF sources for the near future. Use is made of high powers generated by transistor stages (at present, 50 watts of power at 100 MHz is considered feasible; this should increase to 100 watts in 1 to 2 years). By means of cascades of low loss silicon diode frequency multipliers significant power at 2 Gc is obtained. At present, this is limited to about 4 watts; short-term technology advances are expected to push this to 10 watts. Should gallium-arsenide diode performance attain theoretical limits more closely, it is conceivable that 100 watts at 2 Gc may be available after several years of development effort.

Efficiency and reliability are steadily improved as a result of higher power generated by transistor drivers, thus requiring fewer stages of low order multiplication to reach the desired output frequency. Conversion efficiencies of 15 to 30 percent should be readily obtainable in the near-term period.

Turnoff reliability improvement is also to be expected from diode multipliers, since the failure rate versus dissipation function is similar for diodes and transistors.

Up-converters, which simultaneously mix and amplify an intermediate frequency signal to RF by means of nonlinear reactance diode mixers, are also possible candidates for solid-state generation of RF power. In such devices, a narrowband, varacter-diode multiplier furnishes a reference or pump source for the mixing circuit. A tradeoff of multiplier simplicity and efficiency for mixer loss is made. Functional differences, such as modulation handling, must also be considered, since up-converters do not increase frequency and phase deviation as do multiplier chains.

Step-recovery diodes are gaining importance for use as solid-state harmonic generators. The mechanism of rapid reverse charge flow permits simple, high efficiency, low noise, high order multiplier circuits. Present performance is reported to result in about 20 to 30 percent efficiency in multiplying 100 Mc up to 2 Gc, without need for idler circuits as in varacter multipliers. Power levels are limited by internal series resistance and breakdown voltage. Technology advances should soon result in generation of about 1 watt at 2 Gc in a simple high reliable circuit.

5. VACUUM TUBES

Applications requiring 10 watts or more at 2 Gc at present are constrained to the use of vacuum tube sources. Several are available as follows:

- Triodes
- Voltage tunable magnetrons
- Klystrons
- Amplitrons
- Traveling wave tubes

For use in the Advanced Planetary Probe, where frequency stability and noise characteristics are important, tubes which are restricted to applications as power oscillators (the voltage tunable magnetron is an example) must be eliminated from consideration. Frequency stabilization loops are possible, but undesirable for reasons of added complexity.

Triode cavity amplifiers are available up to 20 watts at 2 Gc, with 15 to 30 percent efficiency. Bandwidth is less than 1 per cent, which is not a limitation for deep space use. Life of those tubes is fairly limited to about 10,000 hours, 50,000 hours being an upper limit for tubes operating at lowered efficiency.

Klystrons (electrostatically focused) amplifiers are available for high power narrowband applications. Power levels up to 100 kw are normal, with efficiencies typically between 30 and 40 percent for the high power units, and 5 to 30 percent for the lower power tubes. Weight

and size for 20 watt units are low; for example 2 pounds and 3-1/4 inches diameter. Gain is in the 15 to 30 db range; bandwidth is 0.1 to 0.3 percent, which is more than sufficient for this application. Expected life for klystrons should be as high as 50,000 hours since the gun design is the only significant limiting factor. Noise output is generally sufficiently low for most systems.

"Amplitrons" (crossed-field, backward-wave amplifiers) have been developed for outputs of about 25 watts with 50 percent efficiency. Weight for these tubes are low; one unit (Raytheon QKS 1300) weighs 24 ounces. Requirement for a complex high voltage power supply mated to the individual tube's characteristics is a problem for these devices, resulting in increased total weight. Powers to 100 watts are available; efficiency may be as high as 60 percent. Long life is being demonstrated for the lower power units, although 10,000 hours is a probable maximum figure to be expected. Bandwidths are typically as high as 10 percent. Some characteristics present application problems: low backward insertion noise, noise, low gain, sensitivity to loading and to power supply voltages, and others. One advantage of amplitrons is that redundant amplifiers can be provided without RF switching. With amplitrons, series connection is used, and the deactivated unit presents about 0.5 db insertion loss. Further development is needed if these devices are to become competitive.

Traveling wave tube amplifier flight experience is extensive: Telstar, Relay, Syncom, Surveyor, and Pioneer 6 are some examples. Space application units are limited at present to 50 watts at 40 percent tube efficiency; higher powers are for normal ground use and could be qualified for space in the next few years. Of course, in space applications the constraints of variable RF drive, environmental excursions, aging, and long term power regulation are expected to yield worst case tube efficiency of the order of 35 percent. Life is predicted to reach as high as 90,000 hours for some units in development. Large improvement in efficiency is conceivable possible with new techniques. Wide bandwidth (about 50 percent) is commonplace, eliminating temperature effects on center frequency common with cavity-loaded triodes and klystrons. A disadvantage in this application is the need for a power supply with several stable and high voltages.

APPENDIX F

MODULATION AND BIT SYNCHRONIZATION

1. INTRODUCTION AND SUMMARY

For the Advanced Planetary Probe missions launched in the early 1970's, it was assumed that Mariner IV type modulation and bit synchronization will be used. This is a conservative approach since the Mariner IV system has flight-proven capability and the possible performance improvement may require some development effort. For the more advanced missions, even small communication efficiency improvements should be considered. It is possible that more reliable spacecraft can be achieved for the same capability and weight by turning to coding, rather than higher power transmitters. Redundancy and automatic fault detection and correction can be more easily incorporated in encoders than in power amplifiers.

In Section 2 of this appendix, the bit synchronization problem is considered. It is recognized that the PN sync techniques, in general, are superior and only one other method is briefly mentioned. The Mariner IV telemetry and command links used two-channel PN bit sync systems. Since more efficient single-channel techniques have been developed, the two multiplexing methods had to be compared in order to determine which is most appropriate for the Advanced Planetary Probe. For the telemetry link, because of simpler modulator design and improved efficiency, the single-channel systems should be used for advanced missions. The choice for the command link is not so simple. Since the single-channel detector is more complex, weight, reliability, and performance of the two systems has to be compared before a best approach can be chosen.

In Section 3 suppressed carrier modulation methods are investigated. These techniques offer improvement in efficiency since no power is transmitted in the carrier. Unfortunately, the price of improved data efficiency is the inferior phase-locked loop (PLL) performance and more complex receiver mechanization.

Application of coding for the Advanced Planetary Probe is briefly reviewed in the last section. For the telemetry link, a 128-word biorthogonal code dictionary was selected with potential performance improvement of 2.4 db over the uncoded case. It is recognized that an important constraint on the selection of the spacecraft telecommunication system is the DSIF configuration. As the number of missions supported by DSIF increases, it becomes important to use a minimum amount of mission-dependent equipment. The more complex ground decoder for the biorthogonal coding is the main disadvantage of this technique.

The need for coding the command link is questionable. However, if very low command rejection probabilities are needed, single error-correcting codes could be used.

2. TWO-CHANNEL AND SINGLE-CHANNEL SYNCHRONIZATION

Two basic multiplexing formats have been devised by JPL for telecommunication systems employing PN bit synchronization techniques. In the two-channel scheme, the data and sync channels are linearly summed to form a frequency division multiplexed signal. In the single-channel systems, the binary data and the sync are summed modulo 2 to produce a binary composite waveform.* The TRW Voyager report compares Pioneer 6 I-Q loop telemetry synchronization methods with the PN systems and shows that the two systems do not differ greatly in performance. One of the advantages of the Pioneer method is that the data encoder is simpler since the hardware associated with the PN code generation is eliminated. Another advantage is that self-synchronous coherent carrier systems, resulting in better efficiency as discussed in Section 3, possibly could be developed when PN systems are not used. However, the bit synchronization provided by the I-Q loops may not be as accurate and, therefore, these techniques are not further considered.

The modulators for both two-channel and single-channel systems are fundamentally similar, each requiring a clock, PN generator, data

*J.C. Springett, "Telemetry and Command Techniques for Planetary Spacecraft," JPL Technical Report 32-495, January 15, 1965; TRW Systems, "Phase 1A Voyager Spacecraft," vol. 5, 30 July 1965.

synchronizer, and logical devices. The two-channel modulator is conceptually and practically somewhat more complicated because it requires, in addition, a divider and an analog summing circuit. The single-channel detector, however, is more complex than the two-channel since it requires two additional bandpass filters and two multipliers.

An important advantage of the single-channel system is the use of frequency f_s as the data subcarrier reference rather than $4f_s$ as in the two-channel system. Since both PLL operate at f_s, the phase jitter on $4f_s$ is four times larger than on the f_s reference. Offsetting this advantage is the degradation caused by multiplying two noisy signals in the third multiplier of the single-channel detector.

Clearly, the single-channel system is capable of greater communication efficiency because no power is needed for synchronization. At high bit rates (perhaps above 100 bps), however, the percentage of power used for synchronization is not significant so that both systems have about the same efficiency. At lower bit rates (10 bps) the single-channel system is significantly more efficient than the two-channel format.

2.1 PN Synchronization Systems for Telemetry Link

For the Advanced Planetary Probe it is anticipated that the lowest bit rate will be about 10 bps. In Table F-1, the telemetry performance for this bit rate and the assumed other parameters is demonstrated. The comparison is made for three carrier PLL noise bandwidths: 12, 5, and 1 Hz. The 12 Hz noise bandwidth is presently available, while the realization of the other two bandwidths depends on the availability of phase-stable oscillators. The total required receiver input power divided by the noise density, S_T/Φ, is taken as the comparison criterion. It is seen that for the 10 bps the performance improvement of the single-channel over the two-channel system varies from 1.3 to 2.2 db depending on carrier PLL noise bandwidth, $2B_{LO}$. Since the improvement is maximum at the lowest bit rate, the S_T/Φ, for 100 bps has also been included in Table F-1. As expected, at this bit rate the improvement is only a fraction of a decibel. The theoretical coherent PCM/PSK is included for reference purposes. It assumes that perfect carrier reference and bit sync are available at the receiver. Since the assumed single-channel system does not require power for bit or subcarrier sync,

Table F-1. Comparison of Single-Channel and Two-Channel PN Synchronization Systems

$$P_e^{\,b} = 5 \times 10^{-3} = 2\,B_{LO}(\text{Sync}) = 0.5 \text{ Hz}$$

System Type	Carrier $2\,B_{LO}$ in Hz	$\frac{S_C}{\Phi}$ in $\frac{db}{Hz}$	$\frac{S_S}{\Phi}$ in $\frac{db}{Hz}$	10 bits/sec $\frac{S_D}{\Phi}$ in $\frac{db}{Hz}$	10 bits/sec $\frac{S_T}{\Phi}$ in $\frac{db}{Hz}$	100 bits/sec $\frac{S_D}{\Phi}$ in $\frac{db}{Hz}$	100 bits/sec $\frac{S_T}{\Phi}$ in $\frac{db}{Hz}$
Theoretical PCM/PSK $\frac{S_P T}{\Phi} = 5.2$ db (suppressed carrier)	--	0	0	15.2	15.2	25.2	25.2
Two-channel PCM/PSK/PM	12	16.8	15.4	17	21.2	27	27.8
$\frac{S_D T}{\Phi} = 7$ db	5	13	15.4	17	20.2	27	27.6
Squarewave subcarrier	1	6	15.4	17	19.5	27	27.4
Single-channel PCM/PSK/PM	12	16.8	0	17	19.9	27	27.4
$\frac{S_D T}{\Phi} = 7$ db	5	13	0	17	18.5	27	27.2
Squarewave subcarrier	1	6	0	17	17.3	27	27

only carrier power transmitted in order to obtain coherent reference reduces efficiency of the single-channel PCM/PSK/PM. For this reason self-synchronous carrier systems are briefly discussed in Section 3.

Table F-1 also indicates the potential performance improvement due to narrower PLL noise bandwidths. All of the indicated improvement, however, cannot be achieved because certain amounts of power are wasted in intermodulation products. A comparison criterion which takes this into account is the data modulation loss computed from optimum modulation indices.

2.2 PN Synchronization Systems for Command Link

It appears that 1 bps is adequate for the command link. Some interest in higher bit rates is indicated since the time required to acquire bit sync is reduced for higher bit rates. Another way to reduce bit sync acquisition time is to incorporate automatic acquisition loop. The acquisition time, however, is of major interest only during near-earth operations. At longer communication distances, the propagation delay will predominate. Lower data rates might be considered, but because of the carrier power requirements and the difficulties in mechanization at the lower rates, the total power required does not decrease sufficiently to make such a choice advantageous. Even at 1 bps, rate construction of the subcarrier reference is difficult and results in significant performance degradation. Using any other subcarrier synchronization method, such as a squarer or an I-Q loop, will cause difficulties similar to PN synchronization techniques. For these reasons, only 1 bps transmission rate for command link is considered.

In Table F-2 the command link performance for the assumed parameters is illustrated. Since automatic sync acquisition is not recommended, the sync PLL noise bandwidth was taken to be a conservative 2 Hz. Table F-2 indicates that the performance improvement of the single-channel over the two-channel is 1.4 and 2.2 db for the 20 and 10 Hz carrier PLL noise bandwidth considered. Larger improvements cannot be obtained since most of the transmitted power is in the carrier component. Partly for the same reason, the command link efficiency is much lower than the theoretical PCM/PSK.

The data subcarrier in the two-channel system was assumed to be sinusoidal. At low modulation indices used for the command channel, the sinewave subcarrier provides somewhat better performance than the squarewave since it allows bandpass filtering. The single-channel system

Table F-2. Comparison of Command Link Modulation Techniques

$$P_e{}^b = 1 \times 10^{-5}$$

System Type	Carrier $2B_{LO}$ in Hz	$\frac{S_C}{\Phi}$ in $\frac{db}{Hz}$	$\frac{S_D}{\Phi}$ in $\frac{db}{Hz}$	Sync $2B_{LO}$ = 2 Hz: $\frac{S_S}{\Phi}$ in $\frac{db}{Hz}$	Sync $2B_{LO}$ = 2 Hz: $\frac{S_T}{\Phi}$ in $\frac{db}{Hz}$
Theoretical PCM/PSK	-	-	9.6	-	9.6
Two-channel PCM/PSK/PM sinusoidal subcarrier	20	21	15	18	23.4
	10	18	15	18	22.0
Single-channel PCM/PSK/PM squarewave subcarrier	20	21	15	0	22
	10	18	15	0	19.8

apparently requires a squarewave subcarrier. If a bandpass filter is needed in the data channel, the performance improvement shown in Table F-2 would be reduced.

3. SUPPRESSED CARRIER TECHNIQUES

It is well known that the most efficient modulation technique is the coherent PCM/PSK. To realize this efficiency, however, a coherent carrier reference has to be provided at the receiver. The most common way to establish a coherent phase reference is to transmit a residual carrier component, referred to as pilot tone, which is tracked by the PLL receiver. Since PCM/PSK modulation completely suppresses the carrier, a subcarrier is required. The resultant modulation technique can be described as PCM/PSK/PM, i.e., the PCM data biphase modulates the subcarrier, which in turn phase-modulates the carrier with modulation index less than $\pi/2$ radians. This is the scheme used for Mariner IV links, and was tacitly assumed in Section 2.

Subcarriers are needed for other purposes. For low bit rates and PCM format used, a subcarrier is required in order not to degrade data and PLL performance by the data spectrum which falls inside the loop noise bandwidth. The single-channel PN synchronization systems also require squarewave subcarrier to facilitate modulo-2 addition of data and synchronization components. Since the single-channel PN synchronization systems apparently do not require any power for bit synchronization and the coherent subcarrier reference is obtained as a byproduct, the addition of subcarrier should not degrade communications efficiency. Thus, the main disadvantage of the pilot tone method is that it requires power which could be used for transmitting information. For high bit rates, the data modulation loss (degradation due to the pilot tone transmission) is small, as illustrated in Table F-3. At low bit rates used for the command link,

Table F-3. Modulation Losses for Single-Channel Telemetry Links

PCM/PSK/PM; Squarewave Subcarrier

$$\frac{S_D T}{\Phi} = 7 \text{ db for } P_e{}^b = 5 \times 10^{-3}$$

SNR in 2 B_{LO} = 6 db

Carrier 2 B_{LO}	10 bits/sec		100 bits/sec	
	Carrier Modulation Loss in db	Data Modulation Loss in db	Carrier Modulation Loss in db	Data Modulation Loss in db
12	-3	-3	-10	-0.45
5	-5.5	-1.4	-10	-0.45
1	-10	-0.45	-10	-0.45

however, the modulation loss is of the order of 7 db, as shown in Table F-4. Therefore, suppressed carrier modulation methods which do not require pilot tones to obtain coherent references are of interest.

Table F-4. Modulation Losses for Single Channel Command Link at 1 Bit/Sec

PCM/PSK/PM; Squarewave Subcarrier

$$\frac{S_P T}{\Phi} = 15 \text{ db for } P_e{}^b = 1 \times 10^{-5}$$

SNR in 2 B_{LO} = 8 db

Carrier 2 B_{LO} in Hz	Carrier Modulation Loss in db	Data Modulation Loss in db
20	-1	-7
10	-1.8	-4.7

Two techniques are available to reconstruct a coherent carrier reference by operating on the suppressed carrier signal. The first technique can be described as squarer, followed by a conventional PLL. The second technique is known as the I-Q loop.* Both of these methods are widely used for bit synchronization and coherent subcarrier reconstruction. About the same number of components is required to mechanize each system, and, under some simplifying assumptions, the two schemes are mathematically equivalent.* Therefore in what follows only the squaring loop is considered.

One disadvantage of the I-Q and squaring loops, especially in the case of command link, is that the receiver mechanizations for both of them are somewhat more complex than a simple PLL. Another problem with the self-synchronous technique is the 180 degrees phase ambiguity since both $+\sin(\omega_c t + \phi)$ and $-\sin(\omega_c t + \phi)$ yield the same signal when squared. Although several techniques are available to resolve this ambiguity, it results in more complex equipment.

The performance of the simple PLL and the squaring loop will be considered by comparing loop phase errors and carrier reference phase

*H. L. Van Trees, "Optimum Power Division in Coherent Communication System," IEEE Trans., SET 10 (March 1964).

errors. The mean square phase error in the loop due to the presence of noise is approximately given by

$$\sigma_p^2 = \frac{1}{2\,SNR}$$

where SNR is the signal-to-noise ratio in the loop noise bandwidth. For PLL, the SNR is

$$(SNR)_1 = \frac{S_T M_{LC}}{\Phi 2 B_{LO}}$$

and for the squaring loop it is found that*

$$(SNR)_2 = \frac{S_T^2 \rho^4}{2\Phi(2B'_{LO})\left(2S_T\rho^2 + \Phi B_O\right)}$$

where

ρ^2 = ratio of filtered signal power to unfiltered power at the input of BPF

B_O = bandwidth of BPF preceding the squarer

S_T = total received signal power

M_{LC} = carrier modulation loss

$2B_{LO}$ = PLL noise bandwidth

$2B'_{LO}$ = squaring loop noise bandwidth

Φ = noise spectral density

The 0 db SNR is normally referred to as absolute phase-lock threshold. At this point, the acquisition is difficult and the loop noise error, σ_p, is 1 radian rms ($\sigma_p^2 = 1/SNR$ for low SNR). The carrier reference phase error, σ_{n1}^2, is equal to σ_{p1}^2 for PLL, while for the squaring loop, $\sigma_{n2}^2 = 1/4\,\sigma_{p2}^2$. Thus, for $\sigma_{p1}^2 = \sigma_{p2}^2$ or $(SNR)_1 = (SNR)_2$, the data performance

*J.J. Stiffler, "The Squaring Loop Technique for Binary PSK Synchronization," JPL SPS 37-26, Vol. IV, 31 March 1964.

of the squaring loop system will exceed the data performance of the simple PLL system by at least the data modulation losses given in Tables F-3 and F-4. In general, however, the variance of the phase error for the squaring loop cannot be made equal to (or smaller) than the variance of the simple PLL. This will be illustrated by the following example.

Assuming that $\rho^2 = 1$ and $(2B'_{LO}) = 2 \cdot (2B_{LO})$ and equating $(SNR)_1$ and $(SNR)_2$, we can determine maximum B_O for which the squaring loop is superior to PLL. This maximum B_O, as a function of $2B_{LO}$, is given by

$$B_O = 2 B_{LO} \frac{(SNR)_1}{M_{LC}} \left(\frac{1}{M_{LC}} - 2 \right)$$

From Table F-4, where carrier modulation losses, M_{LC}, are given for command link, it immediately becomes apparent that the squaring loop cannot be made superior to PLL. For the telemetry link, the required maximum B_O for the previously considered bit rates and carrier PLL noise bandwidths are given in Table F-5 for $(SNR)_1 = 6$ db. Unfortunately,

Table F-5. Maximum BPF Bandwidth

Bit Rate	Carrier 2 B_{LO} in Hz	Maximum B_O in Hz
10	12	0
	5	105
	1	320
100	12	3800
	5	1600
	1	320

the performance indicated by the BPF listed in Table F-5 cannot be realized for PN synchronization systems. This becomes apparent when the power spectrum of the synchronization signal is examined. In general, the baseband of this signal is much larger than the bit rate so that $\rho^2 < 1$ and $\sigma_{n2} > \sigma_{n1}$. In other words, the PLL will have shorter acquisition

times and longer time between loss of lock than the squaring loops. Thus, from the loop performance standpoint, suppressed carrier techniques do not appear to be attractive.

It is interesting to point out that for the Pioneer 6 bit synchronization method, the signal baseband is approximately equal to twice the bit rate. In this case, $\rho^2 \simeq 1$ and the performance improvement can be realized with the suppressed carrier schemes.

4. CODING

The present state-of-the-art method for telemetry systems, with few exceptions, is to use the binary uncoded PCM. By this, we mean that the data word length is equal to the number of information bits in the word. In other words, no redundant bits are added to the data words. Furthermore, the detection on the ground is on the bit-by-bit basis as used by Mariner IV and most other spacecraft. It has been well established that the communications efficiency can be improved by adding redundancy at the transmitter. If error detection and/or correction is used to decode the received words on a bit-by-bit basis, the coding is known as error correcting coding. Many spacecraft command links use some sort of error detection schemes. If the redundancy is employed to reduce errors by decoding the entire word in one operation, the coding is known as simplex, orthogonal, or biorthogonal coding.* Although simplex codes are optimum, the difference in performance between and orthogonal or biorthogonal codes is small.

The modulation, as discussed in the preceding section, is taken to be coherent PSK and the disturbance, additive white gaussian noise. In case of error-correcting coding, it is assumed that the two binary symbols are transmitted with equal energy and probability; and in case of orthogonal (or simplex or biorthogonal) coding, all words are equally likely. Under these circumstances, it is known that for both coding techniques the maximum likelihood of correlation detection is achieved in the sense that it minimizes word error probability. It has been established that communications efficiency with simplex coding cannot be exceeded.

*S.W. Golomb, ed., Digital Communication with Space Applications, Prentice-Hall, 1964.

This does not rule out the existence of error-correcting codes which have efficiency equal to the simplex codes. The known error-correcting codes, however, are less efficient than orthogonal codes. For word error probability of the order of 10^{-2}, the performance of certain error-correcting codes is only about 1 db worse than simplex codes.* In this application it is expected that a P_e^w in the neighborhood of 3.5×10^{-2} will be adequate, so that the difference in communication efficiency between the two methods will be of the order of 1 db. On the other hand, for signal-to-noise ratios approaching zero (and therefore $P_e^w \rightarrow 1$), it has been found** that orthogonal codes offer 3.4 db improvement over the error-correcting codes as the length of the code increases without bound. One other disadvantage of the error-correcting codes is that bit error probability in the region of interest (5×10^{-3}) may be larger than for the uncoded case. Since both digital and analog data may be transmitted, the bit error probability will be used as performance criterion. An advantage of the error-correcting coding is the fact that decoders may be simpler. In fact, for large dictionaries, the decoder for orthogonal codes becomes prohibitively complex.

4.1 Coding for Telemetry Link

For the telemetry channel, a biorthogonal coding is assumed since it is more efficient and the complexity is in the ground equipment. The dictionary size has been chosen as 128 words and corresponds to the Mariner IV dictionary. For this size the word length is 64 digits. An elegant and simple way of generating biorthogonal codes, devised by JPL, is shown in Figure F-1. The digit and word synchronization requires careful consideration. One way to obtain both digit and word sync is to use a word-synchronous PN system. Although it appears that the PN code length and the clock frequencies can be chosen to fulfill various constraints, the design of a PN sync system is outside the scope of this task. Another possibility for the word sync is to use the comma-free codes which can

*C. M. Hackett, "Word Error Rate for Group Codes Detected by Correlation and other Means," IEEE Trans. Infer. Theory, January 1963.

**E. C. Posner, "Properties of Error-Correcting Codes at Low Signal-to-Noise Ratios," JPL Tech. Rep. 32-602, 15 June 1964.

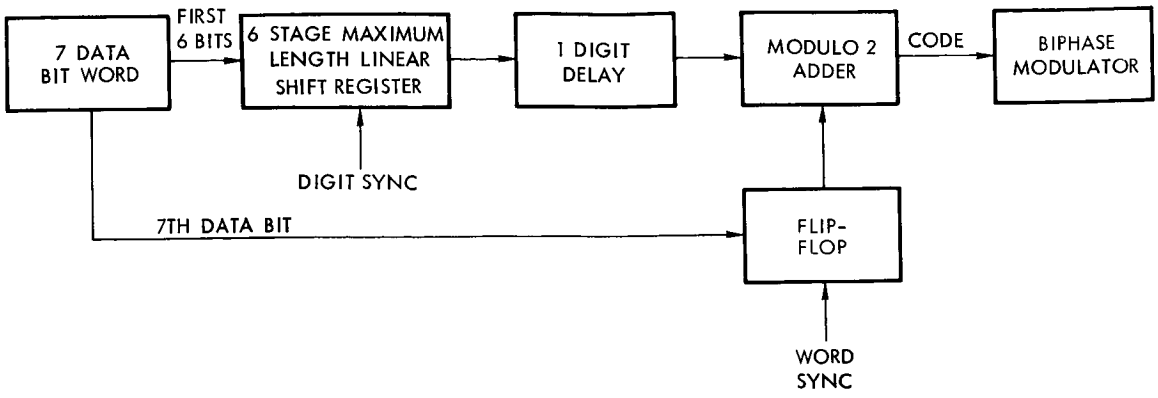

Figure F-1. Biorthogonal Coder

be generated with very little additional hardware.* Before the word sync can be acquired, however, digit sync has to be established. For this reason, the value of the comma-free codes is questionable.

Specifying a bit error probability of 5×10^{-3}, it is found (Golomb, op. cit., Chapter 7) that coding provides 2.4-db improvement. The improvement for lower bit error probabilities is even greater; however, it appears that a bit error rate of 5×10^{-3} is adequate.

The main disadvantage of the biorthogonal coding is the decoder complexity. At the receiver, the 64 words will have to be stored or generated and correlated with the received signals. The 64 correlators can be replaced by an analog-to-digital converter and a computer. Another possible difficulty is the accuracy of the digit and word sync required to realize the theoretical improvement. It appears that the performance degradation for the coded systems, due to sync imperfections will be larger than for the uncoded systems.

4.2 Coding for Command Link

The majority of spacecraft command links at present employ some sort of error- or parity-check coding to decrease the probability of incorrect command acceptance. Since it is recognized that command capability over the omnidirectional antenna can improve mission success probability, further improvement in uplink efficiency is of interest. Furthermore, if the probability of rejecting a command due to bit errors has to be very

*C.C. Wang, "Phase-Coherent and Comma-Free Biorthogonal Telemetry System," IEEE Military Electronics Conference, 1965.

low, say 10^{-4}, coding may be required, assuming that bit error probabilities lower than 10^{-5} could not be achieved dur to impulse noise or other differences from the ideal conditions. Bit error rates of 10^{-5} are normally claimed by TRW and JPL, and no reliability measurements are available for bit error probability lower than 10^{-5}.

Since encoder complexity is the dominating feature for the command channel, error-correcting codes appear to be more appropriate than orthogonal coding. Unfortunately, the decoder even for single-error correction can be considerably more complex than a decoder employing only parity checks.

APPENDIX G

COMMUNICATION SYSTEM NOISE TEMPERATURE

1. INTRODUCTION AND SUMMARY

One of the parameters that determines telecommunications system performance is the system noise temperature or the noise spectral density. In turn, the noise spectral density depends on the antenna temperature. Our main task here is to compute antenna temperature when the ground or spacecraft antenna is pointed at the sun or Jupiter.

Computed trajectories indicate that the sun-probe-earth angles at certain instances will be approximately zero. This means that the spacecraft antenna during these periods will be pointed at the sun. When the spacecraft is in the vicinity of the target, the DSIF antenna may be pointed directly at Jupiter for a short period of time. Again, when the probe gets behind Jupiter, the planet may be in the spacecraft antenna beam. Since the sun and Jupiter radiate a considerable amount of noise around 2300 MHz, this noise will increase antenna noise temperature and degrade system performance. The amount of radiation from Saturn and Neptune is much smaller than from Jupiter and will not degrade system performance.

The spacecraft antenna noise temperature will be affected most seriously by the sun. Figure G-1 shows that in case of the disturbed sun and a 16-foot antenna, the noise density may increase by as much as 12 db/Hz above the nominal -164.4 dbm/Hz level.* The quiet sun, however, will contribute only about 0.3 db/Hz to the system noise spectral density. Fortunately, it is estimated that the uplink performance will be degraded quite infrequently by the disturbed sun. When the probe is near Jupiter and the spacecraft antenna is pointed at the planet, the noise spectral density will increase by a maximum 1.8 db above the nominal -164.4 dbm/Hz level.

---

*This is based on a receiver noise figure of 10 db. In Section 8.4 of Volume 2 a receiver with a noise figure of 5.5 db was selected.

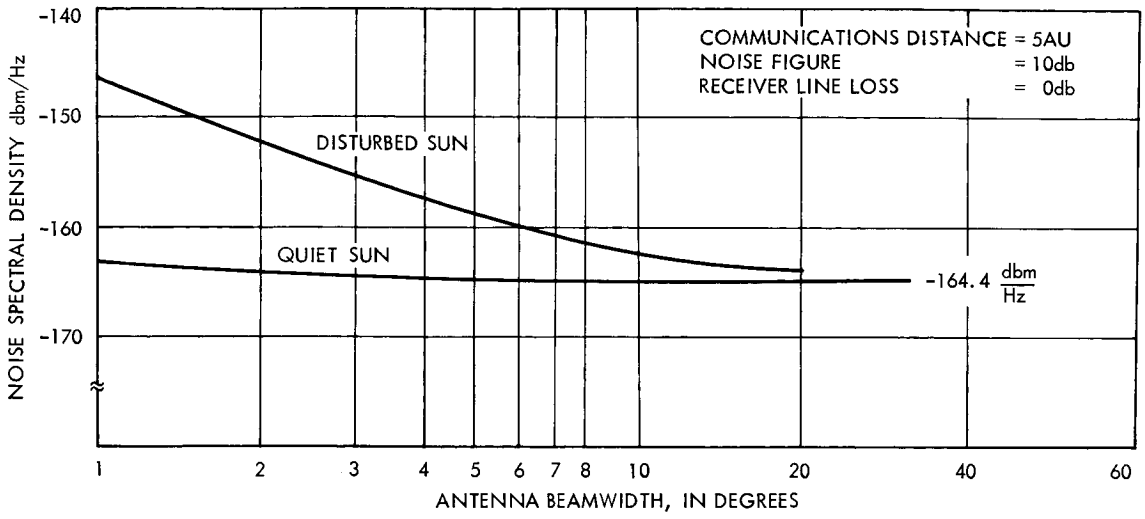

Figure G-1. Receiver Noise Spectral Density Versus Antenna Beamwidth with Antenna Pointed Directly at the Sun

The noise spectral density of the ground system with a 210-foot antenna will increase by 1.7 db/Hz due to Jupiter noise. The noise temperature of the 85-foot antenna, because of its wider beamwidth, will not be affected by the radiation from Jupiter. In Table G-1 the noise spectral densities for various cases is summarized.

2. ANTENNA NOISE TEMPERATURE

The system noise temperature can be approximated by

$$T = \frac{T_a}{L} + \frac{T_o (L-1)}{L} + T_o (NF-1)$$

where

T_a = antenna noise temperature

T_o = ambient temperature = 290 ^{o}K

NF = receiver noise figure

L = receiver line loss to low noise amplifier

The parameter that remains to be computed is the antenna noise temperature. Since contribution of the other sources to the antenna

Table G-1. System Noise Temperatures and Noise Spectral Densities

	Nominal		Disturbed Sun in View		Jupiter in View	
	Temperature (^{o}K)	Noise Density (dbm/Hz)	Temperature (^{o}K)	Noise Density (dbm/Hz)	Temperature (^{o}K)	Noise Density (dbm/Hz)
16-Foot Spacecraft Antenna NF = 10 db L = 0 db T_o = 290^{o}K T_a (sky) = 0^{o}K T_a (disturbed sun) = 43000^{o}K T_a (Jupiter) = 1350^{o}K	2610	-164.4	43000	-152.3	3960	-162.6
210-Foot DSIF Antenna θ_b = 0.1 deg T_o = 290^{o}K T_o (NF-1) = 18^{o}K L = 0.02 db T_a (sky noise) = 10^{o}K T_a (Jupiter noise) = 15^{o}K	30	-183.8	-	-	45	-182.1

temperature is known, only the contribution by the sun or Jupiter has to be calculated. The antenna temperature is given by*

$$T_a = \frac{1}{4\pi} \iint_{\Omega_s} G(\theta_1 \phi)\, T_s\, (\theta_1 \phi)\, d\,\Omega_s$$

where

$T_s(\theta_1 \phi)$ = source brightness temperature

$G(\theta_1 \phi)$ = antenna gain

Ω_s = solid angle subtended by the source at the point of observation

Assuming that the source is directly on the antenna beam axis, for the case when antenna beam solid angle, Ω_b, is much smaller than Ω_s, T_a can be approximated by

$$T_a = \overline{T}_s \left(\frac{\theta_s}{\theta_b} \right)$$

where

$\overline{T}_s$ = average source temperature

θ_s = plane angle subtended by the source

θ_b = plane angle 3 db antenna beamwidth

In the other extreme, when the source is much larger than the antenna beamwidth,

$$T_a \simeq \overline{T}_s$$

The average source temperature can be computed from the measured flux densities using the expression

*J. L. Pawsey and R. N. Bracewell, Radio Astronomy, Oxford Univ. Press, 1955.

$$\overline{T}_s = \frac{s\lambda^2}{2k\Omega_s}$$

where

S = flux density

Ω_s = solid angle subtended by the source at the antenna

λ = wavelength

$k = 1.38 \times 10^{-23}$

For small angles, Ω_s can be accurately approximated by

$$\Omega_s \simeq \frac{\pi}{4} \theta_s^2$$

3. DSIF ANTENNAS POINTED AT JUPITER

For ground-based antennas we obtain the following expression for the antenna temperature by substituting the exptession for $\overline{T}_s$ and Ω_s in that for T_a:

$$T_a = \frac{2s\lambda^2}{\pi k \theta_b^2}$$

The flux from Jupiter as measured on earth at 0.13 meter wavelength* is about 6×10^{-26} w/m^2/Hz. The 210-foot antenna beamwidth, θ_b, is approximately 0.1 degree. Substituting these values in the above equation, the antenna temperature due to the planet is found to be 15 degrees. This results in a total system temperature of 45°K, or a noise spectral density of -182.1 dbm/Hz. Table G-1 indicates that the degradation due to Jupiter is 1.7 db. Since the planet will be in view of the antenna for a short period of time only, the RF noise radiated by Jupiter should not be a serious problem. Of course, the occultation experiment may be significantly degraded.

*A. G. Smith and T. R. Carr, Radio Exploration of the Planetary System, Van Nostrand, 1964.

4. SPACECRAFT ANTENNA POINTED AT THE SUN

The flux density measured on earth* for the quiet sun is given as 1×10^{-20} and for the disturbed sun as 2×10^{-18}. Substituting these in the expression for $\overline{T}_s$, the quiet sun temperature is found to be 1.1×10^5 °K and the disturbed sun temperature is 2.2×10^7 °K.

To compute antenna noise temperature, the angle subtended by the source, θ_s, or equivalent spacecraft range, has to be chosen. From trajectories presented in the Mid-Term Report, it is found that sun-probe-earth angle for Jupiter missions is close to zero at 1 and 5 AU. Since we are more concerned with the uplink performance at 5 AU than at 1 AU, antenna temperature at 5 AU will be calculated. At this range, the antenna temperature due to the disturbed sun for the 16-foot spacecraft antenna is 4.3×10^4 °K. This results in a 12-db degradation of the noise spectral density, as indicated in Table G-1. The degradation for other antennas, expressed as a function of antenna beamwidth, is given in Figure G-1. As shown, the noise spectral density will not be appreciably affected by the quiet sun.

Fortunately, the average duration of the strong outbursts of radiation (disturbances) due to flares is only a few minutes. This does not mean that the sun is quiet the remainder of the time. In general, the observed level of radiation lies somewhat higher than the value used here for the quiet sun. This nominal level, however, is much lower than 2×10^{-18}, so that the antenna temperature will not be significantly raised. Furthermore, from the trajectories it is estimated that for the Jupiter missions the antenna will be pointed at the sun for less than 25 days. Thus, the maximum percentage of the time during which uplink performance can be degraded by the sun is small. For this reason it may be concluded that while the solar radiation may infrequently degrade uplink communications performance, it does not appear to be a serious problem in this application.

---

* A. G. Smith, "Extraterrestrial Noise as a Factor in Space Communications," Proc. IRE, April 1960.

5. SPACECRAFT ANTENNA POINTED AT JUPITER

When the probe is behind Jupiter, the planet may be in the spacecraft antenna beam. Since the spacecraft will be located close to Jupiter, the angular size of the radiation source will be large with respect to the antenna beamwidth. Linear interpolation indicates that the Jupiter and antenna temperature is 1350°K at 2100 MHz. Thus, the noise spectral density will be degraded by 1.8 db, as shown in Table G-1.

APPENDIX H

MIDCOURSE PROPULSION SYSTEM ERROR ANALYSIS

1. INTRODUCTION

The error analysis is based on the assumption that calibration curves will be generated during tests of the midcourse propulsion system under simulated spacecraft environment. These curves will be used to predict system performance based on telemetry inputs from the spacecraft. The telemetry inputs will be propellant tank expulsion gas pressure and propellant temperature. These will be used to determine which calibration curve the system will follow during the subsequent firing.

The errors to be considered are those incurred in measurement and transmittal of the measurements from the spacecraft and those inherent in formulating the calibration curves.

The errors incurred in measurement and transmittal of spacecraft data are those resulting from original calibration errors in the transducers, accuracy capability of the calibrated transducer, and the errors associated with telemetering equipment. It is assumed that the capability of the telemetry equipment will be at least equal to the accuracy capability of the calibrated transducers. This will be done by providing a sufficient number of bits per measurement.

The errors associated with the generation of the calibration curves do not include any errors associated with the expulsion gas loading of the propellant tank based on the assumption that great care will be exercised in tank and bladder fabrication and assembly to obtain reproducible tankage. Great care will also be taken to provide a precise amount of propellant in the tank in order to have an accurate initial gas volume. The errors associated with the propulsion system will be those involved in measuring the tank pressure, thrust, and the effect of simulation of the propulsion system space environment. The major environmental effect will be that associated with reproducing the heat transfer to the gas during blowdown. Transfer rates associated with 1 g earth

environment will be different from those experienced under less than 1 g aboard the spacecraft. Also, the inaccuracies associated with simulating the contribution of heat from the surrounding equipment will introduce additional errors.

The errors associated with changes in viscosity of the propellant during the blowdown mode which affect line resistance and flow rates result in thrust changes. This error with the very low flow rates and relatively large line sizes is a second-order effect.

2. MEASUREMENT ERRORS

Tank pressure measurements will be telemetered to earth. They will be used to determine which calibration curve the engine will follow during the subsequent firing. The thrust error associated with this measurement varies with burn time and is shown in Figure H-1. The

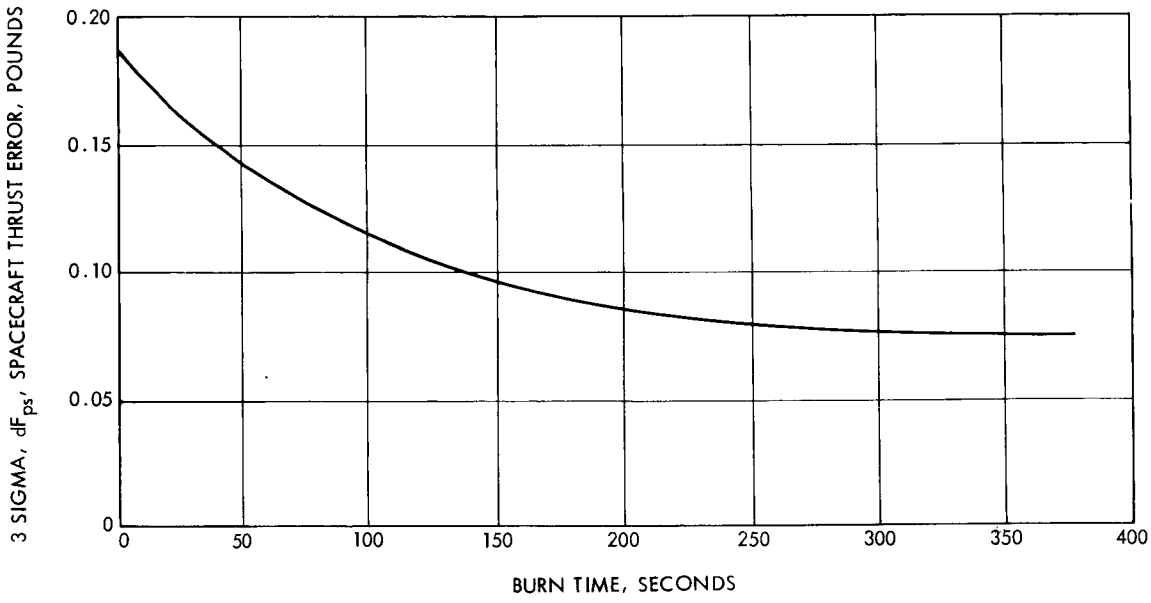

Figure H-1. Spacecraft Thrust Error Due to Tank Pressure Measurement Uncertainty Telemetered to Earth

error in tank pressure as a function of the ability to measure tank pressure, P_{Tas}/P_{Tms}, is

Transducer error, percent	
Calibration	0.25
Measurement	0.50
Telemetry error, percent	0.50
	1.25 percent (3σ)

The transducer and telemetry errors are 99.99 percent values of an assumed rectangular distribution. Straight addition results in a conservative 3σ value.

The tank pressure error is

$$dP_{Ts} = \frac{\partial P_{Tas}}{\partial P_{Tms}} \times P_{Ts}$$

where P_{Ts} is the tank pressure being measured aboard the spacecraft. The thrust error with respect to uncertainties in measurement of tank pressure aboard the spacecraft is

$$dF_{Ps} = \frac{\partial F}{\partial P_{Ts}} \times dP_{Ts}$$

where $\partial F/\partial P_T$ is the change in thrust as a function of tank pressure.

3. CALIBRATION ERRORS

The uncertainties associated with generation of the calibration curves are divided into two groups, proportional and nonproportional errors. The nonproportional uncertainties are divided into those associated with thrust initiation and those occurring during thrust termination.

3.1 Proportional Errors

The test stand transducers can be more accurate than the flight transducers aboard the spacecraft. They do not experience as severe an environment and no weight limitation is involved. Based on this, the measurement error, $\partial P_{Ta}/P_{Tm}$, is:

Transducers calibration error	0.01 percent
Transducers measurement error	0.25
Recorder (includes biased and random errors)	0.25
$\frac{\partial P_{Ta}}{\partial P_{Tm}}$	= 0.51 percent (3σ)

The 0.01 percent calibration accuracy is based on TRW's extremely accurate deadweight calibration system. The recorder accuracy of

0.25 percent is based on TRW's 1000-count digital system with a sampling rate of 625 samples per second. Hysteresis is removed by calibrating in the descending pressure mode, which simulates blowdown system operation. The tank pressure error,

$$dP_T = \frac{\partial P_{Ta}}{\partial P_{Tm}}$$

where P_T is the test stand tank pressure. The thrust error with respect to uncertainties of measuring test stand tank pressure is

$$dF_P = \frac{\partial F}{\partial P_T} \times dP_T$$

A plot of dF_P is given in Figure H-2. The errors involved in measuring the thrust, $\partial F_a / \partial F_m$, are:

Calibration error	0.25 percent
Measurement error	0.25
Recorder error	0.25
$\frac{\partial F_a}{\partial F_m}$ =	0.75 percent (3σ)

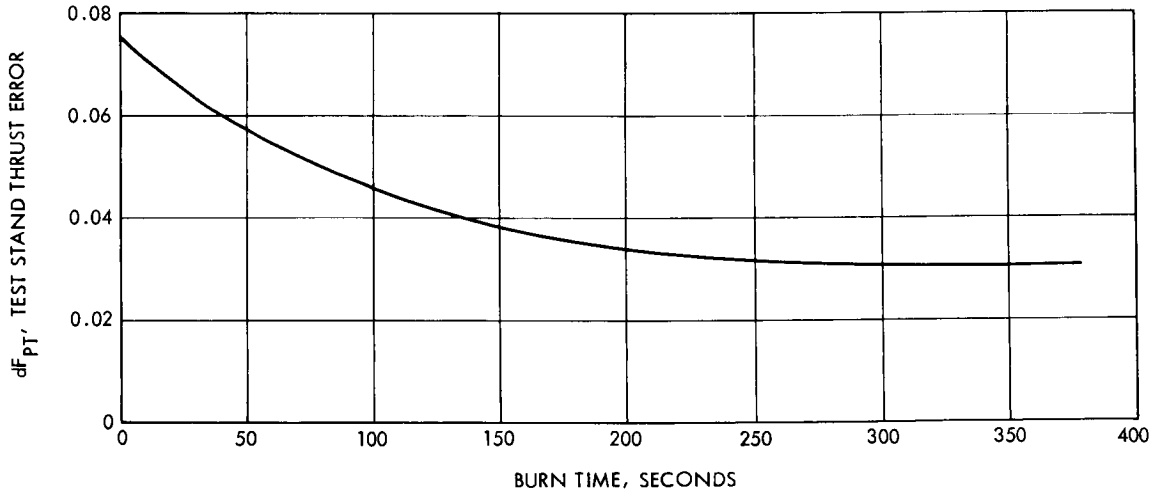

Figure H-2. Test Stand Thrust Error Due to Tank Pressure Measurement Uncertainty

The thrust error due to measurement errors

$$dF_m = \frac{\partial F_a}{\partial F_m} \times F$$

where F is the thrust level. Figure H-3 is a plot of dF_m as a function of firing time at $70^{\circ}F$.

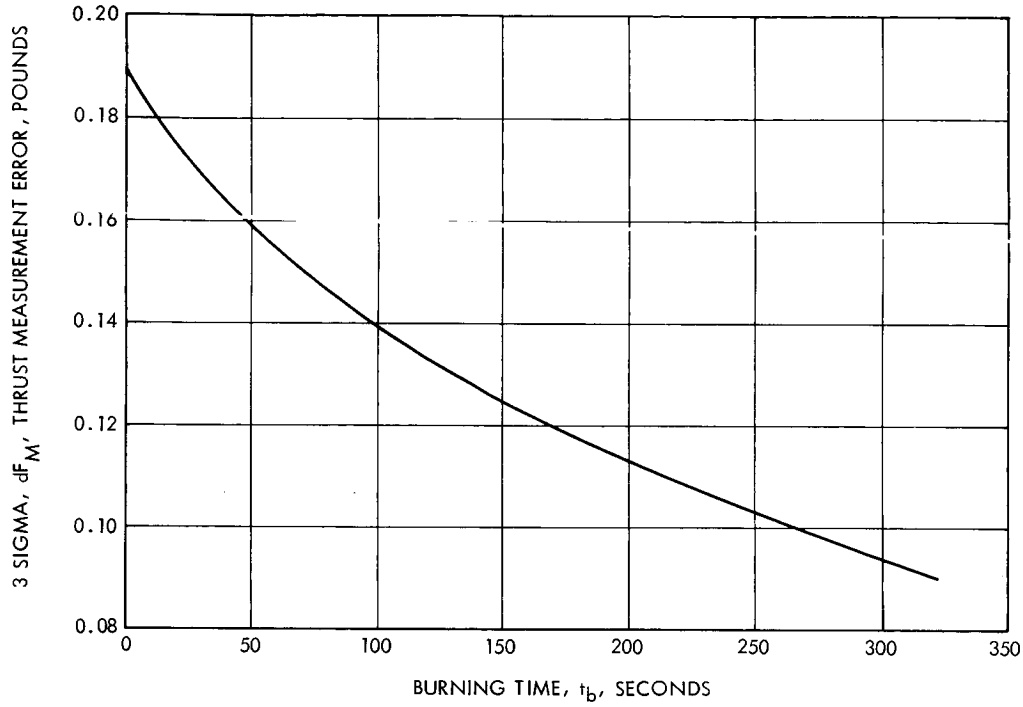

Figure H-3. Test Stand Measurement Error (3σ) Versus Midcourse Propulsion System Burn Time

The next error is that associated with simulating the system environment accurately. For instance, errors will be associated with trying to duplicate spacecraft heat transfer rates to the expulsion gas during the propulsion system blowdown expansion process. Analysis will be performed to determine the effect of the much lower g level on convective heat transfer in an effort to remove as much uncertainty as possible; however, even with the analysis an error will exist. Here it is assumed that the inaccuracy in simulating the heat transfer rates will result in a $5^{\circ}F$ error, i.e., the gas temperature during blowdown at the test stand while generating the calibration curves will be 5 degrees

different from that actually experienced aboard the spacecraft. Therefore dT will be 5^{o}F. Changes in expulsion gas temperature are less critical during the later part of the burn since less expansion takes place with the expulsion of the same increment of propellant.

The thrust error due to expulsion gas temperature change, dF_{GT}, will then be $\partial F/\partial T \times dT$. A plot of dF_{GT} as a function of burn time is given in Figure H-4.

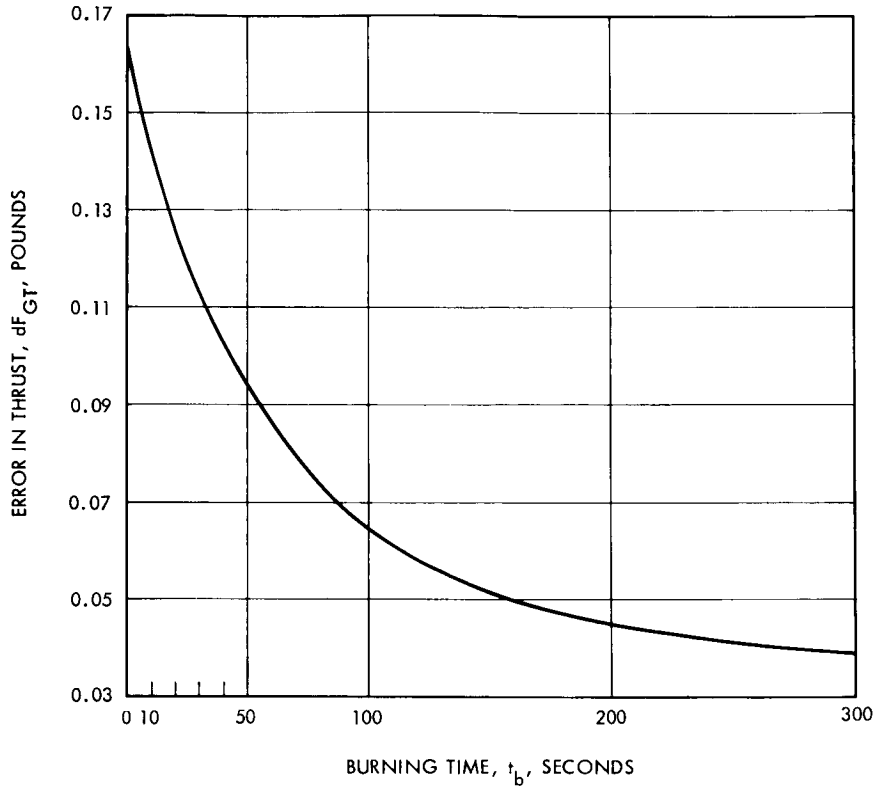

Figure H-4. Error in Midcourse Propulsion System Thrust (3σ) Due to Expulsion Gas Temperature Changes as a Function of Burn Time

The remaining error source is the ability to measure the pressure of the simulated space vacuum environment. The error, due to vacuum measurement, dF_V, is a combination of the errors associated with the pressure measurement and errors introduced in variations of A_e due to manufacturing inaccuracies.

$\partial P_{aa}/\partial P_{am}$ error due to vacuum measurement accuracy is

Transducer calibration error	0.03 percent
Transducer measurement	0.25
Recorder	0.25

$$\frac{\partial P_{aa}}{\partial P_{am}} = 0.53 \text{ percent } (3\sigma)$$

The full range of the transducer P_{vo} is 1 psia for a pressure measurement at 120,000 feet of approximately 0.06 psia. The nominal nozzle exhaust area is 3.12 square inches.

The error in thrust due to inaccuracies of measuring vacuum pressure is:

$$dF_{vm} = \frac{\partial P_{aa}}{\partial P_{am}} \times P_{vo} \times A_{en}$$

where A_{en} is the nozzle exhaust area.

$$dF_{vm} = 0.0053 \times 1 \times 3.12 = 0.000165 \text{ lb } (3\sigma)$$

The error associated with fabrication inaccuracies in the nozzle exhaust area is approximately ± 0.010 inch variation in the effective exhaust diameter. This effective variation includes inaccuracies in nozzle contour and concentricity. The resulting change in nozzle area would be:

$$0.785\ (1.99 \pm 0.010)^2 = 0.651 \text{ in}^2$$

The nominal back pressure in the test cell is 0.06 psia. The error in thrust, therefore, would be $dF_{vf} = 0.651 \times 0.06 = 0.0391$ lb (3σ). The total error in thrust resulting during the blowdown mode of operation is summarized in Table H-1.

The last two errors in Table H-1 are independent of burning time, while the others are not. The proportional impulse errors are summed as a function of time in Figure H-5.

Table H-1. Blowdown Mode Thrust Errors

Error Source	Symbol	3σ Thrust Error (lb)
Spacecraft		
Tank pressure transmittal	dF_{ps}	Figure H-1
Test stand		
Tank pressure setting	dF_{pt}	Figure H-2
Thrust measurement	dF_{m}	Figure H-3
Expulsion gas temperature change	dF_{gt}	Figure H-4
Vacuum measurement	dF_{vm}	0.0165
Thruster nozzle area	dF_{vf}	0.0391

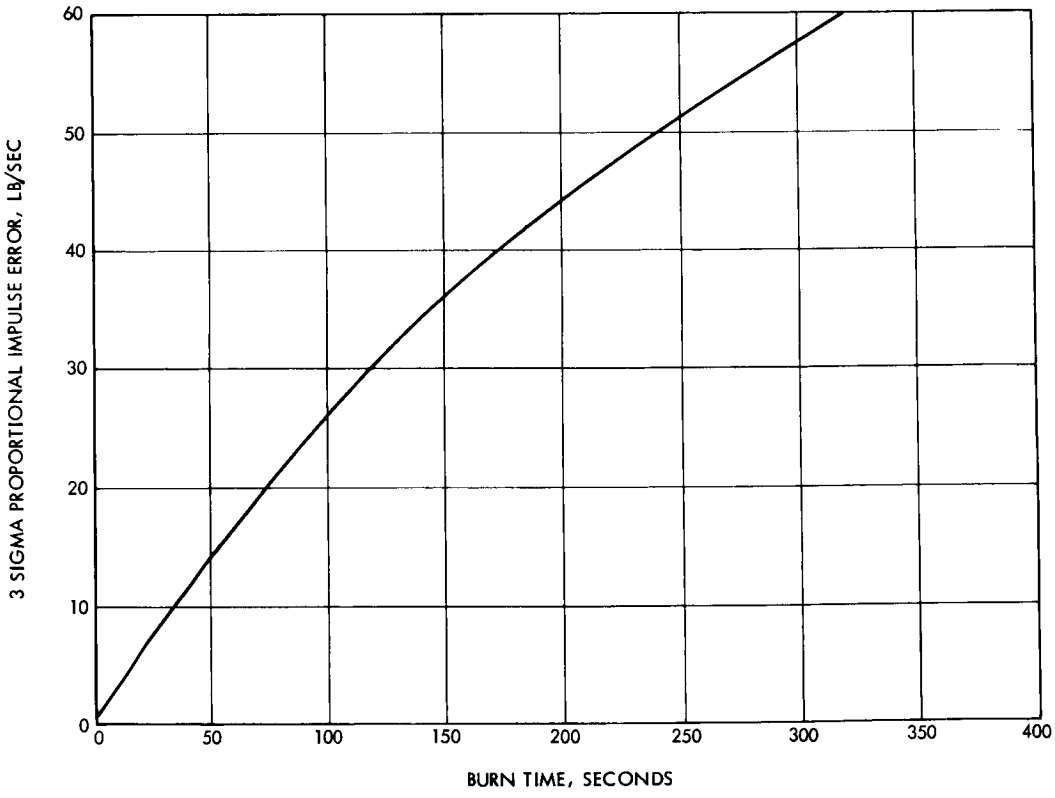

Figure H-5. Proportional Impulse Error (3σ) Versus Burn Time

3.2 Nonproportional Errors

In addition to the above blowdown mode impulse errors, errors are also associated with thrust initiation and termination.

The impulse unpredictability during start involves variations in explosive valve opening time after the fire signal has been given and the timer sequence initiated. It is also affected by variations in fluid transport time since this occurs when thrust buildup commences. The timer is programmed to terminate thrust after a fixed increment of time. Any changes in starting time, therefore, affect the total impulse imparted prior to thrust termination.

Changes in propellant transport time are influenced by uncertainties in tank pressure since this affects the pressure drop available to drive the fluid and by the temperature uncertainties of the propellant since this affects the viscosity of the fluid and the resultant resistance to flow.

The variations associated with propellant ignition delay are assumed to introduce no additional errors because although the starting time is delayed, the accumulated propellant when it reacts will produce an overpressure and additional impulse which will tend to compensate for the impulse lost from the starting delay.

Variations in valve opening time are about 0.004 second. This can result in a 0.2 lb-sec uncertainty.

The transport time required for the propellant to reach the injector is about 0.017 second based on 3 inches of 1/4-inch manifolding and nominal temperature and tank pressure. Assuming a 10 percent variation in time would result in a 0.0017 second change. The total impulse variation would be 0.085 lb-sec.

The errors associated with thrust initiation are summarized in Table H-2.

The impulse errors during thrust termination are different from those associated with either thrust initiation or during the blowdown mode since they are not associated with the timer during the thrust termination sequence.

Table H-2. Thrust Initiation Errors

Error Source			3σ Impulse Error
Valve opening	0.008 sec x 25 lb thrust	=	0.2 lb-sec
Transport time	0.0034 sec x 25 lb thrust	=	0.085 lb-sec
Sum of the squares			0.0472 lb-sec
RSS			0.217 lb-sec

Since the degree of dissociation of the fuel is very nearly independent of flow rate and chamber pressure, the ratio of specific heats and molecular weight will be nearly constant. The thrust coefficient and characteristic exhaust velocity will then be functions of temperature. The specific impulse will then be proportional to the square root of the temperature only.

The impulse error is therefore wholly dependent on the uncertainties associated with the quantity of propellant flowing through the engine during the shutdown sequence. Therefore, the uncertainties to be considered are valve closing time, tank pressure (or expulsion gas temperature), and propellant temperature.

The uncertainties in propellant manifold volume will be eliminated by calibration firings prior to flight.

The propellant flow rate as a function of when the shutoff valve is closed can be obtained from Figure H-6. With a total closing time uncertainty of 0.008 second the propellant passing through the valve can be calculated. Multiplying the propellant quantity by 230 seconds of impulse gives the impulse error involved.

The error due to expulsion gas temperature uncertainty is manifested in a tank pressure uncertainty with respect to which blowdown calibration curve is being followed. The change in flow rate due to expulsion gas temperature errors obtained from Figure H-6 is 0.003 lb-sec for a $40^{\circ}F$ temperature excursion or 0.000075 lb-sec-$^{\circ}F$.

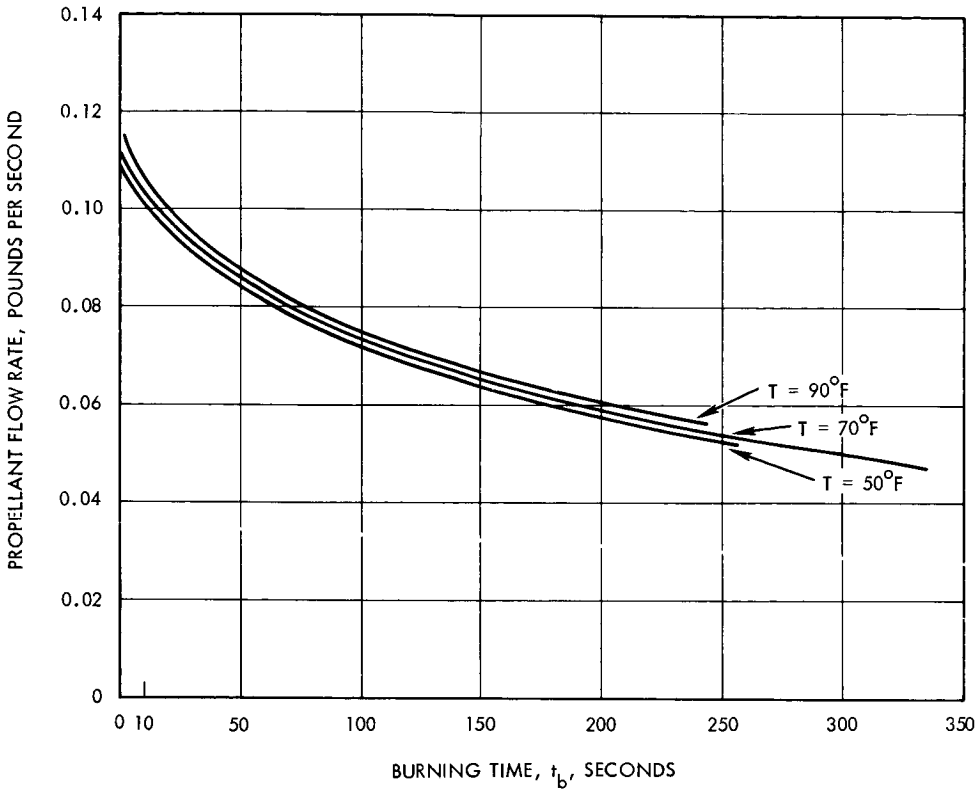

Figure H-6. Propellant Flow Rate Versus Burning Time

Assuming a total uncertainty of 5°F, as for the blowdown mode analysis, results in 0.000375 lb-sec error. This quantity multiplied by the 0.008-second valve closing uncertainty gives the error due to gas expulsion temperature change which results in the pressure change.

The propellant temperature uncertainty results in variations in specific gravity of the propellant which influences the amount of propellant flowing during the 0.008-second valve closing uncertainty. The previous quantities of propellant were computed based on the specific gravity at 70°F. The effect of propellant temperature is calculated by determining the variation of the propellant quantity as a function of specific gravity change over an approximate total 5°F excursion uncertainty.

The variation in density of hydrazine with temperature is shown in Figure H-7. In a 5°F excursion in temperature, the specific gravity varies 0.002 gm/cc.

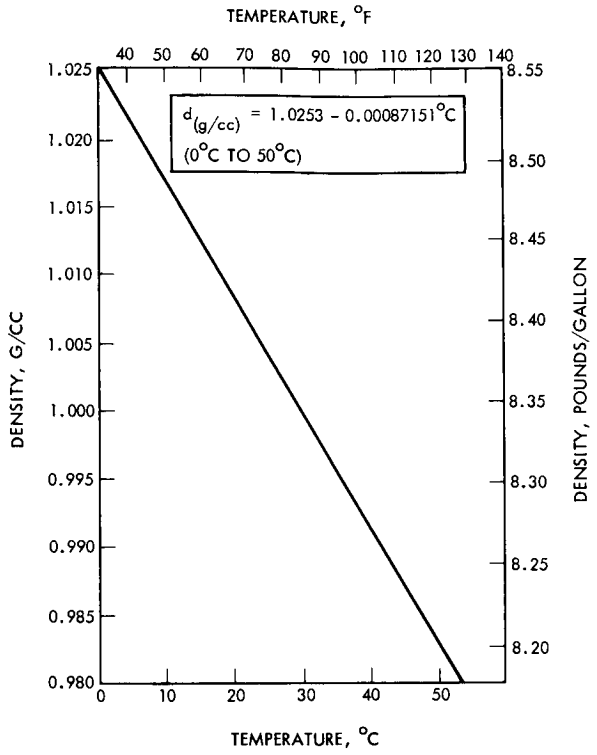

Figure H-7. Density of Hydrazine/Temperature

The results of the above thrust termination uncertainties are shown in Figure H-8.

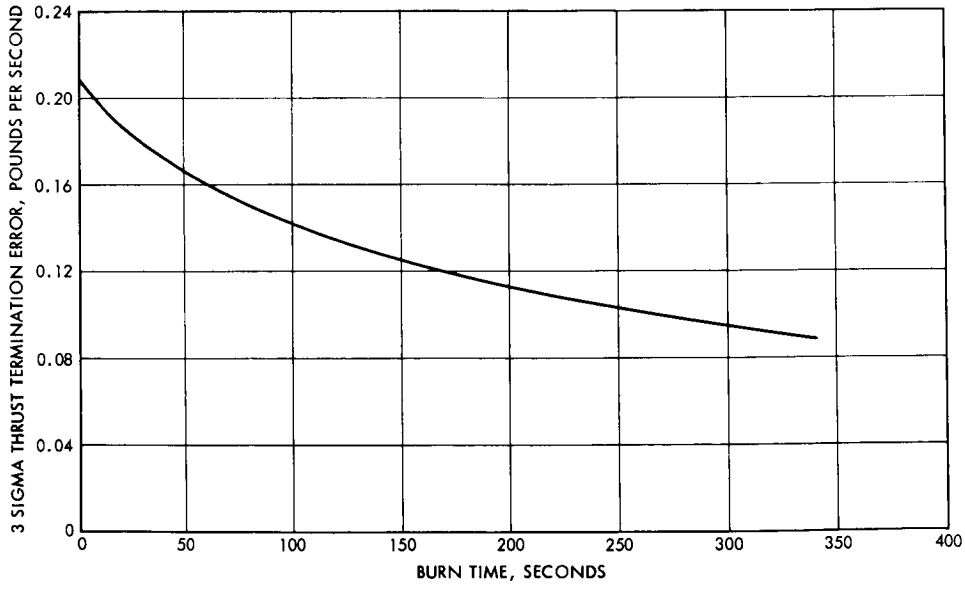

Figure H-8. Thrust Termination Error (3σ) Versus Burn Time

All errors given in Table H-2 and Figures H-5, H-8, and H-9 are summed in Figure H-10. On the basis of this data, and assuming a spacecraft weight of 492 pounds, the velocity increment error as a function of velocity increment is plotted in Figure H-11.

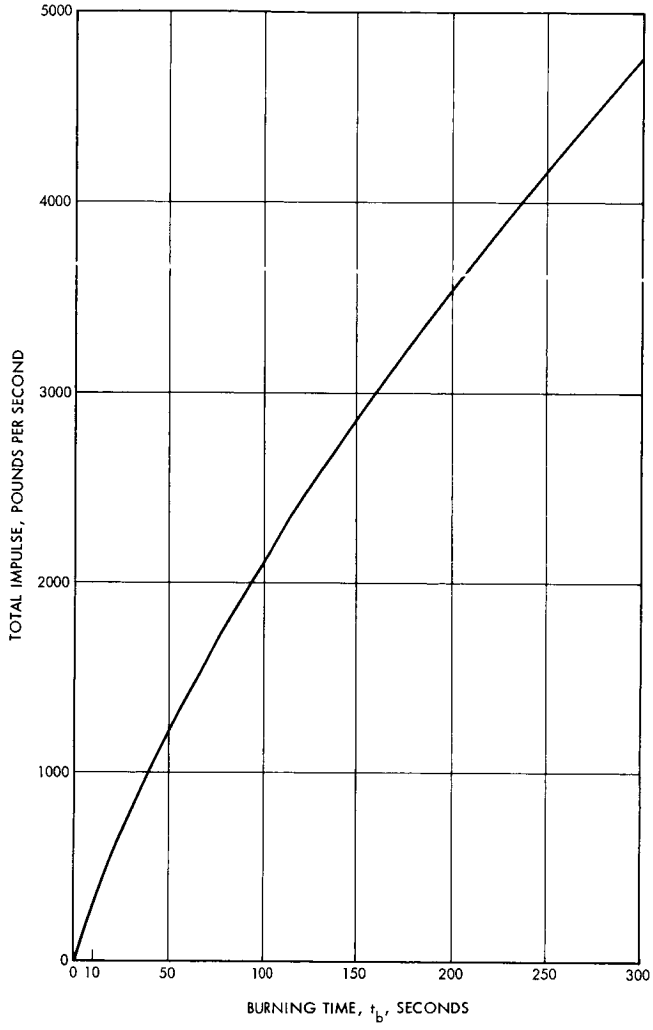

Figure H-9. Nominal Total Pulse Versus Midcourse Propulsion System Burn Time

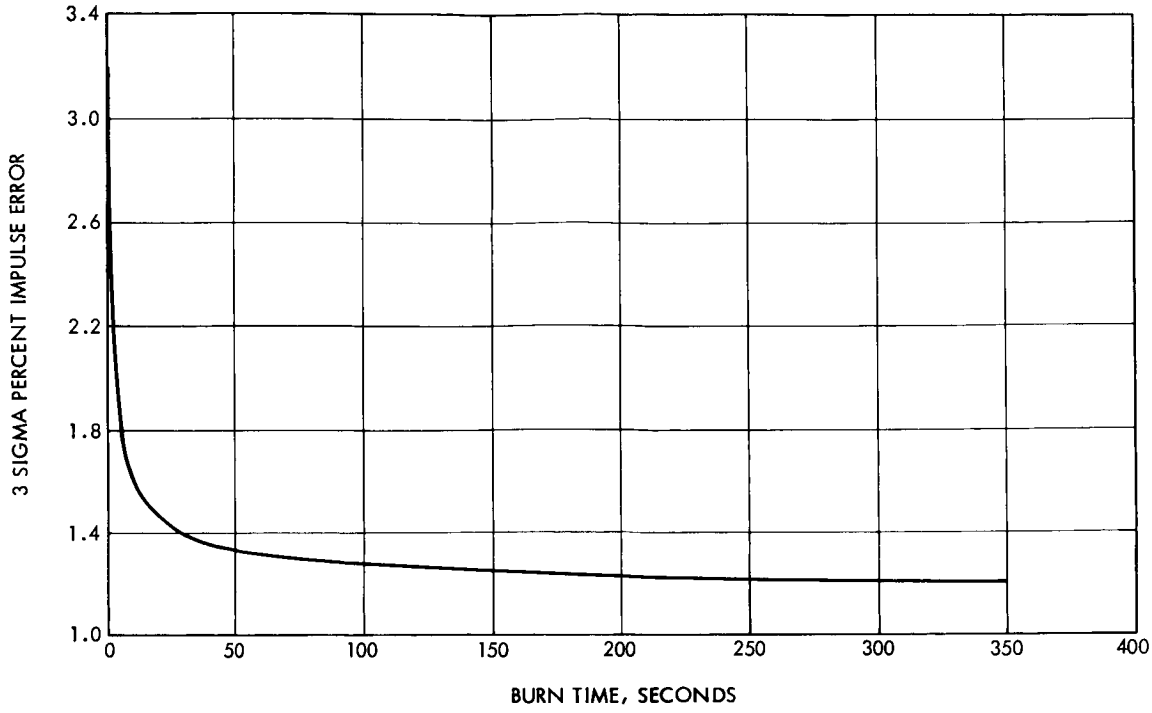

Figure H-10. Percent Impulse Error (3σ) Versus Midcourse Propulsion Burn Time

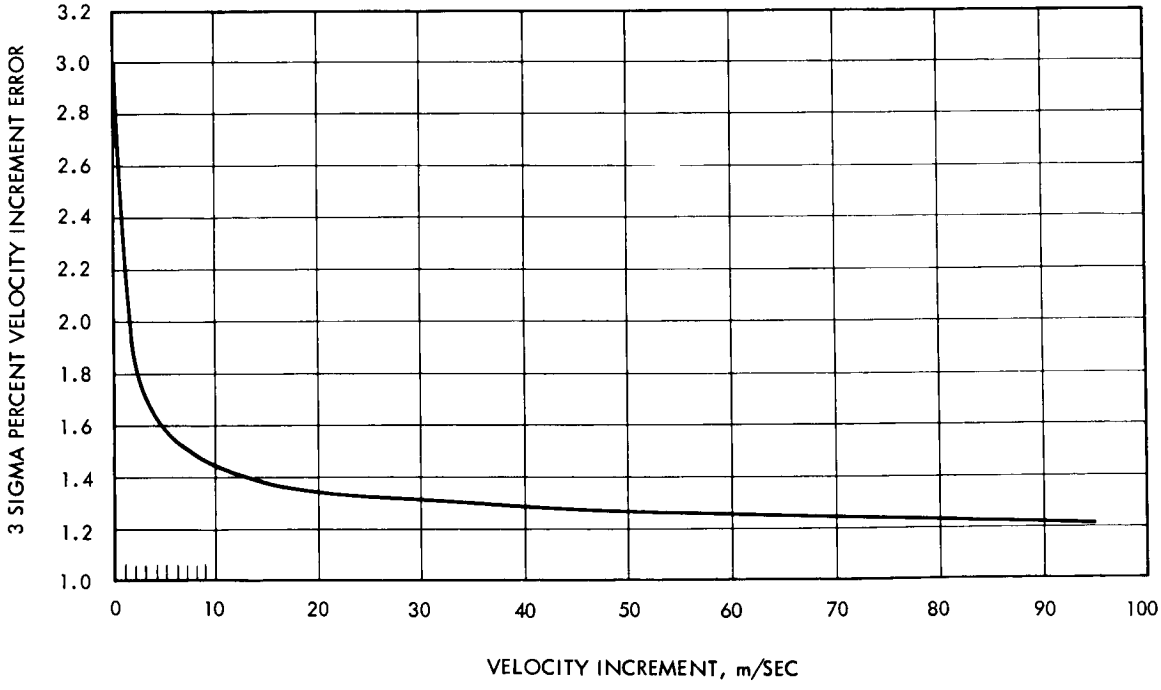

Figure H-11. Percent Velocity Increment Error (3σ) Versus Velocity Increment for 492-Pound Spacecraft

APPENDIX I

RELIABILITY PARTS COUNT ASSESSMENT COMPUTER PROGRAM

1. SCOPE

PARKA 3 is a revised and augmented version of PARKA, a Fortran IV computer program designed to permit rapid reliability assessments of rather complicated systems, in which parts are assumed to follow the exponential failure law. The basic processing block is a subsystem which consists of some configuration of units. Unit failure rate information can be fed in directly or, as is more usual in a preliminary assessment, it is derived from part count data supplied by the cognizant engineer on transmittal forms which permit direct keypunching. So called "logical equations" are supplied which permit the computer to analyze the configuration, each equation representing a portion of the reliability network with subsequent equations embodying previous ones so that ultimately the subsystem is defined. To permit greater flexibility, the starting point for the logical equations is at a level of redundancy one step higher than the units themselves, i.e., at the "basic element" level. A basic element is defined as some redundant configuration of a single unit: (a) n such in parallel, x of which must work; (b) n such in standby redundancy where the standby units may have a nonzero failure rate when "off" but where the switch is ideal. Of course a single unit is included in the above as a special case. Associated with each basic element is a set of L-factors which are analogous to K-factors but pertain only to the specific basic element rather than the system as a whole. These are useful in accounting for units that are "on" for some but not all mission phases and for units that are required for mission success only during certain mission phases. The program multiplies the unit failure rate by the L-factor for a given mission phase before calculating the element reliability for that phase.

The parts within a unit are considered, usually, to be in a series reliability configuration. Indeed this must be the case for units that are subsequently made standby redundant since the algorithm used assumes

an exponential failure law for the unit. Provision is made, however, for calculating a conservative bound to the reliability of a completely redundant unit, i. e., one in which no single part failure causes unit failure. Of course, such units should not be made standby redundant since improper calculation will result.

Up to seven mission phases can be specified and the output for each element consists of a vector of cumulative reliabilities through the indicated phases. If the individual phase is desired (i. e., the conditional probability of surviving the phase given that it is operating at the start), this is obtained by a simple division. These reliability vectors are assembled into a matrix with rows corresponding to the defined elements. An element is defined if it is specified as a basic element or is defined by a logical equation. In general, the input formats are quite liberal; numbers need only occupy their respective fields and need not be justified; blank columns are ignored.

2. USING THE PROGRAM

2. 1 Step 1

Prior to any particular application, a deck of standard generic part failure rates is assembled. A card is prepared for each part type listed on the parts count input form consisting of the part item number, a short alphabetic description, failure rate source, four failure rates corresponding to digital and analog use for both standard and high reliability application, and the number of connections per part. The cards must be ordered to correspond to the parts count form, on which the parts are ordered left to right on each line and continue on succeeding lines (68 parts in all). For programs using special parts not enumerated on the form, additional cards are used to augment the failure rate deck. The special parts are assigned unique consecutive numbers starting with 69 and not exceeding 150 and a corresponding card is added to the failure rate deck. These newly defined numbers are then used to complete the parts count form in the spaces provided. The failure rate deck must end with a blank card.

2.2 Step 2

The parts count form is filled out by the cognizant engineers, one form per unit. Upon receipt of the forms, the reliability analyst edits them and assigns unique consecutive numbers to the units within each subsystem and enters these numbers at the top of the form which will then be punched in columns 2 and 3 of each component cards to identify the unit. Columns 73 to 80 of each card are punched with the information entered in the block at the top right of the form which should contain some sort of subsystem identification. A list of all the unique special parts appearing on the forms is prepared and part type numbers assigned as in Step 1. The forms are then completed by writing the corresponding part type numbers in the shaded blocks preceding the indicated counts for these special parts.

2.3 Step 3

For each unit a unit description card is prepared listing unit number, analog or digital indicator, part level redundancy indicator, short title, and, if unit failure rate is fed directly, $\sum \lambda_i$, $\sum \lambda_i^2$, $\sum \lambda_i^3$, where λ_i are the part failure rates (bits). $\sum \lambda_i^2$ and $\sum \lambda_i^3$ are not needed if the unit is not part level redundant. For units which are part level redundant, these quantities improve the accuracy of the computation but are not essential. When calculating unit failure rates from parts count data, the program also computes $\sum \lambda_i^2$, $\sum \lambda_i^3$ which can then be used directly in subsequent runs.

Steps 2 and 3 constitute the bulk of the work to prepare the data for an assessment. Other input cards will be explained in their appropriate places in sequel.

3. ORGANIZATION OF THE INPUT DECK

The basic input block is a subsystem. Within a subsystem, the data cards can be in any order with the exception that logic cards (defined later) must be in logical order. Various classes of input cards, distinguished by the character in column 1, are recognized by the program. An asterisk in column 1 is used to indicate the end of a subsystem and, thus, by definition, a subsystem block is all cards between asterisk cards (except the first which is not preceded by an asterisk card.

The type of cards permitted within a subsystem block are:

Column 1	Type
C	Component count card
U	Unit descriptor
H	Subsystem header
B	Basic element specification
L	Logical equation
*	End subsystem

No others are valid and, if found, cause a skip to the next subsystem, if any. Card types "C" and "U" have been essentially defined above. "H" is a subsystem title of 71 characters and is optional. "B" and "L" types are used for redundancy calculations (explained below) and, if omitted, the program assumes a series configuration of units for the subsystem.

For a total system, the subsystem blocks are stacked one behind the other. A "$" (column 1) card is used to delimit a system and follows the asterisk card of the last subsystem.

The first four cards of a system set carry no special type character in column 1 and are assumed to be present; thus, none can be omitted. They are:

(a) System Control Card. Selects high-reliability or standard option, selects connection failure rate option, selects boost survivability option, selects "GØBAD" option (defined below).

(b) System Title. (A blank card may be substituted)

(c) Mission phase time increments

(d) K-factors for mission phases

(c) and (d) may be blank in which case no time analysis is made and only failure rates are computed. K-factors are assumed 1.0 unless otherwise specified.

As many systems as desired can be processed sequentially, each ending with a "$" card. The entire stack is preceded by the failure rate deck of Step 1, Section 2 which applies to all succeeding systems.

The last system is followed by an "X" (column 1) card which causes exit off the computer.

One further option is available. If a "Y" (column 1) card is substituted for the "X" card, then instead of exiting, the computer reads a new failure rate table as in the very beginning and another set of systems is analyzed starting all over. Ultimately an "X" card must be present.

4. REDUNDANCY FEATURE

If redundancies are present among the units of a subsystem, these are described by the two card types "B" and "L" which are, respectively, the basic element specification and logical equation cards.

A basic element is considered to be either a binomial combination of a single unit, i.e., a parallel network of n identical units of which X are required for success, or else n identical units in standby redundancy with perfect switching, and where the standby units may have a nonzero failure rate when "off".

The logical equations permit the construction of parallel-series configurations of basic elements and/or elements previously defined by a logical equation. A logical equation is best described by an example:

$$20 = 1*2*3+4*5+6*7+6*7$$

In the above example, 1, 2, 3, 4, 5, 6, and 7 are basic elements or previously defined elements. The new element, 20, is defined to be 1 "and" 2 "and" 3, "or" 4 "and" 5, "or" 6 "and" 7, "or" 6 "and" 7 where the * is interpreted as "and" and the + as "or". Thus 20 represents the network.

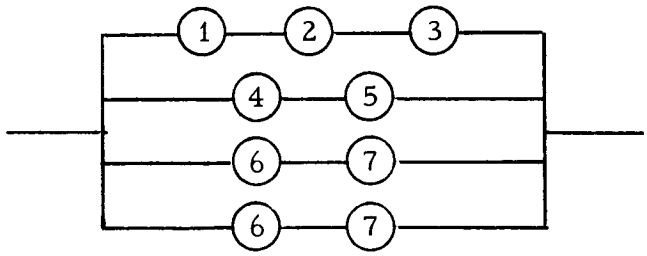

A following equation may now use "20" as previously defined, e.g., 21 = 20*7, which now adds element 7 as an "in line" element to the above network.

No parentheses are allowed and, hence, the most complicated network which can be described in one equation is a parallel network, each branch of which contains series elements. Since defined elements can be used in subsequent equations, this is no essential restriction.

A presently constituted, the logical equations can only be one card long.

The above example of a logical equation (or more properly, a network equation) was purposely kept simple in that the operands are given as single numbers. In actuality, the computer interprets each operand as a possible 9-digit number of the form $\underbrace{XXX}_{N_1}\ \underbrace{YYY}_{N_2}\ \underbrace{ZZZ}_{N_3}$ indicating and "N_1 out of N_2" redundancy of element N_3. This notation permits an entire group of units (defined as N_3) to be made repetitively redundant. Leading zeros need not be present. $N_2 = 0$ is interpreted as $N_2 = 1$ and N_1 is ignored. Thus, N_3 alone (as in the above example) is read as "1 out of 1" of N_3, i.e., the single element, N_3. If $N_2 \neq 0$ then care must be exercised to insure that N_1 is properly indicated. When $N_2 \neq 0$, $N_1 = 0$ indicates simple standby redundancy which can only be a proper application when N_3 refers to an exponential device, i.e., N_3 represents a series configuration of exponential elements. $N_2 \neq 0$, $N_1 \neq 0$ is taken as the usual binomial redundancy case of "N_1 out of N_2" required. If $N_1 > N_2$, N_1 is set to N_2.

Network equations (identified by "L" in column 1) are punches in the card starting with column 3 (column 2 is left blank) and consist of the element number being defined followed by an = sign. The right side consists of operands as described above alternating with operators (+ or *). Blank spaces are ignored and may be freely used for legibility. Any character other than blank, *, +, =, or numerals will invalidate the equation. Also, the equation must be properly formed (no two operators in succession, e.g.).

As presently constituted, the program accepts up to 100 each of basic elements and logical equations.

The machinery outlined above is sufficient for most assessment problems and is quite rapid in execution. There are systems, however, whose reliability logic cannot be expressed as simple networks amenable to the methods above. Included in the program, then, is an algorithm completely different from that for the network equations described above which, unfortunately, runs considerably longer. This method is based on

the theorem for the probability of the union of events and uses a Boolean equation rather than a network equation. These Boolean equations are written in a format exactly like network equations except that now a "B" is entered in column 2. The Boolean equation now represents the event relations which yield success, e.g., in CC.1 CC.2

L B 20 = 1*2*3+4*6*2*3+1*3*5*6+4*5*6

1*2*3 represents the joint event of elements 1, 2, and 3 succeeding, etc.

The union of the four terms enumerates that subjset of the truth table corresponding to success. Of course, the operands are interpreted as single numbers rather than as triplets as for network equations. As before, the left side number represents the new element being defined. The running time to process a Boolean equation varies as 2^n where n = number of terms (number of + signs plus 1). Again, no parentheses are permitted so that the equation must be written as a sum of terms. Because of the increased running time involved, Boolean equations should not be used unnecessarily, i.e., when network type equations will do.

Although logic equation cards can appear anywhere in the block of cards comprising the subsystem, among themselves they must be in logical order, i.e., no equation can refer to an element on its right side which is not either a basic element or an element defined by a previous equation. Thus, the antecedents of an equation must be physically ahead of the equation in the subsystem block (except that basic elements can be anywhere).

5. RESULTS

Following is the printout produced by the PARKA 3 program for the Advanced Planetary Probe. In this printout the following abbreviations are used:

CONNEC . . . . . Connections
CS . . . . . Contact sets
DIP . . . . . Dipped
GT . . . . . Greater than
HIV . . . . . High voltage
LOV . . . . . Low voltage

LT . . . . . Lower than
MEM. CR. . . . . Memory core
MU. LR. BD. . . . . Multilayer board
RELY. . . . . Relay
RELY, L . . . . . Latching relay
SI . . . . . Silicon
SLD . . . . . Solid
SW . . . . . Switching
TERM . . . . . Terminals
TRF . . . . . Transformer
VAR . . . . . Variable
VARAC . . . . . Varactor
WNDGS . . . . . Windings

RELIABILITY ASSESSMENT FOR...
ADVANCED PLANETARY PROBE (PARTS COUNT RELIABILITY ASSESSMENT) (HIREL)

MISSION PROFILE...

PHASE NO.	PHASE Δ TIME (HRS.)	CUMULATIVE TIME (DAYS)	K-FACTOR
1	480.00	20	1.00
2	720.00	50	1.00
3	12720.00	580	1.00
4	4080.00	750	1.00
5	8400.00	1100	1.00
6	12000.00	1600	1.00

COMPONENT PART FAILURE RATES(FAILURES/BILLION HRS.)....

NO.	DESCRIPTION	FAILURE RATE ANALOG	FAILURE RATE DIGITAL	CONNEC/PART
1	RES,CARBCOMP	3	1	2.0
2	RES,MET.FILM	3	3	2.0
3	RES,CARBFILM	17	17	2.0
4	RES,WIRE,ACC	27	27	2.0
5	RES,WIRE,PWR	33	33	2.0
6	RES,VAR,WIRE	40	40	3.0
7	RES,VAR,CCOM	27	27	3.0
8	DIO,SI,GENRL	5	2	2.0
9	DIO,SI,RECT.	5	5	2.0
10	DIO,SI,ZENER	13	13	2.0
11	DIO,SI,SWITC	2	2	2.0
12	DIO,SI,TUNNL	140	140	2.0
13	DIO,SI,VARAC	17	17	2.0
14	DIO,SI,MWMIX	400	400	2.0
15	DIO,SI,MWDET	3233	3233	2.0
16	DIO,GERMANIU	33	33	2.0
17	SCR	17	17	3.0
18	CAP,FIX.CER.	5	5	2.0
19	CAP,CER.FDTH	12	12	2.0
20	CAP,FIX,GLAS	1	1	2.0
21	CAP,MICA DIP	2	2	2.0
22	CAP,MICABUTT	17	17	2.0

23	CAP,FIXPAPER	13	13	2.0
24	CAP,FIXPLAST	13	13	2.0
25	CAP,PAP-PLAS	10	10	2.0
26	CAP,TANTFOIL	13	13	2.0
27	CAP,TANT.SLD	7	7	2.0
28	CAP,TANT.WET	50	50	2.0
29	CAP,VAR.CER.	17	17	3.0
30	CAP,VAR.AIR.	33	33	3.0
31	CAP,VARGLASS	7	7	3.0
32	CONN,COAX	7	7	0.
33	CONN,GEN/PIN	3	3	0.
34	CON,MU.LR.BD	33	33	0.
35	XIST,SI,LT1W	17	7	3.0
36	XIST,SI,GT1W	43	43	3.0
37	XIST,SI,SWIT	7	7	3.0
38	MOS FET	100	100	3.0
39	XIST,SI,MISC	17	17	3.0
40	XIST,GERMANM	100	100	3.0
41	TRF,LF,4TERM	33	33	4.0
42	TRF,RF,4TERM	33	33	4.0
43	TRF,LT100V4T	30	30	4.0
44	TRF,GT100V5T	100	100	5.0
45	TRF,LT100V6T	40	40	6.0
46	TRF,GT100V4T	83	83	4.0
47	MAGAMP2WNDGS	50	50	4.0
48	MAGAMP3WNDGS	50	50	6.0
49	THERMISTOR	50	50	2.0
50	CRYSTAL QTZ	25	25	2.0
51	MEM.CR/HUND.	1	1	0.
52	RELY.GEN.2CS	160	160	6.0
53	RELY.GEN.4CS	187	187	10.0
54	RLY,LG,2CS1W	160	160	6.0
55	RLY,LG,2CS2W	227	227	8.0
56	RLY,SEN,2CS	227	227	6.0
57	COAXSWITCH2W	227	227	6.0
58	COILFILT,LOV	10	10	2.0
59	COILFILT,HIV	83	83	2.0
60	COIL,HI.FREQ	17	17	2.0
61	COIL,ANALOG	4	4	2.0
62	IC,DIG.STOR	22	22	10.0
63	IC,DIG.GATES	16	16	10.0
64	IC,DIG.ISOL	15	15	10.0

65	IC,DIG.ANALG	80	80	10.0
66	DIPLEXER	83	83	6.0
67	ANTENNA,OMNI	17	17	2.0
68	ANTENNA,1GIM	7066	7066	2.0
69	MECHANICALS	10	100	0.
70	FUSE	100	100	-0.
71	SOLAR CELL	20	-0	13.0

ADVANCED PLANETARY PROBE (PARTS COUNT RELIABILITY ASSESSMENT)
SUBSYSTEM 1 DATA HANDLING SUBSYSTEM
UNIT 1 CLOCK (ANALOG)

	COMPONENT PART	QTY	FAILURE RATE	EXTENSION
2	RES,MET.FILM	9	3	27
11	DIO,SI,SWITC	2	2	4
18	CAP,FIX.CER.	2	5	10
21	CAP,MICA DIP	1	2	2
27	CAP,TANT.SLD	4	7	28
35	XIST,SI,LT1W	2	17	34
50	CRYSTAL QTZ	1	25	25
62	IC,DIG.STOR	4	22	88
63	IC,DIG.GATES	4	16	64
64	IC,DIG.ISOL	4	15	60
	TOTAL	33		342
	CONNECTIONS	164	0.500	82
	TOTAL			424

ADVANCED PLANETARY PROBE (PARTS COUNT RELIABILITY ASSESSMENT)
SUBSYSTEM 1 DATA HANDLING SUBSYSTEM
UNIT 2 PROGRAMMER (DIGTAL)

	COMPONENT PART	QTY	FAILURE RATE	EXTENSION
2	RES,MET.FILM	115	3	345
10	DIO,SI,ZENER	1	13	13
11	DIO,SI,SWITC	98	2	196
17	SCR	4	17	68
21	CAP,MICA DIP	48	2	96
27	CAP,TANT.SLD	11	7	77
37	XIST,SI,SWIT	36	7	252
45	TRF,LT100V6T	32	40	1280
62	IC,DIG.STOR	24	22	528
63	IC,DIG.GATES	74	16	1184
64	IC,DIG.ISOL	35	15	525
	TOTAL	478		4564
	CONNECTIONS	2188	0.500	1094
	TOTAL			5658

ADVANCED PLANETARY PROBE (PARTS COUNT RELIABILITY ASSESSMENT)
SUBSYSTEM 1 DATA HANDLING SUBSYSTEM
UNIT 3 PN GENERATOR (DIGTAL)

COMPONENT PART	QTY	FAILURE RATE	EXTENSION
62 IC,DIG.STOR	6	22	132
63 IC,DIG.GATES	6	16	96
64 IC,DIG.ISOL	1	15	15
TOTAL	13		243
CONNECTIONS	130	0.500	65
TOTAL			308

ADVANCED PLANETARY PROBE (PARTS COUNT RELIABILITY ASSESSMENT)
SUBSYSTEM 1 DATA HANDLING SUBSYSTEM
UNIT 4 ANALOG GATES (DIGTAL)

COMPONENT PART	QTY	FAILURE RATE	EXTENSION
2 RES,MET.FILM	240	3	720
11 DIO,SI,SWITC	430	2	860
27 CAP,TANT.SLD	5	7	35
37 XIST,SI,SWIT	34	7	238
62 IC,DIG.STOR	60	22	1320
63 IC,DIG.GATES	80	16	1280
64 IC,DIG.ISOL	5	15	75
TOTAL	854		4528
CONNECTIONS	2902	0.500	1451
TOTAL			5979

ADVANCED PLANETARY PROBE (PARTS COUNT RELIABILITY ASSESSMENT)
SUBSYSTEM 1 DATA HANDLING SUBSYSTEM
UNIT 5 A/D CONVERTER (DATA) (DIGTAL)

	COMPONENT PART	QTY	FAILURE RATE	EXTENSION
1	RES,CARBCOMP	60	1	60
2	RES,MET.FILM	130	3	390
4	RES,WIRE,ACC	30	27	810
10	DIO,SI,ZENER	3	13	39
11	DIO,SI,SWITC	13	2	26
18	CAP,FIX.CER.	10	5	50
27	CAP,TANT.SLD	22	7	154
33	CONN,GEN/PIN	12	3	36
35	XIST,SI,LT1W	20	7	140
37	XIST,SI,SWIT	30	7	210
62	IC,DIG.STOR	17	22	374
63	IC,DIG.GATES	60	16	960
64	IC,DIG.ISOL	60	15	900
	TOTAL	467		4149
	CONNECTIONS	2056	0.500	1028
	TOTAL			5177

ADVANCED PLANETARY PROBE (PARTS COUNT RELIABILITY ASSESSMENT)
SUBSYSTEM 1 DATA HANDLING SUBSYSTEM
UNIT 6 DIGITAL GATES (DIGTAL)

	COMPONENT PART	QTY	FAILURE RATE	EXTENSION
2	RES,MET.FILM	55	3	165
11	DIO,SI,SWITC	90	2	180
26	CAP,TANTFOIL	3	13	39
37	XIST,SI,SWIT	8	7	56
62	IC,DIG.STOR	16	22	352
63	IC,DIG.GATES	32	16	512
	TOTAL	204		1304
	CONNECTIONS	800	0.500	400
	TOTAL			1704

ADVANCED PLANETARY PROBE (PARTS COUNT RELIABILITY ASSESSMENT)
SUBSYSTEM 1 DATA HANDLING SUBSYSTEM
UNIT 7 A/D CONVERTER (TV) (DIGTAL)

	COMPONENT PART	QTY	FAILURE RATE	EXTENSION
1	RES,CARBCOMP	60	1	60
2	RES,MET.FILM	130	3	390
4	RES,WIRE,ACC	30	27	810
10	DIO,SI,ZENER	3	13	39
11	DIO,SI,SWITC	13	2	26
18	CAP,FIX.CER.	10	5	50
27	CAP,TANT.SLD	22	7	154
33	CONN,GEN/PIN	12	3	36
35	XIST,SI,LT1W	20	7	140
37	XIST,SI,SWIT	30	7	210
62	IC,DIG.STOR	17	22	374
63	IC,DIG.GATES	60	16	960
64	IC,DIG.ISOL	60	15	900
	TOTAL	467		4149
	CONNECTIONS	2056	0.500	1028
	TOTAL			5177

ADVANCED PLANETARY PROBE (PARTS COUNT RELIABILITY ASSESSMENT)
SUBSYSTEM 1 DATA HANDLING SUBSYSTEM
UNIT 8 TV CORE BUFFER (DIGTAL)

	COMPONENT PART	QTY	FAILURE RATE	EXTENSION
1	RES,CARBCOMP	50	1	50
2	RES,MET.FILM	130	3	390
4	RES,WIRE,ACC	10	27	270
5	RES,WIRE,PWR	10	33	330
10	DIO,SI,ZENER	38	13	494
11	DIO,SI,SWITC	154	2	308
21	CAP,MICA DIP	7	2	14
27	CAP,TANT.SLD	10	7	70
33	CONN,GEN/PIN	10	3	30
37	XIST,SI,SWIT	60	7	420
45	TRF,LT100V6T	60	40	2400
51	MEM.CR/HUND.	31	1	31
62	IC,DIG.STOR	24	22	528
63	IC,DIG.GATES	22	16	352
64	IC,DIG.ISOL	6	15	90
65	IC,DIG.ANALG	6	80	480
	TOTAL	628		6257
	CONNECTIONS	1938	C.500	969
	TOTAL			7226

ADVANCED PLANETARY PROBE (PARTS COUNT RELIABILITY ASSESSMENT)
SUBSYSTEM 1 DATA HANDLING SUBSYSTEM
UNIT 9 COMBINER (DIGTAL)

	COMPONENT PART	QTY	FAILURE RATE	EXTENSION
2	RES,MET.FILM	15	3	45
11	DIO,SI,SWITC	12	2	24
21	CAP,MICA DIP	3	2	6
27	CAP,TANT.SLD	3	7	21
37	XIST,SI,SWIT	3	7	21
45	TRF,LT100V6T	3	40	120
62	IC,DIG.STOR	4	22	88
63	IC,DIG.GATES	78	16	1248
64	IC,DIG.ISOL	10	15	150
	TOTAL	131		1723
	CONNECTIONS	1013	0.500	506
	TOTAL			2229

ADVANCED PLANETARY PROBE (PARTS COUNT RELIABILITY ASSESSMENT)
SUBSYSTEM 1 DATA HANDLING SUBSYSTEM
UNIT 10 TAPE DECK (DIGTAL)

	COMPONENT PART	QTY	FAILURE RATE	EXTENSION
2	RES,MET.FILM	285	3	855
8	DIO,SI,GENRL	16	2	32
11	DIO,SI,SWITC	16	2	32
18	CAP,FIX.CER.	32	5	160
21	CAP,MICA DIP	43	2	86
27	CAP,TANT.SLD	22	7	154
33	CONN,GEN/PIN	8	3	24
37	XIST,SI,SWIT	66	7	462
39	XIST,SI,MISC	66	17	1122
43	TRF,LT100V4T	4	30	120
52	RELY.GEN.2CS	1	160	160
58	COILFILT,LOV	2	10	20
63	IC,DIG.GATES	1	16	16
69	MECHANICALS	24	100	2400
	TOTAL	586		5643
	CONNECTIONS	1260	0.500	630
	TOTAL			6273

ADVANCED PLANETARY PROBE (PARTS COUNT RELIABILITY ASSESSMENT)
SUBSYSTEM 1 DATA HANDLING SUBSYSTEM
UNIT 11 PARITY LOGIC (DIGTAL)

	COMPONENT PART	QTY	FAILURE RATE	EXTENSION
2	RES,MET.FILM	3	3	9
27	CAP,TANT.SLD	1	7	7
62	IC,DIG.STOR	3	22	66
63	IC,DIG.GATES	10	16	160
64	IC,DIG.ISOL	4	15	60
	TOTAL	21		302
	CONNECTIONS	178	0.500	89
	TOTAL			391

ADVANCED PLANETARY PROBE (PARTS COUNT RELIABILITY ASSESSMENT)
SUBSYSTEM 1 DATA HANDLING SUBSYSTEM
UNIT 12 MEMORY CONTROL (DIGTAL)

	COMPONENT PART	QTY	FAILURE RATE	EXTENSION
2	RES,MET.FILM	4	3	12
11	DIO,SI,SWITC	4	2	8
21	CAP,MICA DIP	2	2	4
37	XIST,SI,SWIT	1	7	7
45	TRF,LT100V6T	1	40	40
62	IC,DIG.STOR	3	22	66
63	IC,DIG.GATES	15	16	240
64	IC,DIG.ISOL	1	15	15
	TOTAL	31		392
	CONNECTIONS	219	0.500	109
	TOTAL			501

ADVANCED PLANETARY PROBE (PARTS COUNT RELIABILITY ASSESSMENT)
SUBSYSTEM 1 DATA HANDLING SUBSYSTEM
UNIT 13 CONTROL LOGIC (DIGTAL)

	COMPONENT PART	QTY	FAILURE RATE	EXTENSION
2	RES,MET.FILM	71	3	213
11	DIO,SI,SWITC	56	2	112
17	SCR	1	17	17
21	CAP,MICA DIP	26	2	52
27	CAP,TANT.SLD	15	7	105
37	XIST,SI,SWIT	22	7	154
45	TRF,LT100V6T	20	40	800
62	IC,DIG.STOR	40	22	880
63	IC,DIG.GATES	190	16	3040
64	IC,DIG.ISOL	60	15	900
	TOTAL	501		6273
	CONNECTIONS	3425	0.500	1712
	TOTAL			7985

ADVANCED PLANETARY PROBE (PARTS COUNT RELIABILITY ASSESSMENT)
SUBSYSTEM 1 DATA HANDLING SUBSYSTEM
UNIT 14 BI-PHASE MODULATOR (DIGTAL)

COMPONENT PART	QTY	FAILURE RATE	EXTENSION
62 IC,DIG.STOR	2	22	44
63 IC,DIG.GATES	5	16	80
64 IC,DIG.ISOL	1	15	15
TOTAL	8		139
CONNECTIONS	80	0.500	40
TOTAL			179

ADVANCED PLANETARY PROBE (PARTS COUNT RELIABILITY ASSESSMENT)
SUBSYSTEM 1 DATA HANDLING SUBSYSTEM
UNIT 15 CLOCK (ANALOG)

COMPONENT PART	QTY	FAILURE RATE	EXTENSION

UNIT INPUTED AS ENTITY...SEE UNIT SUMMARY.

ADVANCED PLANETARY PROBE (PARTS COUNT RELIABILITY ASSESSMENT)
SUBSYSTEM 1 DATA HANDLING SUBSYSTEM
UNIT 16 PROGRAMMER (DIGTAL)

COMPONENT PART	QTY	FAILURE RATE	EXTENSION

UNIT INPUTED AS ENTITY...SEE UNIT SUMMARY.

ADVANCED PLANETARY PROBE (PARTS COUNT RELIABILITY ASSESSMENT)
SUBSYSTEM 1 DATA HANDLING SUBSYSTEM
UNIT 17 PN GENERATOR (DIGTAL)

COMPONENT PART	QTY	FAILURE RATE	EXTENSION

UNIT INPUTED AS ENTITY...SEE UNIT SUMMARY.

ADVANCED PLANETARY PROBE (PARTS COUNT RELIABILITY ASSESSMENT)
SUBSYSTEM 1 DATA HANDLING SUBSYSTEM
UNIT 18 ANALOG GATES (DIGTAL)

COMPONENT PART	QTY	FAILURE RATE	EXTENSION

UNIT INPUTED AS ENTITY...SEE UNIT SUMMARY.

ADVANCED PLANETARY PROBE (PARTS COUNT RELIABILITY ASSESSMENT)
SUBSYSTEM 1 DATA HANDLING SUBSYSTEM
UNIT 19 A/D CONVERTER (DATA) (DIGTAL)

COMPONENT PART	QTY	FAILURE RATE	EXTENSION

UNIT INPUTED AS ENTITY...SEE UNIT SUMMARY.

ADVANCED PLANETARY PROBE (PARTS COUNT RELIABILITY ASSESSMENT)
SUBSYSTEM 1 DATA HANDLING SUBSYSTEM
UNIT 20 DIGITAL GATES (DIGTAL)

COMPONENT PART	QTY	FAILURE RATE	EXTENSION

UNIT INPUTED AS ENTITY...SEE UNIT SUMMARY.

ADVANCED PLANETARY PROBE (PARTS COUNT RELIABILITY ASSESSMENT)
SUBSYSTEM 1 DATA HANDLING SUBSYSTEM
UNIT 21 A/D CONVERTER (TV) (DIGTAL)

COMPONENT PART	QTY	FAILURE RATE	EXTENSION

UNIT INPUTED AS ENTITY...SEE UNIT SUMMARY.

ADVANCED PLANETARY PROBE (PARTS COUNT RELIABILITY ASSESSMENT)
SUBSYSTEM 1 DATA HANDLING SUBSYSTEM
UNIT 22 TV CORE BUFFER (DIGTAL)

COMPONENT PART	QTY	FAILURE RATE	EXTENSION

UNIT INPUTED AS ENTITY...SEE UNIT SUMMARY.

ADVANCED PLANETARY PROBE (PARTS COUNT RELIABILITY ASSESSMENT)
SUBSYSTEM 1 DATA HANDLING SUBSYSTEM
UNIT 23 COMBINER (DIGTAL)

COMPONENT PART	QTY	FAILURE RATE	EXTENSION

UNIT INPUTED AS ENTITY...SEE UNIT SUMMARY.

ADVANCED PLANETARY PROBE (PARTS COUNT RELIABILITY ASSESSMENT)
SUBSYSTEM 1 DATA HANDLING SUBSYSTEM
UNIT 24 TAPE DECK (DIGTAL)

COMPONENT PART	QTY	FAILURE RATE	EXTENSION

UNIT INPUTED AS ENTITY...SEE UNIT SUMMARY.

ADVANCED PLANETARY PROBE (PARTS COUNT RELIABILITY ASSESSMENT)
SUBSYSTEM 1 DATA HANDLING SUBSYSTEM
UNIT 25 PARITY LOGIC (DIGTAL)

COMPONENT PART	QTY	FAILURE RATE	EXTENSION

UNIT INPUTED AS ENTITY...SEE UNIT SUMMARY.

ADVANCED PLANETARY PROBE (PARTS COUNT RELIABILITY ASSESSMENT)
SUBSYSTEM 1 DATA HANDLING SUBSYSTEM
UNIT 26 MEMORY CONTROL (DIGTAL)

COMPONENT PART	QTY	FAILURE RATE	EXTENSION

UNIT INPUTED AS ENTITY...SEE UNIT SUMMARY.

ADVANCED PLANETARY PROBE (PARTS COUNT RELIABILITY ASSESSMENT)
SUBSYSTEM 1 DATA HANDLING SUBSYSTEM
UNIT 27 CONTROL LOGIC (DIGTAL)

COMPONENT PART	QTY	FAILURE RATE	EXTENSION

UNIT INPUTED AS ENTITY...SEE UNIT SUMMARY.

ADVANCED PLANETARY PROBE (PARTS COUNT RELIABILITY ASSESSMENT)
SUBSYSTEM 1 DATA HANDLING SUBSYSTEM
UNIT 28 BI-PHASE MODULATOR (DIGTAL)

COMPONENT PART	QTY	FAILURE RATE	EXTENSION

UNIT INPUTED AS ENTITY...SEE UNIT SUMMARY.

ADVANCED PLANETARY PROBE (PARTS COUNT RELIABILITY ASSESSMENT)
SUBSYSTEM 1 DATA HANDLING SUBSYSTEM
NO. OF COMPONENT PARTS= 4422 SUBSYSTEM FR= 49211

UNIT SUMMARY.....

NO	DESCRIPTION	PART USAGE	FAILURE RATE	SUM FR SQUARED	SUM FR CUBED	
1	CLOCK	ANALOG	424	0.54020E-14	0.99816E-22	
2	PROGRAMMER	DIGTAL	5658	0.94882E-13	0.27670E-20	
3	PN GENERATOR	DIGTAL	308	0.46650E-14	0.91839E-22	
4	ANALOG GATES	DIGTAL	5979	0.56436E-13	0.10067E-20	
5	A/D CONVERTER (DATA)	DIGTAL	5177	0.64633E-13	0.12563E-20	
6	DIGITAL GATES	DIGTAL	1704	0.17690E-13	0.31298E-21	
7	A/D CONVERTER (TV)	DIGTAL	5177	0.64633E-13	0.12563E-20	
8	TV CORE BUFFER	DIGTAL	7226	0.18301E-12	0.79468E-20	
9	COMBINER	DIGTAL	2229	0.29443E-13	0.59041E-21	
10	TAPE DECK	DIGTAL	6273	0.29678E-12	0.28577E-19	
11	PARITY LOGIC	DIGTAL	391	0.49880E-14	0.86828E-22	
12	MEMORY CONTROL	DIGTAL	501	0.72260E-14	0.16126E-21	
13	CONTROL LOGIC	DIGTAL	7985	0.11657E-12	0.27068E-20	
14	BI-PHASE MODULATOR	DIGTAL	179	0.24730E-14	0.45151E-22	
15	CLOCK	ANALOG	424	0.	0.	(PLRD)
16	PROGRAMMER	DIGTAL	5658	0.	0.	(PLRD)
17	PN GENERATOR	DIGTAL	308	0.	0.	(PLRD)
18	ANALOG GATES	DIGTAL	5979	0.	0.	(PLRD)
19	A/D CONVERTER (DATA)	DIGTAL	5177	0.	0.	(PLRD)
20	DIGITAL GATES	DIGTAL	1704	0.	0.	(PLRD)
21	A/D CONVERTER (TV)	DIGTAL	5177	0.	0.	(PLRD)
22	TV CORE BUFFER	DIGTAL	7118	0.	0.	(PLRD)
23	COMBINER	DIGTAL	2229	0.	0.	(PLRD)
24	TAPE DECK	DIGTAL	6273	0.	0.	(PLRD)
25	PARITY LOGIC	DIGTAL	391	0.	0.	(PLRD)
26	MEMORY CONTROL	DIGTAL	501	0.	0.	(PLRD)
27	CONTROL LOGIC	DIGTAL	7985	0.	0.	(PLRD)
28	BI-PHASE MODULATOR	DIGTAL	179	0.	0.	(PLRD)

MISSION RELIABILITIES....

BASIC ELEMENT SPECIFICATIONS

ELEMT NO.	REF. UNIT	REDUN. TYPE	NO. PRESENT	NO. NEEDED	OFF RATIO	PHASE L-FACTORS... 1	2	3	4	5	6
1	1	BINOM	1	1		1.000	1.000	1.000	1.000	1.000	1.000
2	2	BINOM	1	1		1.000	1.000	1.000	1.000	1.000	1.000
3	3	BINOM	1	1		1.000	1.000	1.000	1.000	1.000	1.000
4	4	BINOM	1	1		1.000	1.000	1.000	1.000	1.000	1.000
5	5	BINOM	1	1		1.000	1.000	1.000	1.000	1.000	1.000
6	6	BINOM	1	1		1.000	1.000	1.000	1.000	1.000	1.000
7	7	BINOM	1	1		1.000	1.000	1.000	1.000	1.000	1.000
8	8	BINOM	1	1		1.000	1.000	1.000	1.000	1.000	1.000
9	9	BINOM	1	1		1.000	1.000	1.000	1.000	1.000	1.000
10	10	BINOM	1	1		1.000	1.000	1.000	1.000	1.000	1.000
11	11	BINOM	1	1		1.000	1.000	1.000	1.000	1.000	1.000
12	12	BINOM	1	1		1.000	1.000	1.000	1.000	1.000	1.000
13	13	BINOM	1	1		1.000	1.000	1.000	1.000	1.000	1.000
14	14	BINOM	1	1		1.000	1.000	1.000	1.000	1.000	1.000
15	1	STDBY	2		0.	1.000	1.000	1.000	1.000	1.000	1.000
16	2	STDBY	2		0.	1.000	1.000	1.000	1.000	1.000	1.000
17	3	STDBY	2		0.	1.000	1.000	1.000	1.000	1.000	1.000
18	4	BINOM	2	1		1.000	1.000	1.000	1.000	1.000	1.000
19	5	STDBY	2		0.	1.000	1.000	1.000	1.000	1.000	1.000
20	6	BINOM	2	1		1.000	1.000	1.000	1.000	1.000	1.000
21	7	STDBY	2		0.	1.000	1.000	1.000	1.000	1.000	1.000
22	8	BINOM	2	1		1.000	1.000	1.000	1.000	1.000	1.000
23	9	STDBY	2		0.	1.000	1.000	1.000	1.000	1.000	1.000
24	10	STDBY	2		0.	1.000	1.000	1.000	1.000	1.000	1.000
25	11	STDBY	2		0.	1.000	1.000	1.000	1.000	1.000	1.000
26	12	STDBY	2		0.	1.000	1.000	1.000	1.000	1.000	1.000
27	13	STDBY	2		0.	1.000	1.000	1.000	1.000	1.000	1.000
28	14	STDBY	2		0.	1.000	1.000	1.000	1.000	1.000	1.000
41	15	BINOM	1	1		1.000	1.000	1.000	1.000	1.000	1.000
42	16	BINOM	1	1		1.000	1.000	1.000	1.000	1.000	1.000
43	17	BINOM	1	1		1.000	1.000	1.000	1.000	1.000	1.000
44	18	BINOM	1	1		1.000	1.000	1.000	1.000	1.000	1.000
45	19	BINOM	1	1		1.000	1.000	1.000	1.000	1.000	1.000
46	20	BINOM	1	1		1.000	1.000	1.000	1.000	1.000	1.000
47	21	BINOM	1	1		1.000	1.000	1.000	1.000	1.000	1.000
48	22	BINOM	1	1		1.000	1.000	1.000	1.000	1.000	1.000
49	23	BINOM	1	1		1.000	1.000	1.000	1.000	1.000	1.000
51	25	BINOM	1	1		1.000	1.000	1.000	1.000	1.000	1.000
52	26	BINOM	1	1		1.000	1.000	1.000	1.000	1.000	1.000
53	27	BINOM	1	1		1.000	1.000	1.000	1.000	1.000	1.000

54	28	BINOM	1	1		1.000	1.000	1.000	1.000	1.000	1.000
61	1	BINOM	2	1		1.000	1.000	1.000	1.000	1.000	1.000
62	2	BINOM	2	1		1.000	1.000	1.000	1.000	1.000	1.000
63	3	BINOM	2	1		1.000	1.000	1.000	1.000	1.000	1.000
64	4	BINOM	2	1		1.000	1.000	1.000	1.000	1.000	1.000
65	5	BINOM	2	1		1.000	1.000	1.000	1.000	1.000	1.000
66	6	BINOM	2	1		1.000	1.000	1.000	1.000	1.000	1.000
67	7	BINOM	2	1		1.000	1.000	1.000	1.000	1.000	1.000
68	8	BINOM	2	1		1.000	1.000	1.000	1.000	1.000	1.000
69	9	BINOM	2	1		1.000	1.000	1.000	1.000	1.000	1.000
70	10	BINOM	2	1		1.000	1.000	1.000	1.000	1.000	1.000
71	11	BINOM	2	1		1.000	1.000	1.000	1.000	1.000	1.000
72	12	BINOM	2	1		1.000	1.000	1.000	1.000	1.000	1.000
73	13	BINOM	2	1		1.000	1.000	1.000	1.000	1.000	1.000
74	14	BINOM	2	1		1.000	1.000	1.000	1.000	1.000	1.000
81	1	STDBY	2		0.	0.500	1.000	1.000	1.000	1.000	1.000
82	2	STDBY	2		0.	0.500	1.000	1.000	1.000	1.000	1.000
83	3	STDBY	2		0.	0.500	1.000	1.000	1.000	1.000	1.000
84	4	STDBY	2		0.	0.500	1.000	1.000	1.000	1.000	1.000
85	5	STDBY	2		0.	0.500	1.000	1.000	1.000	1.000	1.000
86	6	STDBY	2		0.	0.500	1.000	1.000	1.000	1.000	1.000
87	7	STDBY	2		0.	0.500	1.000	1.000	1.000	1.000	1.000
88	8	STDBY	2		0.	0.500	1.000	1.000	1.000	1.000	1.000
89	9	STDBY	2		0.	0.500	1.000	1.000	1.000	1.000	1.000
90	10	STDBY	2		0.	0.500	1.000	1.000	1.000	1.000	1.000
91	11	STDBY	2		0.	0.500	1.000	1.000	1.000	1.000	1.000
92	12	STDBY	2		0.	0.500	1.000	1.000	1.000	1.000	1.000
93	13	STDBY	2		0.	0.500	1.000	1.000	1.000	1.000	1.000
94	14	STDBY	2		0.	0.500	1.000	1.000	1.000	1.000	1.000
184	4	BINOM	1	1		0.100	0.100	0.100	0.100	0.100	0.100
186	6	BINOM	1	1		0.200	0.200	0.200	0.200	0.200	0.200
187	7	BINOM	1	1		0.500	0.500	0.500	0.500	0.500	0.500
188	8	BINOM	1	1		0.200	0.200	0.200	0.200	0.200	0.200
190	10	BINOM	1	1		0.500	0.500	0.500	0.500	0.500	0.500
191	10	STDBY	2		0.800	0.500	0.500	0.500	0.500	0.500	0.500
196	6	BINOM	2	1		0.100	0.100	0.100	0.100	0.100	0.100
197	7	BINOM	2	1		0.500	0.500	0.500	0.500	0.500	0.500
198	7	BINOM	2	1		0.200	0.200	0.200	0.200	0.200	0.200
199	4	BINOM	2	1		0.100	0.100	0.100	0.100	0.100	0.100
244	18	BINOM	1	1		0.100	0.100	0.100	0.100	0.100	0.100
246	20	BINOM	1	1		0.100	0.100	0.100	0.100	0.100	0.100
247	21	BINOM	1	1		0.500	0.500	0.500	0.500	0.500	0.500

248	22 BINOM	1	1	0.200	0.200	0.200	0.200	0.200	0.200

LOGICAL EQUATIONS

```
L 29=1*2*3*4*5*6*7*8*9*10*11*12*13*14
L 30=15*16*17*18*19*20*21*22*23*24*25*26*27*28
L 31=1*2
L 32=000002031*3*18*5*20*7*8*9*10*11*12*13*14
L 33=000002031*17*18*19*20*21*22*23*24*25*26*27*28
L 34=000002029
L 35=1*16*3*18*19*20*21*22*24*11*12*27*14*23
L 36=001002029
L 55=41*42*43*44*45*46*47*48*49*70*51*52*53*54
L 95=81*82*83*64*85*66*67*68*89*90*91*92*93*94
L 75=1*62*3*64*5*66*67*68*69*70*71*12*13*14
L 101=15*16*3*4*5*20*7*8*10*11*12*27*14*23
L 102=1*2*3*4*19*6*21*22*10*25*26*27*14*13
L 192=1*2*3*184*5*186*187*188*9*190*11*12*13*14
L 193=002031*17*184*19*186*187*188*23*190*25*26*27*28
L 194=002031*3*184*5*186*187*188*190*11*12*13*14*9
L 201=002192
L 202=81*82*83*199*85*196*197*198*89*191*91*92*93*94
L 203=1*62*3*199*5*196*197*198*69*70*71*12*13*14
L 204=1*2*3*184*5*186*9*11*12*13*14
L 205=1*2*3*4*5*6*9*11*12*13*14
L 206=15*16*17*18*19*20*23*25*26*27*28
L 207=15*16*17*199*19*196*23*25*26*27*28
L 208=2031
L 209=208*3*18*5*20*9*11*12*13*14
L 210=208*3*199*5*196*9*11*12*13*14
L 211=208*17*18*19*20*23*25*26*27*28
L 212=208*17*199*19*196*25*26*27*28
L 213=1*2*3*4*19*6* 9*11*26*27*14
L 214=1*2*3*199*19*196*9*11*26*27*14
L 215=208*17*44*45*46*9*11*26*27*14
L 249=15*16*3*4*5*246*7*8*23*10*11*12*27*14
L 250=1*2*3*4*19*6*247*248*10*15*26*27*14
L 261=2*13*1
L 262=2261
L 263=3*14
L 264=2263
L 265=6*9*11
```

```
L 266=186*9*11
L 267=4*5
L 268=184*5
L 269=2265
L 270=2266
L 271=2267
L 272=2268
L 273=262*264*269*271*26
L 274=262*264*270*272*26
L 275=2205
L 276=2204
```

MISSION PHASE RELIABILITIES

ELEMT	PHASE 1	2	3	4	5	6
1	0.9997965	0.9994913	0.9941153	0.9923970	0.9888688	0.9838502
2	0.9972878	0.9932334	0.9242623	0.9031704	0.8612494	0.8047149
3	0.9998522	0.9996305	0.9957218	0.9944713	0.9919018	0.9882425
4	0.9971342	0.9928509	0.9201416	0.8979670	0.8539816	0.7948566
5	0.9975181	0.9938069	0.9304715	0.9110240	0.8722556	0.8197164
6	0.9991824	0.9979573	0.9765594	0.9697936	0.9560112	0.9366612
7	0.9975181	0.9938069	0.9304715	0.9110240	0.8722556	0.8197164
8	0.9965375	0.9913663	0.9043074	0.8780357	0.8263256	0.7576919
9	0.9989306	0.9973288	0.9694487	0.9606722	0.9428523	0.9179672
10	0.9969935	0.9925007	0.9163837	0.8932275	0.8473790	0.7859334
11	0.9998123	0.9995309	0.9945721	0.9929867	0.9897307	0.9850978
12	0.9997595	0.9993990	0.9930503	0.9910225	0.9868607	0.9809455
13	0.9961745	0.9904638	0.8948034	0.8661216	0.8099328	0.7359273
14	0.9999141	0.9997852	0.9975114	0.9967832	0.9952855	0.9931500
15	1.0000000	0.9999999	0.9999826	0.9999710	0.9999378	0.9998689
16	0.9999963	0.9999771	0.9970566	0.9951529	0.9898952	0.9795531
17	1.0000000	0.9999999	0.9999908	0.9999847	0.9999671	0.9999306
18	0.9999918	0.9999489	0.9936226	0.9895893	0.9786786	0.9579162
19	0.9999969	0.9999808	0.9975248	0.9959187	0.9914692	0.9826734
20	0.9999993	0.9999958	0.9994505	0.9990876	0.9980650	0.9959882
21	0.9999969	0.9999808	0.9975248	0.9959187	0.9914692	0.9826734
22	0.9999880	0.9999255	0.9908429	0.9851247	0.9698372	0.9412868
23	0.9999994	0.9999964	0.9995285	0.9992163	0.9983350	0.9965393
24	0.9999955	0.9999718	0.9964024	0.9940854	0.9877111	0.9752516
25	1.0000000	0.9999999	0.9999852	0.9999753	0.9999471	0.9998884
26	1.0000000	0.9999998	0.9999758	0.9999596	0.9999133	0.9998173
27	0.9999927	0.9999544	0.9942619	0.9906092	0.9806699	0.9615802

28	1.0000000	1.0000000	0.9999969	0.9999948	0.9999889	0.9999765
41	1.0000000	0.9999999	0.9999826	0.9999710	0.9999378	0.9998689
42	0.9999963	0.9999771	0.9970566	0.9951529	0.9898952	0.9795531
43	1.0000000	0.9999999	0.9999908	0.9999847	0.9999671	0.9999306
44	0.9999959	0.9999744	0.9967229	0.9946080	0.9887789	0.9773505
45	0.9999969	0.9999808	0.9975248	0.9959187	0.9914692	0.9826734
46	0.9999997	0.9999979	0.9997231	0.9995391	0.9990180	0.9979504
47	0.9999969	0.9999808	0.9975248	0.9959187	0.9914692	0.9826734
48	0.9999942	0.9999637	0.9954038	0.9924606	0.9844075	0.9688023
49	0.9999994	0.9999964	0.9995285	0.9992163	0.9983350	0.9965393
51	1.0000000	0.9999999	0.9999852	0.9999753	0.9999471	0.9998884
52	1.0000000	0.9999998	0.9999758	0.9999596	0.9999133	0.9998173
53	0.9999927	0.9999544	0.9942619	0.9906092	0.9806699	0.9615802
54	1.0000000	1.0000000	0.9999969	0.9999948	0.9999889	0.9999765
61	1.0000000	0.9999997	0.9999654	0.9999422	0.9998761	0.9997392
62	0.9999926	0.9999542	0.9942638	0.9906240	0.9807483	0.9618637
63	1.0000000	0.9999999	0.9999817	0.9999694	0.9999344	0.9998618
64	0.9999918	0.9999489	0.9936226	0.9895893	0.9786786	0.9579162
65	0.9999938	0.9999616	0.9951658	0.9920833	0.9836814	0.9674978
66	0.9999993	0.9999958	0.9994505	0.9990876	0.9980650	0.9959882
67	0.9999938	0.9999616	0.9951658	0.9920833	0.9836814	0.9674978
68	0.9999880	0.9999255	0.9908429	0.9851247	0.9698372	0.9412868
69	0.9999989	0.9999929	0.9990666	0.9984533	0.9967341	0.9932706
70	0.9999910	0.9999438	0.9930083	0.9885996	0.9767068	0.9541755
71	1.0000000	0.9999998	0.9999705	0.9999508	0.9998945	0.9997779
72	0.9999999	0.9999996	0.9999517	0.9999194	0.9998274	0.9996369
73	0.9999854	0.9999091	0.9889337	0.9820766	0.9638745	0.9302656
74	1.0000000	0.9999999	0.9999938	0.9999897	0.9999778	0.9999531
81	1.0000000	0.9999999	0.9999832	0.9999718	0.9999389	0.9998705
82	0.9999991	0.9999853	0.9971547	0.9952771	0.9900692	0.9797899
83	1.0000000	1.0000000	0.9999911	0.9999851	0.9999677	0.9999315
84	0.9999990	0.9999836	0.9968319	0.9947458	0.9889716	0.9776118
85	0.9999992	0.9999877	0.9976075	0.9960236	0.9916167	0.9828754
86	0.9999999	0.9999987	0.9997325	0.9995512	0.9990355	0.9979753
87	0.9999992	0.9999877	0.9976075	0.9960236	0.9916167	0.9828754
88	0.9999985	0.9999760	0.9954245	0.9924370	0.9842331	0.9682989
89	0.9999999	0.9999977	0.9995444	0.9992368	0.9983646	0.9965812
90	0.9999989	0.9999819	0.9965219	0.9942363	0.9879216	0.9755359
91	1.0000000	0.9999999	0.9999857	0.9999760	0.9999480	0.9998898
92	1.0000000	0.9999999	0.9999766	0.9999606	0.9999149	0.9998196
93	0.9999982	0.9999708	0.9944511	0.9908464	0.9809959	0.9620117
94	1.0000000	1.0000000	0.9999970	0.9999950	0.9999891	0.9999768

184	0.9997130	0.9992828	0.9917118	0.9892955	0.9843394	0.9773022
186	0.9998364	0.9995911	0.9952673	0.9938844	0.9910432	0.9869985
187	0.9987583	0.9968986	0.9646095	0.9544758	0.9339462	0.9053819
188	0.9993065	0.9982673	0.9800838	0.9743218	0.9625654	0.9460161
190	0.9984956	0.9962433	0.9572793	0.9451071	0.9205319	0.8865289
191	0.9999980	0.9999873	0.9983527	0.9972780	0.9942855	0.9883211
196	1.0000000	1.0000000	0.9999944	0.9999906	0.9999799	0.9999575
197	0.9999985	0.9999904	0.9987475	0.9979275	0.9956369	0.9910474
198	0.9999997	0.9999985	0.9997952	0.9996591	0.9992729	0.9984806
199	0.9999999	0.9999995	0.9999313	0.9998854	0.9997547	0.9994848
244	1.0000000	0.9999997	0.9999656	0.9999425	0.9998767	0.9997404
246	1.0000000	1.0000000	0.9999972	0.9999953	0.9999899	0.9999787
247	0.9999992	0.9999952	0.9993662	0.9989477	0.9977688	0.9953754
248	0.9999998	0.9999985	0.9998062	0.9996772	0.9993112	0.9985592
29	0.9766555	0.9426566	0.5040816	0.4123850	0.2727580	0.1511168
30	0.9999568	0.9997309	0.9666201	0.9458520	0.8911848	0.7934537
31	0.9970849	0.9927282	0.9188233	0.8963037	0.8516626	0.7917190
32	0.9831169	0.9582783	0.6042609	0.5194450	0.3787340	0.2388798
33	0.9999562	0.9997275	0.9662060	0.9451898	0.8899027	0.7911848
34	0.9997254	0.9983235	0.8493861	0.7776747	0.6271171	0.4366825
35	0.9990918	0.9975708	0.9427267	0.9157530	0.8499677	0.7407612
36	0.9994550	0.9967117	0.7540649	0.6547086	0.4711190	0.2793973
55	0.9999629	0.9997687	0.9710460	0.9528734	0.9045898	0.8168155
95	0.9999681	0.9997549	0.9648258	0.9428171	0.8849844	0.7821663
75	0.9929846	0.9823905	0.7885220	0.7267821	0.6054958	0.4524987
101	0.9851183	0.9631659	0.6413384	0.5611215	0.4243013	0.2819695
102	0.9863832	0.9662131	0.6591471	0.5793511	0.4403943	0.2923745
192	0.9852486	0.9635286	0.6498747	0.5727556	0.4415925	0.3045565
193	0.9961001	0.9902221	0.8824747	0.8470948	0.7743977	0.6733130
194	0.9881249	0.9705608	0.7048940	0.6354586	0.5124967	0.3756853
201	0.9998907	0.9993267	0.9299549	0.8919501	0.8025360	0.6666434
202	0.9999924	0.9999167	0.9855927	0.9762325	0.9506964	0.9019699
203	0.9930096	0.9825442	0.8040171	0.7502456	0.6462920	0.5150572
204	0.9886454	0.9718548	0.7180856	0.6516598	0.5336183	0.4010926
205	0.9854501	0.9640212	0.6537389	0.5771633	0.4465857	0.3095784
206	0.9999764	0.9998529	0.9815050	0.9698049	0.9383390	0.8795768
207	0.9999852	0.9999076	0.9882742	0.9807809	0.9603854	0.9214033
208	0.9999957	0.9999735	0.9966122	0.9944274	0.9884097	0.9766240
209	0.9919697	0.9799970	0.7836605	0.7270018	0.6200998	0.4893700
210	0.9919784	0.9800506	0.7890652	0.7352298	0.6346691	0.5126410
211	0.9999758	0.9998494	0.9810846	0.9691260	0.9369891	0.8770616
212	0.9999852	0.9999077	0.9883169	0.9808630	0.9606032	0.9219591

213	0.9919238	0.9798935	0.7841811	0.7281405	0.6227598	0.4942454
214	0.9955885	0.9889689	0.8726312	0.8360297	0.7625947	0.6634818
215	0.9986383	0.9965279	0.9472604	0.9273555	0.8815927	0.8081524
249	0.9851189	0.9631699	0.6416892	0.5616313	0.4251197	0.2830993
250	0.9901850	0.9756012	0.7446730	0.6808455	0.5638210	0.4268995
261	0.9932706	0.9832613	0.8221663	0.7763079	0.6897895	0.5826476
262	0.9999773	0.9998591	0.9831568	0.9728738	0.9459558	0.8973779
263	0.9997663	0.9994158	0.9932439	0.9912723	0.9872255	0.9814730
264	1.0000000	0.9999998	0.9999771	0.9999618	0.9999181	0.9998273
265	0.9979266	0.9948246	0.9415855	0.9251198	0.8921209	0.8470110
266	0.9985798	0.9964533	0.9596234	0.9481008	0.9248117	0.8925304
267	0.9946594	0.9867020	0.8561656	0.8180695	0.7448902	0.6515570
268	0.9972319	0.9930941	0.9227595	0.9012720	0.8585955	0.8011107
269	0.9999978	0.9999866	0.9982596	0.9971238	0.9939597	0.9876501
270	0.9999990	0.9999937	0.9991737	0.9986293	0.9970997	0.9940064
271	0.9999857	0.9999112	0.9891208	0.9823444	0.9642741	0.9306778
272	0.9999962	0.9999761	0.9969370	0.9949576	0.9894947	0.9787619
273	0.9999608	0.9997565	0.9707227	0.9528733	0.9064981	0.8245622
274	0.9999724	0.9998286	0.9792894	0.9665653	0.9331461	0.8727448
275	0.9998936	0.9993449	0.9316088	0.8943896	0.8065891	0.6725726
276	0.9999353	0.9996001	0.9558915	0.9307218	0.8687703	0.7675160

ADVANCED PLANETARY PROBE (PARTS COUNT RELIABILITY ASSESSMENT)
SUBSYSTEM 3 PROPULSION SUBSYSTEM
UNIT 1 EXPLOSIVE VALVES 1LB (ANALOG)

COMPONENT PART	QTY	FAILURE RATE	EXTENSION

UNIT INPUTED AS ENTITY...SEE UNIT SUMMARY.

ADVANCED PLANETARY PROBE (PARTS COUNT RELIABILITY ASSESSMENT)
SUBSYSTEM 3 PROPULSION SUBSYSTEM
UNIT 2 HYDRZNE TNK A BLDR .15LB (ANALOG)

COMPONENT PART	QTY	FAILURE RATE	EXTENSION

UNIT INPUTED AS ENTITY...SEE UNIT SUMMARY.

ADVANCED PLANETARY PROBE (PARTS COUNT RELIABILITY ASSESSMENT)
SUBSYSTEM 3 PROPULSION SUBSYSTEM
UNIT 3 LNE A FTTNGS 2LB (ANALOG)

COMPONENT PART	QTY	FAILURE RATE	EXTENSION

UNIT INPUTED AS ENTITY...SEE UNIT SUMMARY.

ADVANCED PLANETARY PROBE (PARTS COUNT RELIABILITY ASSESSMENT)
SUBSYSTEM 3 PROPULSION SUBSYSTEM
UNIT 4 HYDRZNE FLL DRA VLVE.15 (ANALOG)

COMPONENT PART	QTY	FAILURE RATE	EXTENSION

UNIT INPUTED AS ENTITY...SEE UNIT SUMMARY.

ADVANCED PLANETARY PROBE (PARTS COUNT RELIABILITY ASSESSMENT)
SUBSYSTEM 3 PROPULSION SUBSYSTEM
UNIT 5 NITROGEN FILL VALVE.15 (ANALOG)

COMPONENT PART	QTY	FAILURE RATE	EXTENSION

UNIT INPUTED AS ENTITY...SEE UNIT SUMMARY.

ADVANCED PLANETARY PROBE (PARTS COUNT RELIABILITY ASSESSMENT)
SUBSYSTEM 3 PROPULSION SUBSYSTEM
UNIT 6 PROPELLANT FILTER .50 (ANALOG)

COMPONENT PART	QTY	FAILURE RATE	EXTENSION

UNIT INPUTED AS ENTITY...SEE UNIT SUMMARY.

ADVANCED PLANETARY PROBE (PARTS COUNT RELIABILITY ASSESSMENT)
SUBSYSTEM 3 PROPULSION SUBSYSTEM
UNIT 7 25LB THRUST ENGINE 1.20 (ANALOG)

COMPONENT PART	QTY	FAILURE RATE	EXTENSION

UNIT INPUTED AS ENTITY...SEE UNIT SUMMARY.

ADVANCED PLANETARY PROBE (PARTS COUNT RELIABILITY ASSESSMENT)
SUBSYSTEM 3 PROPULSION SUBSYSTEM
UNIT 8 TANK (PRESSURIZATION) (ANALOG)

COMPONENT PART	QTY	FAILURE RATE	EXTENSION

UNIT INPUTED AS ENTITY...SEE UNIT SUMMARY.

ADVANCED PLANETARY PROBE (PARTS COUNT RELIABILITY ASSESSMENT)
SUBSYSTEM 3 PROPULSION SUBSYSTEM
UNIT 9 LINES(PRESSURIZATION) (ANALOG)

COMPONENT PART	QTY	FAILURE RATE	EXTENSION

UNIT INPUTED AS ENTITY...SEE UNIT SUMMARY.

ADVANCED PLANETARY PROBE (PARTS COUNT RELIABILITY ASSESSMENT)
SUBSYSTEM 3 PROPULSION SUBSYSTEM
UNIT 10 EXPLOSIVE VALVES(PRESS) (ANALOG)

COMPONENT PART	QTY	FAILURE RATE	EXTENSION

UNIT INPUTED AS ENTITY...SEE UNIT SUMMARY.

ADVANCED PLANETARY PROBE (PARTS COUNT RELIABILITY ASSESSMENT)
SUBSYSTEM 3 PROPULSION SUBSYSTEM
UNIT 11 FILTER (PRESS) (ANALOG)

COMPONENT PART	QTY	FAILURE RATE	EXTENSION

UNIT INPUTED AS ENTITY...SEE UNIT SUMMARY.

ADVANCED PLANETARY PROBE (PARTS COUNT RELIABILITY ASSESSMENT)
SUBSYSTEM 3 PROPULSION SUBSYSTEM
UNIT 12 LATCHING SOL VALVE (ANALOG)

COMPONENT PART	QTY	FAILURE RATE	EXTENSION

UNIT INPUTED AS ENTITY...SEE UNIT SUMMARY.

ADVANCED PLANETARY PROBE (PARTS COUNT RELIABILITY ASSESSMENT)
SUBSYSTEM 3 PROPULSION SUBSYSTEM
UNIT 13 HIGH PRESS SWITCH (ANALOG)

COMPONENT PART	QTY	FAILURE RATE	EXTENSION

UNIT INPUTED AS ENTITY...SEE UNIT SUMMARY.

ADVANCED PLANETARY PROBE (PARTS COUNT RELIABILITY ASSESSMENT)
SUBSYSTEM 3 PROPULSION SUBSYSTEM
UNIT 14 BURST DISC AND RELF VALV (ANALOG)

COMPONENT PART	QTY	FAILURE RATE	EXTENSION

UNIT INPUTED AS ENTITY...SEE UNIT SUMMARY.

ADVANCED PLANETARY PROBE (PARTS COUNT RELIABILITY ASSESSMENT)
SUBSYSTEM 3 PROPULSION SUBSYSTEM
UNIT 15 GAS TEMP. .15 (ANALOG)

COMPONENT PART	QTY	FAILURE RATE	EXTENSION

UNIT INPUTED AS ENTITY...SEE UNIT SUMMARY.

ADVANCED PLANETARY PROBE (PARTS COUNT RELIABILITY ASSESSMENT)
SUBSYSTEM 3 PROPULSION SUBSYSTEM
UNIT 16 TANK PRESS. .3 (ANALOG)

COMPONENT PART	QTY	FAILURE RATE	EXTENSION

UNIT INPUTED AS ENTITY...SEE UNIT SUMMARY.

ADVANCED PLANETARY PROBE (PARTS COUNT RELIABILITY ASSESSMENT)
SUBSYSTEM 3 PROPULSION SUBSYSTEM
UNIT 17 PROPEL MNFLD TEMP. .3 (ANALOG)

COMPONENT PART	QTY	FAILURE RATE	EXTENSION

UNIT INPUTED AS ENTITY...SEE UNIT SUMMARY.

ADVANCED PLANETARY PROBE (PARTS COUNT RELIABILITY ASSESSMENT)
SUBSYSTEM 3 PROPULSION SUBSYSTEM
UNIT 18 CHAMBER PRESS .3 (ANALOG)

COMPONENT PART	QTY	FAILURE RATE	EXTENSION

UNIT INPUTED AS ENTITY...SEE UNIT SUMMARY.

ADVANCED PLANETARY PROBE (PARTS COUNT RELIABILITY ASSESSMENT)
SUBSYSTEM 3 PROPULSION SUBSYSTEM
UNIT 19 REGULATOR (ANALOG)

COMPONENT PART	QTY	FAILURE RATE	EXTENSION

UNIT INPUTED AS ENTITY...SEE UNIT SUMMARY.

ADVANCED PLANETARY PROBE (PARTS COUNT RELIABILITY ASSESSMENT)
SUBSYSTEM 3 PROPULSION SUBSYSTEM
NO. OF COMPONENT PARTS= 0 SUBSYSTEM FR= 0

UNIT SUMMARY.....

NO	DESCRIPTION	PART USAGE	FAILURE RATE	SUM FR SQUARED	SUM FR CUBED
1	EXPLOSIVE VALVES 1LB	ANALOG	93	0.	0.
2	HYDRZNE TNK A BLDR .15LB	ANALOG	120	0.	0.
3	LNE A FTTNGS 2LB	ANALOG	30	0.	0.
4	HYDRZNE FLL DRA VLVE.15	ANALOG	125	0.	0.
5	NITROGEN FILL VALVE.15	ANALOG	125	0.	0.
6	PROPELLANT FILTER .50	ANALOG	31	0.	0.
7	25LB THRUST ENGINE 1.20	ANALOG	7750	0.	0.
8	TANK (PRESSURIZATION)	ANALOG	120	0.	0.
9	LINES(PRESSURIZATION)	ANALOG	30	0.	0.
10	EXPLOSIVE VALVES(PRESS)	ANALOG	93	0.	0.
11	FILTER (PRESS)	ANALOG	31	0.	0.
12	LATCHING SOL VALVE	ANALOG	6200	0.	0.
13	HIGH PRESS SWITCH	ANALOG	30	0.	0.
14	BURST DISC AND RELF VALV	ANALOG	30	0.	0.
15	GAS TEMP. .15	ANALOG	30	0.	0.
16	TANK PRESS. .3	ANALOG	30	0.	0.
17	PROPEL MNFLD TEMP. .3	ANALOG	30	0.	0.
18	CHAMBER PRESS .3	ANALOG	30	0.	0.
19	REGULATOR	ANALOG	1000	0.	0.

MISSION RELIABILITIES....

BASIC ELEMENT SPECIFICATIONS

ELEMT NO.	REF. UNIT	REDUN. TYPE	NO. PRESENT	NO. NEEDED	OFF RATIO	PHASE L-FACTORS... 1	2	3	4	5	6
1	1	BINOM	1	1		1.000	1.000	1.000	1.000	1.000	1.000
2	2	BINOM	1	1		1.000	1.000	1.000	1.000	1.000	1.000
3	3	BINOM	1	1		1.000	1.000	1.000	1.000	1.000	1.000
4	4	BINOM	1	1		1.000	1.000	1.000	1.000	1.000	1.000
5	5	BINOM	1	1		1.000	1.000	1.000	1.000	1.000	1.000
6	6	BINOM	1	1		1.000	1.000	1.000	1.000	1.000	1.000
7	7	BINOM	1	1		1.000	1.000	1.000	1.000	1.000	1.000

24	7	BINOM	2	1	1.000	1.000	1.000	1.000	1.000	1.000
8	8	BINOM	1	1	1.000	1.000	1.000	1.000	1.000	1.000
9	9	BINOM	1	1	1.000	1.000	1.000	1.000	1.000	1.000
10	10	BINOM	1	1	1.000	1.000	1.000	1.000	1.000	1.000
11	11	BINOM	1	1	1.000	1.000	1.000	1.000	1.000	1.000
12	12	BINOM	2	2	1.000	1.000	1.000	1.000	1.000	1.000
13	13	BINOM	1	1	1.000	1.000	1.000	1.000	1.000	1.000
14	14	BINOM	1	1	1.000	1.000	1.000	1.000	1.000	1.000
15	15	BINOM	1	1	0.100	0.100	0.100	1.000	1.000	1.000
16	16	BINOM	1	1	0.100	0.100	0.100	1.000	1.000	1.000
17	17	BINOM	1	1	0.100	0.100	0.100	1.000	1.000	1.000
18	18	BINOM	1	1	0.100	0.100	0.100	1.000	1.000	1.000
22	19	BINOM	1	1	1.000	1.000	1.000	1.000	1.000	1.000

LOGICAL EQUATIONS

L 25=1*2*3*4*5*6*24*15*16*17*18
L 26=23*20
L 15=1*2*3*4*5*6*7*8*9*10*11*12*13*14*1*3*4*5*5*9*9*11*11*11
L 19=1*2*3*4*5*6*7*15*16*17*18
L 20=8*9*10*11*12*13*14*15*16*17*18
L 21=19*20
L 23=21*22

MISSION PHASE RELIABILITIES

	PHASE					
ELEMT	1	2	3	4	5	6
1	0.9999554	0.9998884	0.9987063	0.9983274	0.9975478	0.9964352
2	0.9999424	0.9998560	0.9983310	0.9978423	0.9968370	0.9954026
3	0.9999856	0.9999640	0.9995825	0.9994601	0.9992083	0.9988487
4	0.9999400	0.9998500	0.9982615	0.9977525	0.9967054	0.9952115
5	0.9999400	0.9998500	0.9982615	0.9977525	0.9967054	0.9952115
6	0.9999851	0.9999628	0.9995686	0.9994422	0.9991819	0.9988103
7	0.9962869	0.9907431	0.8977353	0.8697930	0.8149732	0.7425983
24	0.9999862	0.9999143	0.9895419	0.9830461	0.9657651	0.9337444
8	0.9999424	0.9998560	0.9983310	0.9978423	0.9968370	0.9954026
9	0.9999856	0.9999640	0.9995825	0.9994601	0.9992083	0.9988487
10	0.9999554	0.9998864	0.9987063	0.9983274	0.9975478	0.9964352
11	0.9999851	0.9999628	0.9995686	0.9994422	0.9991819	0.9988103
12	0.9940657	0.9852302	0.8414674	0.7999548	0.7208242	0.6211641
13	0.9999856	0.9999640	0.9995825	0.9994601	0.9992083	0.9988487
14	0.9999856	0.9999640	0.9995825	0.9994601	0.9992083	0.9988487

15	0.9896575	0.9743441	0.7397128	0.6771503	0.5645098	0.4353062
16	0.9999986	0.9999964	0.9999582	0.9998358	0.9995839	0.9992241
17	0.9999986	0.9999964	0.9999582	0.9998358	0.9995839	0.9992241
18	0.9999986	0.9999964	0.9999582	0.9998358	0.9995839	0.9992241
22	0.9995201	0.9988007	0.9861764	0.9821610	0.9739454	0.9623279
25	0.9997290	0.9992714	0.9821863	0.9731784	0.9509128	0.9123069
26	0.7813277	0.9829059	0.9424648	0.6028640	0.5117601	0.3675108
15	0.9896575	0.9743441	0.7397128	0.6771503	0.5645098	0.4353062
19	0.9857306	0.9647074	0.6591576	0.5831642	0.4531737	0.3160813
20	0.9836226	0.9595581	0.6194794	0.5381777	0.4028368	0.2663299
21	0.9695869	0.9256928	0.4083345	0.3138460	0.1825551	0.0841819
23	0.9691217	0.9245827	0.4026899	0.3082473	0.1777987	0.0810106

ADVANCED PLANETARY PROBE (PARTS COUNT RELIABILITY ASSESSMENT)
SUBSYSTEM 1 TELECOMMUNICATION SUBSYSTEM
UNIT 1 OMNI ANTENNA (ANALOG)

COMPONENT PART	QTY	FAILURE RATE	EXTENSION

UNIT INPUTED AS ENTITY...SEE UNIT SUMMARY.

ADVANCED PLANETARY PROBE (PARTS COUNT RELIABILITY ASSESSMENT)
SUBSYSTEM 1 TELECOMMUNICATION SUBSYSTEM
UNIT 2 TRACKING (MED GAIN) ANT (ANALOG)

COMPONENT PART	QTY	FAILURE RATE	EXTENSION

UNIT INPUTED AS ENTITY...SEE UNIT SUMMARY.

ADVANCED PLANETARY PROBE (PARTS COUNT RELIABILITY ASSESSMENT)
SUBSYSTEM 1 TELECOMMUNICATION SUBSYSTEM
UNIT 3 TELEMETRY (HI GAIN) ANT (ANALOG)

COMPONENT PART	QTY	FAILURE RATE	EXTENSION

UNIT INPUTED AS ENTITY...SEE UNIT SUMMARY.

ADVANCED PLANETARY PROBE (PARTS COUNT RELIABILITY ASSESSMENT)
SUBSYSTEM 1 TELECOMMUNICATION SUBSYSTEM
UNIT 4 DIPLEXER(A3) (ANALOG)

COMPONENT PART	QTY	FAILURE RATE	EXTENSION

UNIT INPUTED AS ENTITY...SEE UNIT SUMMARY.

ADVANCED PLANETARY PROBE (PARTS COUNT RELIABILITY ASSESSMENT)
SUBSYSTEM 1 TELECOMMUNICATION SUBSYSTEM
UNIT 5 CIRCULATION SW CS1 (ANALOG)

COMPONENT PART	QTY	FAILURE RATE	EXTENSION

UNIT INPUTED AS ENTITY...SEE UNIT SUMMARY.

ADVANCED PLANETARY PROBE (PARTS COUNT RELIABILITY ASSESSMENT)
SUBSYSTEM 1 TELECOMMUNICATION SUBSYSTEM
UNIT 6 4 PORT HYBRID (ANALOG)

COMPONENT PART	QTY	FAILURE RATE	EXTENSION

UNIT INPUTED AS ENTITY...SEE UNIT SUMMARY.

ADVANCED PLANETARY PROBE (PARTS COUNT RELIABILITY ASSESSMENT)
SUBSYSTEM 1 TELECOMMUNICATION SUBSYSTEM
UNIT 7 ANTENNA SELECTOR (DIGTAL)

COMPONENT PART	QTY	FAILURE RATE	EXTENSION

UNIT INPUTED AS ENTITY...SEE UNIT SUMMARY.

ADVANCED PLANETARY PROBE (PARTS COUNT RELIABILITY ASSESSMENT)
SUBSYSTEM 1 TELECOMMUNICATION SUBSYSTEM
UNIT 8 POWER AMP SELECT/MON (DIGTAL)

COMPONENT PART	QTY	FAILURE RATE	EXTENSION

UNIT INPUTED AS ENTITY...SEE UNIT SUMMARY.

ADVANCED PLANETARY PROBE (PARTS COUNT RELIABILITY ASSESSMENT)
SUBSYSTEM 1 TELECOMMUNICATION SUBSYSTEM
UNIT 9 S-BAND RECEIVER NO1 (ANALOG)

COMPONENT PART	QTY	FAILURE RATE	EXTENSION

UNIT INPUTED AS ENTITY...SEE UNIT SUMMARY.

ADVANCED PLANETARY PROBE (PARTS COUNT RELIABILITY ASSESSMENT)
SUBSYSTEM 1 TELECOMMUNICATION SUBSYSTEM
UNIT 1C POWER AMP,TWT (ANALOG)

COMPONENT PART	QTY	FAILURE RATE	EXTENSION

UNIT INPUTED AS ENTITY...SEE UNIT SUMMARY.

ADVANCED PLANETARY PROBE (PARTS COUNT RELIABILITY ASSESSMENT)
SUBSYSTEM 1 TELECOMMUNICATION SUBSYSTEM
UNIT 11 POWER AMP,SOLID STATE (ANALOG)

COMPONENT PART	QTY	FAILURE RATE	EXTENSION

UNIT INPUTED AS ENTITY...SEE UNIT SUMMARY.

ADVANCED PLANETARY PROBE (PARTS COUNT RELIABILITY ASSESSMENT)
SUBSYSTEM 1 TELECOMMUNICATION SUBSYSTEM
UNIT 12 MODULATOR EXCITER (ANALOG)

COMPONENT PART	QTY	FAILURE RATE	EXTENSION

UNIT INPUTED AS ENTITY...SEE UNIT SUMMARY.

ADVANCED PLANETARY PROBE (PARTS COUNT RELIABILITY ASSESSMENT)
SUBSYSTEM 1 TELECOMMUNICATION SUBSYSTEM
UNIT 13 RECEIVER SELECTOR (ANALOG)

COMPONENT PART	QTY	FAILURE RATE	EXTENSION

UNIT INPUTED AS ENTITY...SEE UNIT SUMMARY.

ADVANCED PLANETARY PROBE (PARTS COUNT RELIABILITY ASSESSMENT)
SUBSYSTEM 1 TELECOMMUNICATION SUBSYSTEM
UNIT 14 TWT POWER SUPPLY (ANALOG)

COMPONENT PART	QTY	FAILURE RATE	EXTENSION

UNIT INPUTED AS ENTITY...SEE UNIT SUMMARY.

ADVANCED PLANETARY PROBE (PARTS COUNT RELIABILITY ASSESSMENT)
SUBSYSTEM 1 TELECOMMUNICATION SUBSYSTEM
UNIT 15 TWT POWER SUPPLY (OFF) (ANALOG)

COMPONENT PART	QTY	FAILURE RATE	EXTENSION

UNIT INPUTED AS ENTITY...SEE UNIT SUMMARY.

ADVANCED PLANETARY PROBE (PARTS COUNT RELIABILITY ASSESSMENT)
SUBSYSTEM 1 TELECOMMUNICATION SUBSYSTEM
UNIT 16 POWER AMP,TWT (OFF) (ANALOG)

COMPONENT PART	QTY	FAILURE RATE	EXTENSION

UNIT INPUTED AS ENTITY...SEE UNIT SUMMARY.

ADVANCED PLANETARY PROBE (PARTS COUNT RELIABILITY ASSESSMENT)
SUBSYSTEM 1 TELECOMMUNICATION SUBSYSTEM
UNIT 17 S-BAND RECEIVER (OFF) (ANALOG)

COMPONENT PART	QTY	FAILURE RATE	EXTENSION

UNIT INPUTED AS ENTITY...SEE UNIT SUMMARY.

ADVANCED PLANETARY PROBE (PARTS COUNT RELIABILITY ASSESSMENT)
SUBSYSTEM 1 TELECOMMUNICATION SUBSYSTEM
UNIT 18 MODULATOR EXCITOR (OFF) (ANALOG)

COMPONENT PART	QTY	FAILURE RATE	EXTENSION

UNIT INPUTED AS ENTITY...SEE UNIT SUMMARY.

ADVANCED PLANETARY PROBE (PARTS COUNT RELIABILITY ASSESSMENT)
SUBSYSTEM 1 TELECOMMUNICATION SUBSYSTEM
UNIT 19 TRANSMITTER I (ANALOG)

COMPONENT PART	QTY	FAILURE RATE	EXTENSION

UNIT INPUTED AS ENTITY...SEE UNIT SUMMARY.

ADVANCED PLANETARY PROBE (PARTS COUNT RELIABILITY ASSESSMENT)
SUBSYSTEM 1 TELECOMMUNICATION SUBSYSTEM
UNIT 20 TRANSMITTER II (ANALOG)

COMPONENT PART	QTY	FAILURE RATE	EXTENSION

UNIT INPUTED AS ENTITY...SEE UNIT SUMMARY.

ADVANCED PLANETARY PROBE (PARTS COUNT RELIABILITY ASSESSMENT)
SUBSYSTEM 1 TELECOMMUNICATION SUBSYSTEM
UNIT 21 ANT-DIPLEXER (ANALOG)

COMPONENT PART	QTY	FAILURE RATE	EXTENSION

UNIT INPUTED AS ENTITY...SEE UNIT SUMMARY.

ADVANCED PLANETARY PROBE (PARTS COUNT RELIABILITY ASSESSMENT)
SUBSYSTEM 1 TELECOMMUNICATION SUBSYSTEM
UNIT 22 S-BAND RECEIVER NO2 (ANALOG)

COMPONENT PART	QTY	FAILURE RATE	EXTENSION

UNIT INPUTED AS ENTITY...SEE UNIT SUMMARY.

ADVANCED PLANETARY PROBE (PARTS COUNT RELIABILITY ASSESSMENT)
SUBSYSTEM 1 TELECOMMUNICATION SUBSYSTEM
UNIT 23 DIPLEXER(A2) (ANALOG)

COMPONENT PART	QTY	FAILURE RATE	EXTENSION

UNIT INPUTED AS ENTITY...SEE UNIT SUMMARY.

ADVANCED PLANETARY PROBE (PARTS COUNT RELIABILITY ASSESSMENT)
SUBSYSTEM 1 TELECOMMUNICATION SUBSYSTEM
UNIT 24 DIPLEXER(A4) (ANALOG)

COMPONENT PART	QTY	FAILURE RATE	EXTENSION

UNIT INPUTED AS ENTITY...SEE UNIT SUMMARY.

ADVANCED PLANETARY PROBE (PARTS COUNT RELIABILITY ASSESSMENT)
SUBSYSTEM 1 TELECOMMUNICATION SUBSYSTEM
UNIT 25 CIRCULATION SW CS2 (ANALOG)

COMPONENT PART	QTY	FAILURE RATE	EXTENSION

UNIT INPUTED AS ENTITY...SEE UNIT SUMMARY.

ADVANCED PLANETARY PROBE (PARTS COUNT RELIABILITY ASSESSMENT)
SUBSYSTEM 1 TELECOMMUNICATION SUBSYSTEM
UNIT 26 CIRCULATION SW CS3 (ANALOG)

COMPONENT PART	QTY	FAILURE RATE	EXTENSION

UNIT INPUTED AS ENTITY...SEE UNIT SUMMARY.

ADVANCED PLANETARY PROBE (PARTS COUNT RELIABILITY ASSESSMENT)
SUBSYSTEM 1 TELECOMMUNICATION SUBSYSTEM
UNIT 27 ANT-DIP(A2) (ANALOG)

COMPONENT PART	QTY	FAILURE RATE	EXTENSION

UNIT INPUTED AS ENTITY...SEE UNIT SUMMARY.

ADVANCED PLANETARY PROBE (PARTS COUNT RELIABILITY ASSESSMENT)
SUBSYSTEM 1 TELECOMMUNICATION SUBSYSTEM
UNIT 28 CIRCULATING SW CS4 (ANALOG)

COMPONENT PART	QTY	FAILURE RATE	EXTENSION

UNIT INPUTED AS ENTITY...SEE UNIT SUMMARY.

ADVANCED PLANETARY PROBE (PARTS COUNT RELIABILITY ASSESSMENT)
SUBSYSTEM 1 TELECOMMUNICATION SUBSYSTEM
UNIT 29 CIRCULATING SW CS5 (ANALOG)

COMPONENT PART	QTY	FAILURE RATE	EXTENSION

UNIT INPUTED AS ENTITY...SEE UNIT SUMMARY.

ADVANCED PLANETARY PROBE (PARTS COUNT RELIABILITY ASSESSMENT)
SUBSYSTEM 1 TELECOMMUNICATION SUBSYSTEM
UNIT 30 CIRCULATING SW CS6 (ANALOG)

COMPONENT PART	QTY	FAILURE RATE	EXTENSION

UNIT INPUTED AS ENTITY...SEE UNIT SUMMARY.

ADVANCED PLANETARY PROBE (PARTS COUNT RELIABILITY ASSESSMENT)
SUBSYSTEM 1 TELECOMMUNICATION SUBSYSTEM
UNIT 31 CIRCULATING SW CS7 (ANALOG)

COMPONENT PART	QTY	FAILURE RATE	EXTENSION

UNIT INPUTED AS ENTITY...SEE UNIT SUMMARY.

ADVANCED PLANETARY PROBE (PARTS COUNT RELIABILITY ASSESSMENT)
SUBSYSTEM 1 TELECOMMUNICATION SUBSYSTEM
UNIT 32 TWT AND CONVERTER (ANALOG)

COMPONENT PART	QTY	FAILURE RATE	EXTENSION

UNIT INPUTED AS ENTITY...SEE UNIT SUMMARY.

ADVANCED PLANETARY PROBE (PARTS COUNT RELIABILITY ASSESSMENT)
SUBSYSTEM 1 TELECOMMUNICATION SUBSYSTEM
NO. OF COMPONENT PARTS= 0 SUBSYSTEM FR= 0

UNIT SUMMARY.....

NO	DESCRIPTION	PART USAGE	FAILURE RATE	SUM FR SQUARED	SUM FR CUBED
1	OMNI ANTENNA	ANALOG	18	0.	0.
2	TRACKING (MED GAIN) ANT	ANALOG	18	0.	0.
3	TELEMETRY (HI GAIN) ANT	ANALOG	37	0.	0.
4	DIPLEXER(A3)	ANALOG	83	0.	0.
5	CIRCULATION SW CS1	ANALOG	83	0.	0.
6	4 PORT HYBRID	ANALOG	83	0.	0.
7	ANTENNA SELECTOR	DIGTAL	905	0.	0.
8	POWER AMP SELECT/MON	DIGTAL	1444	0.	0.
9	S-BAND RECEIVER NO1	ANALOG	6318	0.	0.
10	POWER AMP,TWT	ANALOG	3333	0.	0.
11	POWER AMP,SOLID STATE	ANALOG	2000	0.	0.
12	MODULATOR EXCITER	ANALOG	1952	0.	0.
13	RECEIVER SELECTOR	ANALOG	905	0.	0.
14	TWT POWER SUPPLY	ANALOG	5254	0.	0.
15	TWT POWER SUPPLY (OFF)	ANALOG	2627	0.	0.
16	POWER AMP,TWT (OFF)	ANALOG	333	0.	0.
17	S-BAND RECEIVER (OFF)	ANALOG	5700	0.	0.
18	MODULATOR EXCITOR (OFF)	ANALOG	1236	0.	0.
19	TRANSMITTER I	ANALOG	3952	0.	0.
20	TRANSMITTER II	ANALOG	10539	0.	0.
21	ANT-DIPLEXER	ANALOG	120	0.	0.
22	S-BAND RECEIVER NO2	ANALOG	6318	0.	0.
23	DIPLEXER(A2)	ANALOG	83	0.	0.
24	DIPLEXER(A4)	ANALOG	83	0.	0.
25	CIRCULATION SW CS2	ANALOG	83	0.	0.
26	CIRCULATION SW CS3	ANALOG	83	0.	0.
27	ANT-DIP(A2)	ANALOG	101	0.	0.
28	CIRCULATING SW CS4	ANALOG	83	0.	0.
29	CIRCULATING SW CS5	ANALOG	83	0.	0.
30	CIRCULATING SW CS6	ANALOG	83	0.	0.
31	CIRCULATING SW CS7	ANALOG	83	0.	0.
32	TWT AND CONVERTER	ANALOG	8587	0.	0.

MISSION RELIABILITIES....

BASIC ELEMENT SPECIFICATIONS

ELEMT NO.	REF. UNIT	REDUN. TYPE	NO. PRESENT	NO. NEEDED	OFF RATIO	PHASE L-FACTORS... 1	2	3	4	5	6
1	1	BINOM	1	1		1.000	1.000	1.000	1.000	1.000	1.000
2	2	BINOM	1	1		1.000	1.000	1.000	1.000	1.000	1.000
3	3	BINOM	1	1		1.000	1.000	1.000	1.000	1.000	1.000
4	4	BINOM	1	1		1.000	1.000	1.000	1.000	1.000	1.000
5	5	BINOM	1	1		1.000	1.000	1.000	1.000	1.000	1.000
6	6	BINOM	1	1		1.000	1.000	1.000	1.000	1.000	1.000
7	7	BINOM	1	1		1.000	1.000	1.000	1.000	1.000	1.000
8	8	BINOM	1	1		1.000	1.000	1.000	1.000	1.000	1.000
9	9	BINOM	1	1		1.000	1.000	1.000	1.000	1.000	1.000
10	10	BINOM	1	1		1.000	1.000	1.000	1.000	1.000	1.000
11	11	BINOM	1	1		1.000	1.000	1.000	1.000	1.000	1.000
12	12	BINOM	1	1		1.000	1.000	1.000	1.000	1.000	1.000
13	13	BINOM	1	1		1.000	1.000	1.000	1.000	1.000	1.000
14	14	BINOM	1	1		1.000	1.000	1.000	1.000	1.000	1.000
15	15	BINOM	1	1		1.000	1.000	1.000	1.000	1.000	1.000
16	16	BINOM	1	1		1.000	1.000	1.000	1.000	1.000	1.000
17	17	BINOM	1	1		1.000	1.000	1.000	1.000	1.000	1.000
35	18	BINOM	1	1		1.000	1.000	1.000	1.000	1.000	1.000
36	19	STDBY	2		0.630	1.000	1.000	1.000	1.000	1.000	1.000
37	20	STDBY	2		0.398	1.000	1.000	1.000	1.000	1.000	1.000
39	21	STDBY	3		0.842	1.000	1.000	1.000	1.000	1.000	1.000
42	9	BINOM	2	1		1.000	1.000	1.000	1.000	1.000	1.000
45	22	BINOM	1	1		1.000	1.000	1.000	1.000	1.000	1.000
46	23	BINOM	1	1		1.000	1.000	1.000	1.000	1.000	1.000
47	24	BINOM	1	1		1.000	1.000	1.000	1.000	1.000	1.000
48	25	BINOM	1	1		1.000	1.000	1.000	1.000	1.000	1.000
49	26	BINOM	1	1		1.000	1.000	1.000	1.000	1.000	1.000
50	21	BINOM	1	1		1.000	1.000	1.000	1.000	1.000	1.000
51	27	BINOM	1	1		1.000	1.000	1.000	1.000	1.000	1.000
53	28	BINOM	1	1		1.000	1.000	1.000	1.000	1.000	1.000
54	29	BINOM	1	1		1.000	1.000	1.000	1.000	1.000	1.000
55	30	BINOM	1	1		1.000	1.000	1.000	1.000	1.000	1.000
56	31	BINOM	1	1		1.000	1.000	1.000	1.000	1.000	1.000
58	32	STDBY	2		0.344	1.000	1.000	1.000	1.000	1.000	1.000

LOGICAL EQUATIONS

```
L 18=1*4
L 19=002018*002009
L 20=1*4*9
L 21=2*4*9
L 22=2*4*001002009
L 23=11*12
L 24=3*23
L 25=2*23
L 26=002023
L 27=3*26
L 28=002011
L 29=002012
L 30=3*28*29
L 31=001003021
L 32=12*16*15
L 33=12*14*10
L 34=35*16*15
L 38=36*3
L 40=36*39
L 41=39*36
L 43=39*42
L 44=41*42
LB52=51*9+50*45+51*48*49*45+50*48*49*9+51*48*49*45*13+50*48*49*9*13
LB57=39*32+3*33+39*55*56*8*33+3*55*56*8*32
L 59=58*39*42*12
L 60=58*39*12*9
L 70= 20*5*25*7*13
L 71=1002020*5*48*49*7
L 72=2033
L 73=71*72
```

MISSION PHASE RELIABILITIES

	PHASE					
ELEMT	1	2	3	4	5	6
1	0.9999914	0.9999784	0.9997495	0.9996760	0.9995249	0.9993090
2	0.9999914	0.9999784	0.9997495	0.9996760	0.9995249	0.9993090
3	0.9999822	0.9999556	0.9994851	0.9993342	0.9990237	0.9985802
4	0.9999602	0.9999004	0.9988453	0.9985071	0.9978112	0.9968179
5	0.9999602	0.9999004	0.9988453	0.9985071	0.9978112	0.9968179
6	0.9999602	0.9999004	0.9988453	0.9985071	0.9978112	0.9968179
7	0.9995657	0.9989146	0.9874814	0.9838420	0.9763912	0.9658449

8	0.9993071	0.9982687	0.9801002	0.9743429	0.9625959	0.9460597
9	0.9969719	0.9924471	0.9158098	0.8925043	0.8463729	0.7845765
10	0.9984014	0.9960084	0.9546644	0.9417702	0.9157689	0.8798646
11	0.9990405	0.9976029	0.9725440	0.9646403	0.9485697	0.9260750
12	0.9990635	0.9976603	0.9731940	0.9654741	0.9497725	0.9277836
13	0.9995657	0.9989146	0.9874814	0.9838420	0.9763912	0.9658449
14	0.9974813	0.9937150	0.9294747	0.9097622	0.8704843	0.8172963
15	0.9987398	0.9968526	0.9640927	0.9538146	0.9329975	0.9040444
16	0.9998402	0.9996005	0.9953754	0.9940239	0.9912473	0.9872942
17	0.9972677	0.9931833	0.9237221	0.9024879	0.8602949	0.8034181
35	0.9994069	0.9985179	0.9829420	0.9779977	0.9678962	0.9536463
36	0.9999971	0.9999817	0.9976493	0.9961241	0.9918989	0.9835472
37	0.9999822	0.9998893	0.9866084	0.9783505	0.9565324	0.9165612
39	0.1580000	0.1580000	0.1580000	0.1580000	0.1580000	0.1580000
42	0.9999908	0.9999430	0.9929120	0.9884447	0.9763987	0.9535927
45	0.9969719	0.9924471	0.9158098	0.8925043	0.8463729	0.7845765
46	0.9999602	0.9999004	0.9988453	0.9985071	0.9978112	0.9968179
47	0.9999602	0.9999004	0.9988453	0.9985071	0.9978112	0.9968179
48	0.9999602	0.9999004	0.9988453	0.9985071	0.9978112	0.9968179
49	0.9999602	0.9999004	0.9988453	0.9985071	0.9978112	0.9968179
50	0.9999424	0.9998560	0.9983310	0.9978423	0.9968370	0.9954026
51	0.9999515	0.9998788	0.9985951	0.9981836	0.9973371	0.9961291
53	0.9999602	0.9999004	0.9988453	0.9985071	0.9978112	0.9968179
54	0.9999602	0.9999004	0.9988453	0.9985071	0.9978112	0.9968179
55	0.9999602	0.9999004	0.9988453	0.9985071	0.9978112	0.9968179
56	0.9999602	0.9999004	0.9988453	0.9985071	0.9978112	0.9968179
58	0.9999886	0.9999292	0.9912497	0.9857579	0.9710099	0.9432761
18	0.9999515	0.9998788	0.9985951	0.9981836	0.9973371	0.9961291
19	0.9999954	0.9999714	0.9963511	0.9940018	0.9875403	0.9749162
20	0.9969236	0.9923268	0.9145232	0.8908831	0.8441192	0.7815395
21	0.9969236	0.9923268	0.9145232	0.8908831	0.8441192	0.7815395
22	0.9999423	0.9998218	0.9915170	0.9866493	0.9737987	0.9499015
23	0.9981048	0.9952688	0.9464739	0.9313352	0.9009254	0.8591972
24	0.9980871	0.9952246	0.9459866	0.9307152	0.9000458	0.8579773
25	0.9980962	0.9952473	0.9462368	0.9310335	0.9004974	0.8586035
26	0.9999982	0.9999888	0.9985412	0.9975867	0.9949215	0.9895862
27	0.9999804	0.9999444	0.9980271	0.9969225	0.9939501	0.9881812
28	0.9999995	0.9999971	0.9996196	0.9993673	0.9986542	0.9971976
29	0.9999996	0.9999973	0.9996375	0.9993970	0.9987169	0.9973272
30	0.9999813	0.9999500	0.9987427	0.9980998	0.9963991	0.9931203
31	1.0000000	0.9999995	0.9993755	0.9987008	0.9962123	0.9895740
32	0.9976450	0.9941229	0.9339102	0.9153800	0.8783793	0.8281005

33	0.9949540	0.9874328	0.8635505	0.8272056	0.7571230	0.6671785
34	0.9979879	0.9949775	0.9432647	0.9272538	0.8951407	0.8511845
38	0.9999793	0.9999373	0.9971356	0.9954609	0.9909365	0.9821507
40	0.1579996	0.1579971	0.1576286	0.1573876	0.1567200	0.1554005
41	0.1579996	0.1579971	0.1576286	0.1573876	0.1567200	0.1554005
43	0.1579986	0.1579910	0.1568801	0.1561743	0.1542710	0.1506677
44	0.1579981	0.1579881	0.1565113	0.1555689	0.1530212	0.1481887
-52	0.9999908	0.9999429	0.9929091	0.9884396	0.9763872	0.9535667
-57	0.9999699	0.9998685	0.9881756	0.9810239	0.9621950	0.9277667
59	0.1578488	0.1576102	0.1513388	0.1486348	0.1422747	0.1318577
60	0.1573723	0.1564287	0.1395870	0.1342080	0.1233281	0.1084870
70	0.9941220	0.9853697	0.8428507	0.8016557	0.7230732	0.6239851
71	0.9994368	0.9985574	0.9768748	0.9677805	0.9464241	0.9109976
72	0.9999872	0.9999207	0.9902359	0.9841282	0.9677770	0.9371841
73	0.9994240	0.9984782	0.9673365	0.9524201	0.9159274	0.8537724

ADVANCED PLANETARY PROBE (PARTS COUNT RELIABILITY ASSESSMENT)
SUBSYSTEM 2 ATTITUDE CONTROL SUBSYSTEM A
UNIT 1 SOLAR CELL ASSEMBLY (ANALOG)

COMPONENT PART	QTY	FAILURE RATE	EXTENSION
71 SOLAR CELL	2	20	40
TOTAL	2		40
CONNECTIONS	26	0.500	13
TOTAL			53

ADVANCED PLANETARY PROBE (PARTS COUNT RELIABILITY ASSESSMENT)
SUBSYSTEM 2 ATTITUDE CONTROL SUBSYSTEM A
UNIT 2 FREQUENCY DIVIDER (DIGTAL)

COMPONENT PART	QTY	FAILURE RATE	EXTENSION

UNIT INPUTED AS ENTITY...SEE UNIT SUMMARY.

ADVANCED PLANETARY PROBE (PARTS COUNT RELIABILITY ASSESSMENT)
SUBSYSTEM 2 ATTITUDE CONTROL SUBSYSTEM A
UNIT 3 COMMAND FLIP FLOP (DIGTAL)

COMPONENT PART	QTY	FAILURE RATE	EXTENSION
62 IC,DIG.STOR	1	22	22
TOTAL	1		22
CONNECTIONS	10	0.500	5
TOTAL			27

ADVANCED PLANETARY PROBE (PARTS COUNT RELIABILITY ASSESSMENT)
SUBSYSTEM 2 ATTITUDE CONTROL SUBSYSTEM A
UNIT 4 LEVEL DETECTOR (ANALOG)

COMPONENT PART	QTY	FAILURE RATE	EXTENSION
1 RES,CARBCOMP	8	3	24
18 CAP,FIX.CER.	4	5	20
35 XIST,SI,LT1W	2	17	34
62 IC,DIG.STOR	1	22	22
63 IC,DIG.GATES	2	16	32
TOTAL	17		132
CONNECTIONS	60	0.500	30
TOTAL			162

ADVANCED PLANETARY PROBE (PARTS COUNT RELIABILITY ASSESSMENT)
SUBSYSTEM 2 ATTITUDE CONTROL SUBSYSTEM A
UNIT 5 ZERO CROSSING DETECTOR (ANALOG)

	COMPONENT PART	QTY	FAILURE RATE	EXTENSION
1	RES,CARBCOMP	7	3	21
7	RES,VAR,CCOM	1	27	27
18	CAP,FIX.CER.	4	5	20
35	XIST,SI,LT1W	2	17	34
62	IC,DIG.STOR	2	22	44
63	IC,DIG.GATES	2	16	32
	TOTAL	18		178
	CONNECTIONS	71	0.500	35
	TOTAL			213

ADVANCED PLANETARY PROBE (PARTS COUNT RELIABILITY ASSESSMENT)
SUBSYSTEM 2 ATTITUDE CONTROL SUBSYSTEM A
UNIT 6 PREAMPLIFIER (ANALOG)

	COMPONENT PART	QTY	FAILURE RATE	EXTENSION
1	RES,CARBCOMP	10	3	30
7	RES,VAR,CCOM	1	27	27
18	CAP,FIX.CER.	2	5	10
35	XIST,SI,LT1W	5	17	85
	TOTAL	18		152
	CONNECTIONS	42	0.500	21
	TOTAL			173

ADVANCED PLANETARY PROBE (PARTS COUNT RELIABILITY ASSESSMENT)
SUBSYSTEM 2 ATTITUDE CONTROL SUBSYSTEM A
UNIT 7 REVERSIBLE COUNTER (DIGTAL)

COMPONENT PART	QTY	FAILURE RATE	EXTENSION
62 IC,DIG.STOR	7	22	154
TOTAL	7		154
CONNECTIONS	70	0.500	35
TOTAL			189

ADVANCED PLANETARY PROBE (PARTS COUNT RELIABILITY ASSESSMENT)
SUBSYSTEM 2 ATTITUDE CONTROL SUBSYSTEM A
UNIT 8 FREQUENCY DIVIDER (DIGTAL)

COMPONENT PART	QTY	FAILURE RATE	EXTENSION
62 IC,DIG.STOR	7	22	154
TOTAL	7		154
CONNECTIONS	70	0.500	35
TOTAL			189

ADVANCED PLANETARY PROBE (PARTS COUNT RELIABILITY ASSESSMENT)
SUBSYSTEM 2 ATTITUDE CONTROL SUBSYSTEM A
UNIT 9 CONTROL LOGIC (DIGTAL)

COMPONENT PART	QTY	FAILURE RATE	EXTENSION
62 IC,DIG.STOR	2	22	44
63 IC,DIG.GATES	5	16	80
TOTAL	7		124
CONNECTIONS	70	0.500	35
TOTAL			159

ADVANCED PLANETARY PROBE (PARTS COUNT RELIABILITY ASSESSMENT)
SUBSYSTEM 2 ATTITUDE CONTROL SUBSYSTEM A
UNIT 10 S/C ANGLE REGISTER (DIGTAL)

COMPONENT PART	QTY	FAILURE RATE	EXTENSION
62 IC,DIG.STOR	7	22	154
TOTAL	7		154
CONNECTIONS	70	0.500	35
TOTAL			189

ADVANCED PLANETARY PROBE (PARTS COUNT RELIABILITY ASSESSMENT) A
SUBSYSTEM 2 ATTITUDE CONTROL SUBSYSTEM
UNIT 11 REF TIMING REG. COMPAR (DIGTAL)

COMPONENT PART	QTY	FAILURE RATE	EXTENSION
62 IC,DIG.STOR	11	22	242
TOTAL	11		242
CONNECTIONS	110	0.500	55
TOTAL			297

ADVANCED PLANETARY PROBE (PARTS COUNT RELIABILITY ASSESSMENT) A
SUBSYSTEM 2 ATTITUDE CONTROL SUBSYSTEM
UNIT 12 GATING LOGIC (DIGTAL)

COMPONENT PART	QTY	FAILURE RATE	EXTENSION
63 IC,DIG.GATES	16	16	256
TOTAL	16		256
CONNECTIONS	160	0.500	80
TOTAL			336

ADVANCED PLANETARY PROBE (PARTS COUNT RELIABILITY ASSESSMENT)
SUBSYSTEM 2 ATTITUDE CONTROL SUBSYSTEM A
UNIT 13 SOL VALVE DRIVERS (DIGTAL)

COMPONENT PART	QTY	FAILURE RATE	EXTENSION
1 RES,CARBCOMP	7	1	7
5 RES,WIRE,PWR	1	33	33
18 CAP,FIX.CER.	4	5	20
35 XIST,SI,LT1W	1	7	7
36 XIST,SI,GT1W	1	43	43
TOTAL	14		110
CONNECTIONS	30	0.500	15
TOTAL			125

ADVANCED PLANETARY PROBE (PARTS COUNT RELIABILITY ASSESSMENT)
SUBSYSTEM 2 ATTITUDE CONTROL SUBSYSTEM A
UNIT 14 EXPLOSIVE VALVE DRIVERS (DIGTAL)

COMPONENT PART	QTY	FAILURE RATE	EXTENSION
1 RES,CARBCOMP	4	1	4
3 RES,CARBFILM	1	17	17
18 CAP,FIX.CER.	1	5	5
27 CAP,TANT.SLD	1	7	7
36 XIST,SI,GT1W	1	43	43
TOTAL	8		76
CONNECTIONS	17	0.500	8
TOTAL			84

ADVANCED PLANETARY PROBE (PARTS COUNT RELIABILITY ASSESSMENT)
SUBSYSTEM 2 ATTITUDE CONTROL SUBSYSTEM
UNIT 15 NITROGEN TANK (ANALOG)

COMPONENT PART QTY FAILURE RATE EXTENSION

UNIT INPUTED AS ENTITY...SEE UNIT SUMMARY.

A

ADVANCED PLANETARY PROBE (PARTS COUNT RELIABILITY ASSESSMENT)
SUBSYSTEM 2 ATTITUDE CONTROL SUBSYSTEM
UNIT 16 REGULATOR (ANALOG)

COMPONENT PART QTY FAILURE RATE EXTENSION

UNIT INPUTED AS ENTITY...SEE UNIT SUMMARY.

A

ADVANCED PLANETARY PROBE (PARTS COUNT RELIABILITY ASSESSMENT)
SUBSYSTEM 2 ATTITUDE CONTROL SUBSYSTEM
UNIT 17 RELIEF VALVE (ANALOG)

COMPONENT PART QTY FAILURE RATE EXTENSION

UNIT INPUTED AS ENTITY...SEE UNIT SUMMARY.

A

ADVANCED PLANETARY PROBE (PARTS COUNT RELIABILITY ASSESSMENT)
SUBSYSTEM 2 ATTITUDE CONTROL SUBSYSTEM A
UNIT 18 SOLENOID VALVES (ANALOG)

COMPONENT PART	QTY	FAILURE RATE	EXTENSION

UNIT INPUTED AS ENTITY...SEE UNIT SUMMARY.

ADVANCED PLANETARY PROBE (PARTS COUNT RELIABILITY ASSESSMENT)
SUBSYSTEM 2 ATTITUDE CONTROL SUBSYSTEM A
UNIT 19 FILL VALVE (ANALOG)

COMPONENT PART	QTY	FAILURE RATE	EXTENSION

UNIT INPUTED AS ENTITY...SEE UNIT SUMMARY.

ADVANCED PLANETARY PROBE (PARTS COUNT RELIABILITY ASSESSMENT)
SUBSYSTEM 2 ATTITUDE CONTROL SUBSYSTEM A
UNIT 20 LINES AND FITTINGS (ANALOG)

COMPONENT PART	QTY	FAILURE RATE	EXTENSION

UNIT INPUTED AS ENTITY...SEE UNIT SUMMARY.

ADVANCED PLANETARY PROBE (PARTS COUNT RELIABILITY ASSESSMENT)
SUBSYSTEM 2 ATTITUDE CONTROL SUBSYSTEM A
UNIT 21 FILTER (ANALOG)

COMPONENT PART	QTY	FAILURE RATE	EXTENSION

UNIT INPUTED AS ENTITY...SEE UNIT SUMMARY.

ADVANCED PLANETARY PROBE (PARTS COUNT RELIABILITY ASSESSMENT)
SUBSYSTEM 2 ATTITUDE CONTROL SUBSYSTEM A
UNIT 22 LOW PRESSURE TRANSDUCER (ANALOG)

COMPONENT PART	QTY	FAILURE RATE	EXTENSION

UNIT INPUTED AS ENTITY...SEE UNIT SUMMARY.

ADVANCED PLANETARY PROBE (PARTS COUNT RELIABILITY ASSESSMENT)
SUBSYSTEM 2 ATTITUDE CONTROL SUBSYSTEM A
UNIT 23 HIGH PRESSURE TRANSDUCER (ANALOG)

COMPONENT PART	QTY	FAILURE RATE	EXTENSION

UNIT INPUTED AS ENTITY...SEE UNIT SUMMARY.

ADVANCED PLANETARY PROBE (PARTS COUNT RELIABILITY ASSESSMENT)
SUBSYSTEM 2 ATTITUDE CONTROL SUBSYSTEM A
NO. OF COMPONENT PARTS= 133 SUBSYSTEM FR= 2196

UNIT SUMMARY.....

NO	DESCRIPTION	PART USAGE	FAILURE RATE	SUM FR SQUARED	SUM FR CUBED
1	SOLAR CELL ASSEMBLY	ANALOG	53	0.80000E-15	0.16000E-22
2	FREQUENCY DIVIDER	DIGTAL	189	0.	0.
3	COMMAND FLIP FLOP	DIGTAL	27	0.48400E-15	0.10648E-22
4	LEVEL DETECTOR	ANALOG	162	0.17460E-14	0.29382E-22
5	ZERO CROSSING DETECTOR	ANALOG	213	0.29500E-14	0.59686E-22
6	PREAMPLIFIER	ANALOG	173	0.23140E-14	0.44768E-22
7	REVERSIBLE COUNTER	DIGTAL	189	0.33880E-14	0.74536E-22
8	FREQUENCY DIVIDER	DIGTAL	189	0.33880E-14	0.74536E-22
9	CONTROL LOGIC	DIGTAL	159	0.22480E-14	0.41776E-22
10	S/C ANGLE REGISTER	DIGTAL	189	0.33880E-14	0.74536E-22
11	REF TIMING REG. COMPAR	DIGTAL	297	0.53240E-14	0.11713E-21
12	GATING LOGIC	DIGTAL	336	0.40960E-14	0.65536E-22
13	SOL VALVE DRIVERS	DIGTAL	125	0.30940E-14	0.11629E-21
14	EXPLOSIVE VALVE DRIVERS	DIGTAL	84	0.22160E-14	0.84892E-22
15	NITROGEN TANK	ANALOG	120	0.	0.
16	REGULATOR	ANALOG	1000	0.	0.
17	RELIEF VALVE	ANALOG	10	0.	0.
18	SOLENOID VALVES	ANALOG	6200	0.	0.
19	FILL VALVE	ANALOG	10	0.	0.
20	LINES AND FITTINGS	ANALOG	30	0.	0.
21	FILTER	ANALOG	120	0.	0.
22	LOW PRESSURE TRANSDUCER	ANALOG	30	0.	0.
23	HIGH PRESSURE TRANSDUCER	ANALOG	30	0.	0.

MISSION RELIABILITIES....

BASIC ELEMENT SPECIFICATIONS

ELEMT NO.	REF. UNIT	REDUN. TYPE	NO. PRESENT	NO. NEEDED	OFF RATIO	PHASE L-FACTORS... 1	2	3	4	5	6
1	1	BINOM	1	1		1.000	1.000	1.000	1.000	1.000	1.000
2	2	BINOM	1	1		1.000	1.000	1.000	1.000	1.000	1.000
3	3	BINOM	1	1		1.000	1.000	1.000	1.000	1.000	1.000

4	4	BINOM	1	1		1.000	1.000	1.000	1.000	1.000	1.000
5	5	BINOM	1	1		1.000	1.000	1.000	1.000	1.000	1.000
6	6	BINOM	1	1		1.000	1.000	1.000	1.000	1.000	1.000
7	7	BINOM	1	1		1.000	1.000	1.000	1.000	1.000	1.000
8	8	BINOM	1	1		1.000	1.000	1.000	1.000	1.000	1.000
9	9	BINOM	1	1		1.000	1.000	1.000	1.000	1.000	1.000
10	10	BINOM	1	1		1.000	1.000	1.000	1.000	1.000	1.000
11	11	BINOM	1	1		1.000	1.000	1.000	1.000	1.000	1.000
12	12	BINOM	1	1		1.000	1.000	1.000	1.000	1.000	1.000
13	13	BINOM	1	1		1.000	1.000	1.000	1.000	1.000	1.000
14	14	BINOM	1	1		1.000	1.000	1.000	1.000	1.000	1.000
21	1	BINOM	2	1		1.000	1.000	1.000	1.000	1.000	1.000
22	2	STDBY	2		0.	1.000	1.000	1.000	1.000	1.000	1.000
23	3	BINOM	2	1		1.000	1.000	1.000	1.000	1.000	1.000
24	4	BINOM	2	1		1.000	1.000	1.000	1.000	1.000	1.000
25	5	BINOM	2	1		1.000	1.000	1.000	1.000	1.000	1.000
26	6	BINOM	2	1		1.000	1.000	1.000	1.000	1.000	1.000
27	7	BINOM	3	2		1.000	1.000	1.000	1.000	1.000	1.000
28	8	BINOM	3	2		1.000	1.000	1.000	1.000	1.000	1.000
29	9	BINOM	3	2		1.000	1.000	1.000	1.000	1.000	1.000
30	10	BINOM	3	2		1.000	1.000	1.000	1.000	1.000	1.000
31	11	BINOM	3	2		1.000	1.000	1.000	1.000	1.000	1.000
32	12	BINOM	3	2		1.000	1.000	1.000	1.000	1.000	1.000
33	13	BINOM	2	1		1.000	1.000	1.000	1.000	1.000	1.000
34	14	BINOM	2	1		1.000	1.000	1.000	1.000	1.000	1.000
40	15	BINOM	1	1		1.000	1.000	1.000	1.000	1.000	1.000
41	16	BINOM	1	1		1.000	1.000	1.000	1.000	1.000	1.000
42	17	BINOM	1	1		1.000	1.000	1.000	1.000	1.000	1.000
43	18	BINOM	1	1		1.000	1.000	1.000	1.000	1.000	1.000
44	19	BINOM	1	1		1.000	1.000	1.000	1.000	1.000	1.000
45	20	BINOM	1	1		1.000	1.000	1.000	1.000	1.000	1.000
46	21	BINOM	1	1		1.000	1.000	1.000	1.000	1.000	1.000
50	18	BINOM	2	1		1.000	1.000	1.000	1.000	1.000	1.000

LOGICAL EQUATIONS

```
L 35=21*22*23*24*25*26*27*28*29*30*31*32*33*34*21*23*24*25*25*29*29
L 36=35*31*31*31
L 39=34*7
L 40=34*23
L 41=34*26
L 47=40*41*42*43*44*45*46
```

L 48=40*46*41
L 49=00100204 8
L 51=48*50*42*44
L 52=51*36

MISSION PHASE RELIABILITIES

	PHASE					
ELEMT	1	2	3	4	5	6
1	0.9999746	0.9999364	0.9992625	0.9990465	0.9986018	0.9979669
2	0.9999093	0.9997732	0.9973726	0.9966038	0.9950228	0.9927687
3	0.9999870	0.9999676	0.9996242	0.9995141	0.9992874	0.9989637
4	0.9999222	0.9998056	0.9977475	0.9970882	0.9957323	0.9937985
5	0.9998978	0.9997444	0.9970394	0.9961733	0.9943926	0.9918542
6	0.9999170	0.9997924	0.9975947	0.9968908	0.9954432	0.9933788
7	0.9999093	0.9997732	0.9973726	0.9966038	0.9950228	0.9927687
8	0.9999093	0.9997732	0.9973726	0.9966038	0.9950228	0.9927687
9	0.9999237	0.9998092	0.9977892	0.9971421	0.9958112	0.9939130
10	0.9999093	0.9997732	0.9973726	0.9966038	0.9950228	0.9927687
11	0.9998574	0.9996437	0.9958743	0.9946683	0.9921899	0.9886600
12	0.9998387	0.9995969	0.9953338	0.9939702	0.9911688	0.9871805
13	0.9999400	0.9998500	0.9982615	0.9977525	0.9967054	0.9952115
14	0.9999597	0.9998992	0.9988314	0.9984891	0.9977849	0.9967796
21	1.0000000	1.0000000	0.9999995	0.9999991	0.9999980	0.9999959
22	1.0000000	1.0000000	0.9999965	0.9999942	0.9999876	0.9999738
23	1.0000000	1.0000000	0.9999999	0.9999998	0.9999995	0.9999989
24	1.0000000	1.0000000	0.9999949	0.9999915	0.9999818	0.9999615
25	1.0000000	0.9999999	0.9999912	0.9999854	0.9999686	0.9999336
26	1.0000000	1.0000000	0.9999942	0.9999903	0.9999792	0.9999562
27	1.0000000	0.9999998	0.9999793	0.9999655	0.9999259	0.9998439
28	1.0000000	0.9999998	0.9999793	0.9999655	0.9999259	0.9998439
29	1.0000000	0.9999999	0.9999854	0.9999755	0.9999475	0.9998893
30	1.0000000	0.9999998	0.9999793	0.9999655	0.9999259	0.9998439
31	0.9999999	0.9999996	0.9999491	0.9999150	0.9998180	0.9996171
32	0.9999999	0.9999995	0.9999349	0.9998914	0.9997674	0.9995112
33	1.0000000	1.0000000	0.9999970	0.9999949	0.9999891	0.9999771
34	1.0000000	1.0000000	0.9999986	0.9999977	0.9999951	0.9999896
40	1.0000000	1.0000000	0.9999985	0.9999975	0.9999946	0.9999885
41	1.0000000	0.9999999	0.9999928	0.9999880	0.9999743	0.9999458
42	0.9999952	0.9999880	0.9998608	0.9998200	0.9997360	0.9996161
43	0.9970284	0.9925876	0.9173153	0.8944019	0.8490137	0.7881396
44	0.9999952	0.9999880	0.9998608	0.9998200	0.9997360	0.9996161
45	0.9999856	0.9999640	0.9995825	0.9994601	0.9992083	0.9988487

46	0.9999424	0.9998560	0.9983310	0.9978423	0.9968370	0.9954026
50	0.9999912	0.9999451	0.9931632	0.9888490	0.9772031	0.9551152
35	0.9999997	0.9999980	0.9997266	0.9995436	0.9990215	0.9979400
36	0.9999995	0.9999968	0.9995739	0.9992888	0.9984760	0.9967942
39	0.9999093	0.9997732	0.9973712	0.9966015	0.9950179	0.9927584
40	1.0000000	1.0000000	0.9999985	0.9999975	0.9999946	0.9999885
41	1.0000000	0.9999999	0.9999928	0.9999880	0.9999743	0.9999458
47	0.9969471	0.9923851	0.9151392	0.8916564	0.8451855	0.7829600
48	0.9999424	0.9998559	0.9983223	0.9978279	0.9968060	0.9953372
49	1.0000000	1.0000000	0.9999972	0.9999953	0.9999898	0.9999783
51	0.9999240	0.9997770	0.9912211	0.9863460	0.9735678	0.9499319
52	0.9999234	0.9997738	0.9907987	0.9856445	0.9720841	0.9468866

ADVANCED PLANETARY PROBE (PARTS COUNT RELIABILITY ASSESSMENT)
SUBSYSTEM 3 COMMAND DECODING AND DISTRIBUTING SUBSYSTEM (CDDS)
UNIT 1 DETECTOR (ANALOG)

	COMPONENT PART	QTY	FAILURE RATE	EXTENSION
1	RES,CARBCOMP	70	3	210
2	RES,MET.FILM	30	3	90
8	DIO,SI,GENRL	49	5	245
18	CAP,FIX.CER.	30	5	150
27	CAP,TANT.SLD	5	7	35
35	XIST,SI,LT1W	36	17	612
45	TRF,LT100V6T	4	40	160
61	COIL,ANALOG	2	4	8
62	IC,DIG.STOR	27	22	594
63	IC,DIG.GATES	24	16	384
65	IC,DIG.ANALG	1	80	80
	TOTAL	278		2568
	CONNECTIONS	1024	0.500	512
	TOTAL			3080

ADVANCED PLANETARY PROBE (PARTS COUNT RELIABILITY ASSESSMENT)
SUBSYSTEM 3 COMMAND DECODING AND DISTRIBUTING SUBSYSTEM (CDDS)
UNIT 2 INPUT SELECTOR-DECODER (DIGTAL)

	COMPONENT PART	QTY	FAILURE RATE	EXTENSION
2	RES,MET.FILM	12	3	36
8	DIO,SI,GENRL	8	2	16
20	CAP,FIX,GLAS	4	1	4
37	XIST,SI,SWIT	12	7	84
62	IC,DIG.STOR	29	22	638
63	IC,DIG.GATES	100	16	1600
	TOTAL	165		2378
	CONNECTIONS	1374	0.500	687
	TOTAL			3065

ADVANCED PLANETARY PROBE (PARTS COUNT RELIABILITY ASSESSMENT)
SUBSYSTEM 3 COMMAND DECODING AND DISTRIBUTING SUBSYSTEM (CDDS)
UNIT 3 OUTPUT SELECTOR-DECODER (DIGTAL)

	COMPONENT PART	QTY	FAILURE RATE	EXTENSION
2	RES,MET.FILM	88	3	264
8	DIO,SI,GENRL	104	2	208
20	CAP,FIX,GLAS	20	1	20
37	XIST,SI,SWIT	300	7	2100
62	IC,DIG.STOR	41	22	902
63	IC,DIG.GATES	128	16	2048
	TOTAL	681		5542
	CONNECTIONS	3014	0.500	1507
	TOTAL			7049

ADVANCED PLANETARY PROBE (PARTS COUNT RELIABILITY ASSESSMENT)
SUBSYSTEM 3 COMMAND DECODING AND DISTRIBUTING SUBSYSTEM (CDDS)
UNIT 4 COMPUTER SEQUENCER (DIGTAL)

	COMPONENT PART	QTY	FAILURE RATE	EXTENSION
2	RES,MET.FILM	47	3	141
11	DIO,SI,SWITC	3	2	6
20	CAP,FIX,GLAS	3	1	3
37	XIST,SI,SWIT	28	7	196
51	MEM.CR/HUND.	5	1	5
62	IC,DIG.STOR	10	22	220
63	IC,DIG.GATES	24	16	384
64	IC,DIG.ISOL	3	15	45
	TOTAL	123		1000
	CONNECTIONS	560	0.500	280
	TOTAL			1280

ADVANCED PLANETARY PROBE (PARTS COUNT RELIABILITY ASSESSMENT)
SUBSYSTEM 3 COMMAND DECODING AND DISTRIBUTING SUBSYSTEM (CDDS)
UNIT 5 TIMING AND MODE SELECT (DIGTAL)

	COMPONENT PART	QTY	FAILURE RATE	EXTENSION
2	RES,MET.FILM	7	3	21
11	DIO,SI,SWITC	2	2	4
20	CAP,FIX,GLAS	2	1	2
37	XIST,SI,SWIT	4	7	28
62	IC,DIG.STOR	3	22	66
63	IC,DIG.GATES	12	16	192
	TOTAL	30		313
	CONNECTIONS	184	0.500	92
	TOTAL			405

ADVANCED PLANETARY PROBE (PARTS COUNT RELIABILITY ASSESSMENT)
SUBSYSTEM 3 COMMAND DECODING AND DISTRIBUTING SUBSYSTEM (CDDS)
UNIT 6 OUTPUT DRIVER (DIGTAL)

	COMPONENT PART	QTY	FAILURE RATE	EXTENSION
2	RES,MET.FILM	12	3	36
8	DIO,SI,GENRL	10	2	20
18	CAP,FIX.CER.	2	5	10
37	XIST,SI,SWIT	30	7	210
62	IC,DIG.STOR	1	22	22
63	IC,DIG.GATES	4	16	64
	TOTAL	59		362
	CONNECTIONS	188	0.500	94
	TOTAL			456

ADVANCED PLANETARY PROBE (PARTS COUNT RELIABILITY ASSESSMENT)
SUBSYSTEM 3 COMMAND DECODING AND DISTRIBUTING SUBSYSTEM (CDDS)
UNIT 7 DETECTOR-(INT.RED) (ANALOG)

	COMPONENT PART	QTY	FAILURE RATE	EXTENSION
1	RES,CARBCOMP	70	3	210
2	RES,MET.FILM	30	3	90
8	DIO,SI,GENRL	49	5	245
18	CAP,FIX.CER.	30	5	150
27	CAP,TANT.SLD	5	7	35
35	XIST,SI,LT1W	36	17	612
45	TRF,LT100V6T	4	40	160
61	COIL,ANALOG	2	4	8
62	IC,DIG.STOR	27	22	594
63	IC,DIG.GATES	24	16	384
65	IC,DIG.ANALG	1	80	80
	TOTAL	278		2568
	CONNECTIONS	1024	0.500	512
	TOTAL			3080

ADVANCED PLANETARY PROBE (PARTS COUNT RELIABILITY ASSESSMENT)
SUBSYSTEM 3 COMMAND DECODING AND DISTRIBUTING SUBSYSTEM (CDDS)
UNIT 8 INPUT SELECTOR (DIGTAL)

COMPONENT PART	QTY	FAILURE RATE	EXTENSION
2 RES,MET.FILM	12	3	36
8 DIO,SI,GENRL	8	2	16
20 CAP,FIX,GLAS	4	1	4
37 XIST,SI,SWIT	12	7	84
62 IC,DIG.STOR	29	22	638
63 IC,DIG.GATES	100	16	1600
TOTAL	165		2378
CONNECTIONS	1374	0.500	687
TOTAL			3065

ADVANCED PLANETARY PROBE (PARTS COUNT RELIABILITY ASSESSMENT)
SUBSYSTEM 3 COMMAND DECODING AND DISTRIBUTING SUBSYSTEM (CDDS)
UNIT 9 OUTPUT SELECTOR-DECODER (DIGTAL)

	COMPONENT PART	QTY	FAILURE RATE	EXTENSION
2	RES,MET.FILM	88	3	264
8	DIO,SI,GENRL	104	2	208
20	CAP,FIX,GLAS	20	1	20
37	XIST,SI,SWIT	300	7	2100
62	IC,DIG.STOR	41	22	902
63	IC,DIG.GATES	128	16	2048
	TOTAL	681		5542
	CONNECTIONS	3014	0.500	1507
	TOTAL			7049

ADVANCED PLANETARY PROBE (PARTS COUNT RELIABILITY ASSESSMENT)
SUBSYSTEM 3 COMMAND DECODING AND DISTRIBUTING SUBSYSTEM (CDDS)
UNIT 10 COMPUTER SEQUENCER (DIGTAL)

	COMPONENT PART	QTY	FAILURE RATE	EXTENSION
2	RES,MET.FILM	47	3	141
11	DIO,SI,SWITC	3	2	6
20	CAP,FIX,GLAS	3	1	3
37	XIST,SI,SWIT	28	7	196
51	MEM.CR/HUND.	5	1	5
62	IC,DIG.STOR	10	22	220
63	IC,DIG.GATES	24	16	384
64	IC,DIG.ISOL	3	15	45
	TOTAL	123		1000
	CONNECTIONS	560	0.500	280
	TOTAL			1280

ADVANCED PLANETARY PROBE (PARTS COUNT RELIABILITY ASSESSMENT)
SUBSYSTEM 3 COMMAND DECODING AND DISTRIBUTING SUBSYSTEM (CDDS)
UNIT 11 TIMING AND MODE SELECT (DIGTAL)

	COMPONENT PART	QTY	FAILURE RATE	EXTENSION
2	RES,MET.FILM	7	3	21
11	DIO,SI,SWITC	2	2	4
20	CAP,FIX,GLAS	2	1	2
37	XIST,SI,SWIT	4	7	28
62	IC,DIG.STOR	3	22	66
63	IC,DIG.GATES	12	16	192
	TOTAL	30		313
	CONNECTIONS	184	0.500	92
	TOTAL			405

ADVANCED PLANETARY PROBE (PARTS COUNT RELIABILITY ASSESSMENT)
SUBSYSTEM 3 COMMAND DECODING AND DISTRIBUTING SUBSYSTEM (CDDS)
UNIT 12 OUTPUT DRIVER (DIGTAL)

COMPONENT PART	QTY	FAILURE RATE	EXTENSION
2 RES,MET.FILM	12	3	36
8 DIO,SI,GENRL	10	2	20
18 CAP,FIX.CER.	2	5	10
37 XIST,SI,SWIT	30	7	210
62 IC,DIG.STOR	1	22	22
63 IC,DIG.GATES	4	16	64
TOTAL	59		362
CONNECTIONS	188	0.500	94
TOTAL			456

ADVANCED PLANETARY PROBE (PARTS COUNT RELIABILITY ASSESSMENT)
SUBSYSTEM 3 COMMAND DECODING AND DISTRIBUTING SUBSYSTEM (CDDS)
UNIT 13 COMMAND DISTRIBUTION (DIGTAL)

COMPONENT PART	QTY	FAILURE RATE	EXTENSION
8 DIO,SI,GENRL	300	2	600
27 CAP,TANT.SLD	3	7	21
53 RELY.GEN.4CS	6	187	1122
~~55 RLY,LG,2C S2W~~ 17 SIL. CONT. RECT.	150	~~187~~ 17	~~28050~~ 2250
TOTAL	459		~~35793~~ 1993
CONNECTIONS	1866	0.500	933
TOTAL			2926 ~~36726~~

Multiplying by a rate bias factor of .1

293

ADVANCED PLANETARY PROBE (PARTS COUNT RELIABILITY ASSESSMENT)
SUBSYSTEM 3 COMMAND DECODING AND DISTRIBUTING SUBSYSTEM (CDDS)
NO. OF COMPONENT PARTS= 3131 SUBSYSTEM FR= 67396

UNIT SUMMARY.....

NO	DESCRIPTION	PART USAGE	FAILURE RATE	SUM FR SQUARED	SUM FR CUBED	
1	DETECTOR	ANALOG	3080	0.45568E-13	0.13451E-20	
2	INPUT SELECTOR-DECODER	DIGTAL	3065	0.40368E-13	0.72290E-21	
3	OUTPUT SELECTOR-DECODER	DIGTAL	7049	0.68540E-13	0.10670E-20	
4	COMPUTER SEQUENCER	DIGTAL	1280	0.13474E-13	0.22581E-21	
5	TIMING AND MODE SELECT	DIGTAL	405	0.47930E-14	0.82675E-22	
6	OUTPUT DRIVER	DIGTAL	456	0.31760E-14	0.37976E-22	
7	DETECTOR-(INT.RED)	ANALOG	3080	0.45568E-13	0.13451E-20	(PLRD
8	INPUT SELECTOR	DIGTAL	3065	0.40368E-13	0.72290E-21	(PLRD
9	OUTPUT SELECTOR-DECODER	DIGTAL	7049	0.68540E-13	0.10670E-20	(PLRD
10	COMPUTER SEQUENCER	DIGTAL	1280	0.13474E-13	0.22581E-21	(PLRD
11	TIMING AND MODE SELECT	DIGTAL	405	0.47930E-14	0.82675E-22	(PLRD
12	OUTPUT DRIVER	DIGTAL	456	0.31760E-14	0.37976E-22	(PLRD
13	COMMAND DISTRIBUTION	DIGTAL	~~36726~~	0.79405E-11	0.17938E-17	

172

MISSION RELIABILITIES....

BASIC ELEMENT SPECIFICATIONS

ELEMT NO.	REF. UNIT	REDUN. TYPE	NO. PRESENT	NO. NEEDED	OFF RATIO	PHASE L-FACTORS... 1	2	3	4	5	6
1	1	BINOM	1	1		1.000	1.000	1.000	1.000	1.000	1.000
2	2	BINOM	1	1		1.000	1.000	1.000	1.000	1.000	1.000
3	3	BINOM	1	1		1.000	1.000	1.000	1.000	1.000	1.000
4	4	BINOM	1	1		1.000	1.000	1.000	1.000	1.000	1.000
5	5	BINOM	1	1		1.000	1.000	1.000	1.000	1.000	1.000
6	6	BINOM	1	1		1.000	1.000	1.000	1.000	1.000	1.000
11	1	BINOM	2	1		1.000	1.000	1.000	1.000	1.000	1.000
12	2	BINOM	2	1		1.000	1.000	1.000	1.000	1.000	1.000
13	3	BINOM	2	1		1.000	1.000	1.000	1.000	1.000	1.000
14	4	BINOM	2	1		1.000	1.000	1.000	1.000	1.000	1.000
15	5	BINOM	2	1		1.000	1.000	1.000	1.000	1.000	1.000
16	6	BINOM	2	1		1.000	1.000	1.000	1.000	1.000	1.000
17	7	BINOM	1	1		1.000	1.000	1.000	1.000	1.000	1.000

18	8	BINOM	1	1	1.000	1.000	1.000	1.000	1.000	1.000
19	9	BINOM	1	1	1.000	1.000	1.000	1.000	1.000	1.000
20	10	BINOM	1	1	1.000	1.000	1.000	1.000	1.000	1.000
21	11	BINOM	1	1	1.000	1.000	1.000	1.000	1.000	1.000
22	12	BINOM	1	1	1.000	1.000	1.000	1.000	1.000	1.000
33	13	BINOM	1	1	1.000	1.000	1.000	1.000	1.000	1.000
34	13	BINOM	1	1	0.100	0.100	0.100	0.100	0.100	0.100

LOGICAL EQUATIONS

```
L  7=1*2*3*4*5*6
L 23=11*12*13*14*15*16
L 24=17*18*19*20*21*22
L 25=000002007
L 26=001002007
L 28=1*2
L 29=001002028
L 30=29*13*14*15*16
L 37=28*33
L 38=28*34
```

MISSION PHASE RELIABILITIES

	PHASE					
ELEMT	1	2	3	4	5	6
1	0.9985227	0.9963108	0.9580325	0.9460688	0.9219060	0.8884544
2	0.9985299	0.9963287	0.9582325	0.9463243	0.9222712	0.8889663
3	0.9966222	0.9915769	0.9065382	0.8808376	0.8301959	0.7628594
4	0.9993858	0.9984652	0.9823402	0.9772234	0.9667726	0.9520364
5	0.9998056	0.9995141	0.9943783	0.9927365	0.9893650	0.9845683
6	0.9997811	0.9994529	0.9936726	0.9918256	0.9880338	0.9826420
11	0.9999978	0.9999864	0.9982387	0.9970914	0.9939013	0.9875576
12	0.9999978	0.9999865	0.9982555	0.9971189	0.9939582	0.9876715
13	0.9999886	0.9999290	0.9912649	0.9858003	0.9711666	0.9437643
14	0.9999996	0.9999976	0.9996881	0.9994812	0.9988959	0.9976995
15	1.0000000	0.9999998	0.9999684	0.9999472	0.9998869	0.9997619
16	0.9999999	0.9999997	0.9999600	0.9999332	0.9998568	0.9996987
17	0.9999989	0.9999932	0.9991110	0.9985258	0.9968827	0.9935635
18	0.9999989	0.9999933	0.9991191	0.9985392	0.9969106	0.9936205
19	0.9999943	0.9999645	0.9954957	0.9926098	0.9847099	0.9693899
20	0.9999998	0.9999988	0.9998444	0.9997407	0.9994463	0.9988404
21	1.0000000	0.9999999	0.9999846	0.9999743	0.9999449	0.9998838
22	1.0000000	0.9999999	0.9999802	0.9999670	0.9999292	0.9998508

33	0.9825260	0.9568858	0.5997599	0.5162996	0.3792474	0.2440753
34	0.9982387	0.9956026	0.9501622	0.9360309	0.9075954	0.8684651
7	0.9926662	0.9817663	0.8077819	0.7587902	0.6670809	0.5549574
23	0.9999838	0.9998991	0.9874140	0.9794755	0.9581071	0.9179181
24	0.9999919	0.9999495	0.9935450	0.9893840	0.9779426	0.9556425
25	0.9999730	0.9998327	0.9802136	0.9682390	0.9371445	0.8817518
26	0.9999462	0.9996675	0.9630522	0.9418178	0.8891649	0.8019370
28	0.9970547	0.9926531	0.9180179	0.8952878	0.8502473	0.7898059
29	0.9999913	0.9999460	0.9932789	0.9890354	0.9775741	0.9558185
30	0.9999795	0.9998722	0.9842250	0.9743691	0.9480961	0.8995067
37	0.9796322	0.9498557	0.5505903	0.4622368	0.3224541	0.1927721
38	0.9952986	0.9882880	0.8722659	0.8380171	0.7716805	0.6859189

ADVANCED PLANETARY PROBE (PARTS COUNT RELIABILITY ASSESSMENT)
SUBSYSTEM 4 POWER SUBSYSTEM
UNIT 1 SHUNT REGULATOR (ANALOG)

	COMPONENT PART	QTY	FAILURE RATE	EXTENSION
1	RES,CARBCOMP	17	3	51
2	RES,MET.FILM	3	3	9
5	RES,WIRE,PWR	1	33	33
8	DIO,SI,GENRL	6	5	30
10	DIO,SI,ZENER	2	13	26
18	CAP,FIX.CER.	1	5	5
28	CAP,TANT.WET	2	50	100
33	CONN,GEN/PIN	3	3	9
35	XIST,SI,LT1W	6	17	102
36	XIST,SI,GT1W	2	43	86
	TOTAL	43		451
	CONNECTIONS	88	0.500	44
	TOTAL			495

ADVANCED PLANETARY PROBE (PARTS COUNT RELIABILITY ASSESSMENT)
SUBSYSTEM 4 POWER SUBSYSTEM
UNIT 2 ENERGY STORAGE (ANALOG)

	COMPONENT PART	QTY	FAILURE RATE	EXTENSION
1	RES,CARBCOMP	1	3	3
8	DIO,SI,GENRL	1	5	5
28	CAP,TANT.WET	200	50	10000
	TOTAL	202		10008
	CONNECTIONS	404	0.500	202
	TOTAL			10210

ADVANCED PLANETARY PROBE (PARTS COUNT RELIABILITY ASSESSMENT)
SUBSYSTEM 4 POWER SUBSYSTEM
UNIT 3 CONTROL INVERTER-RECTIF (ANALOG)

	COMPONENT PART	QTY	FAILURE RATE	EXTENSION
1	RES,CARBCOMP	4	3	12
5	RES,WIRE,PWR	2	33	66
8	DIO,SI,GENRL	3	5	15
9	DIO,SI,RECT.	2	5	10
18	CAP,FIX.CER.	3	5	15
28	CAP,TANT.WET	2	50	100
33	CONN,GEN/PIN	2	3	6
36	XIST,SI,GT1W	2	43	86
45	TRF,LT100V6T	2	40	80
58	COILFILT,LOV	1	10	10
	TOTAL	23		400
	CONNECTIONS	52	0.500	26
	TOTAL			426

ADVANCED PLANETARY PROBE (PARTS COUNT RELIABILITY ASSESSMENT)
SUBSYSTEM 4 POWER SUBSYSTEM
UNIT 4 1 CHANNEL SCIENCE DISTRI (ANALOG)

	COMPONENT PART	QTY	FAILURE RATE	EXTENSION
1	RES,CARBCOMP	11	3	33
2	RES,MET.FILM	1	3	3
8	DIO,SI,GENRL	4	5	20
9	DIO,SI,RECT.	4	5	20
10	DIO,SI,ZENER	1	13	13
18	CAP,FIX.CER.	3	5	15
26	CAP,TANTFOIL	1	13	13
35	XIST,SI,LT1W	4	17	68
45	TRF,LT100V6T	1	40	40
48	MAGAMP3WNDGS	1	50	50
55	RLY,LG,2CS2W	1	227	227
	TOTAL	32		502
	CONNECTIONS	82	0.500	41
	TOTAL			543

ADVANCED PLANETARY PROBE (PARTS COUNT RELIABILITY ASSESSMENT)
SUBSYSTEM 4 POWER SUBSYSTEM
UNIT 5 EQUIPMENT CONVERTER (ANALOG)

	COMPONENT PART	QTY	FAILURE RATE	EXTENSION
1	RES,CARBCOMP	19	3	57
2	RES,MET.FILM	8	3	24
8	DIO,SI,GENRL	33	5	165
10	DIO,SI,ZENER	4	13	52
11	DIO,SI,SWITC	6	2	12
18	CAP,FIX.CER.	12	5	60
21	CAP,MICA DIP	2	2	4
26	CAP,TANTFOIL	15	13	195
33	CONN,GEN/PIN	40	3	120
35	XIST,SI,LT1W	4	17	68
36	XIST,SI,GT1W	4	43	172
43	TRF,LT100V4T	2	30	60
45	TRF,LT100V6T	2	40	80
58	COILFILT,LOV	17	10	170
70	FUSE	1	100	100
	TOTAL	169		1339
	CONNECTIONS	276	0.500	138
	TOTAL			1477

ADVANCED PLANETARY PROBE (PARTS COUNT RELIABILITY ASSESSMENT)
SUBSYSTEM 4 POWER SUBSYSTEM
UNIT 6 TWT CONVERTER (ANALOG)

	COMPONENT PART	QTY	FAILURE RATE	EXTENSION
1	RES,CARBCOMP	15	3	45
2	RES,MET.FILM	11	3	33
8	DIO,SI,GENRL	42	5	210
10	DIO,SI,ZENER	3	13	39
11	DIO,SI,SWITC	6	2	12
18	CAP,FIX.CER.	8	5	40
22	CAP,MICABUTT	1	17	17
26	CAP,TANTFOIL	13	13	169
33	CONN,GEN/PIN	13	3	39
35	XIST,SI,LT1W	4	17	68
36	XIST,SI,GT1W	4	43	172
45	TRF,LT100V6T	2	40	80
46	TRF,GT100V4T	4	83	332
58	COILFILT,LOV	5	10	50
70	FUSE	1	100	100
	TOTAL	132		1406
	CONNECTIONS	260	0.500	130
	TOTAL			1536

ADVANCED PLANETARY PROBE (PARTS COUNT RELIABILITY ASSESSMENT)
SUBSYSTEM 4 POWER SUBSYSTEM
UNIT 7 SHUNT REG (NO SING FAIL) (ANALOG)

	COMPONENT PART	QTY	FAILURE RATE	EXTENSION
1	RES,CARBCOMP	17	3	51
2	RES,MET.FILM	3	3	9
5	RES,WIRE,PWR	1	33	33
8	DIO,SI,GENRL	6	5	30
10	DIO,SI,ZENER	2	13	26
18	CAP,FIX.CER.	1	5	5
28	CAP,TANT.WET	2	50	100
33	CONN,GEN/PIN	3	3	9
35	XIST,SI,LT1W	6	17	102
36	XIST,SI,GT1W	2	43	86
	TOTAL	43		451
	CONNECTIONS	88	0.500	44
	TOTAL			495

ADVANCED PLANETARY PROBE (PARTS COUNT RELIABILITY ASSESSMENT)
SUBSYSTEM 4 POWER SUBSYSTEM
UNIT 8 ENERGY STORAGE (ANALOG)

	COMPONENT PART	QTY	FAILURE RATE	EXTENSION
1	RES,CARBCOMP	1	3	3
8	DIO,SI,GENRL	1	5	5
28	CAP,TANT.WET	200	50	10000
	TOTAL	202		10008
	CONNECTIONS	404	0.500	202
	TOTAL			10210

ADVANCED PLANETARY PROBE (PARTS COUNT RELIABILITY ASSESSMENT)
SUBSYSTEM 4 POWER SUBSYSTEM
UNIT 9 CONTROL INVERTER (ANALOG)

	COMPONENT PART	QTY	FAILURE RATE	EXTENSION
1	RES,CARBCOMP	4	3	12
5	RES,WIRE,PWR	2	33	66
8	DIO,SI,GENRL	3	5	15
9	DIO,SI,RECT.	2	5	10
18	CAP,FIX.CER.	3	5	15
28	CAP,TANT.WET	2	50	100
33	CONN,GEN/PIN	2	3	6
36	XIST,SI,GT1W	2	43	86
45	TRF,LT100V6T	2	40	80
58	COILFILT,LOV	1	10	10
	TOTAL	23		400
	CONNECTIONS	52	0.500	26
	TOTAL			426

ADVANCED PLANETARY PROBE (PARTS COUNT RELIABILITY ASSESSMENT)
SUBSYSTEM 4 POWER SUBSYSTEM
UNIT 10 1 CHANNEL SCIENCE (ANALOG)

	COMPONENT PART	QTY	FAILURE RATE	EXTENSION
1	RES,CARBCOMP	11	3	33
2	RES,MET.FILM	1	3	3
8	DIO,SI,GENRL	4	5	20
9	DIO,SI,RECT.	4	5	20
10	DIO,SI,ZENER	1	13	13
18	CAP,FIX.CER.	3	5	15
26	CAP,TANTFOIL	1	13	13
35	XIST,SI,LT1W	4	17	68
45	TRF,LT100V6T	1	40	40
48	MAGAMP3WNDGS	1	50	50
55	RLY,LG,2CS2W	1	227	227
	TOTAL	32		502
	CONNECTIONS	82	0.500	41
	TOTAL			543

ADVANCED PLANETARY PROBE (PARTS COUNT RELIABILITY ASSESSMENT)
SUBSYSTEM 4 POWER SUBSYSTEM
UNIT 11 THERMOELCTRC COUPLE ASY (ANALOG)

COMPONENT PART	QTY	FAILURE RATE	EXTENSION

UNIT INPUTED AS ENTITY...SEE UNIT SUMMARY.

ADVANCED PLANETARY PROBE (PARTS COUNT RELIABILITY ASSESSMENT)
SUBSYSTEM 4 POWER SUBSYSTEM
UNIT 12 HOT JUNCTION ELECTRODE (ANALOG)

COMPONENT PART	QTY	FAILURE RATE	EXTENSION

UNIT INPUTED AS ENTITY...SEE UNIT SUMMARY.

ADVANCED PLANETARY PROBE (PARTS COUNT RELIABILITY ASSESSMENT)
SUBSYSTEM 4 POWER SUBSYSTEM
UNIT 13 FOLLOWER (ANALOG)

COMPONENT PART	QTY	FAILURE RATE	EXTENSION
TOTAL	0		0
CONNECTIONS	0	0.500	0
TOTAL			0

ADVANCED PLANETARY PROBE (PARTS COUNT RELIABILITY ASSESSMENT)
SUBSYSTEM 4 POWER SUBSYSTEM
UNIT 14 FOLLOWER SPRING (ANALOG)

COMPONENT PART	QTY	FAILURE RATE	EXTENSION

UNIT INPUTED AS ENTITY...SEE UNIT SUMMARY.

ADVANCED PLANETARY PROBE (PARTS COUNT RELIABILITY ASSESSMENT)
SUBSYSTEM 4 POWER SUBSYSTEM
UNIT 15 INSULATION SHIMS (ANALOG)

COMPONENT PART	QTY	FAILURE RATE	EXTENSION
TOTAL	0		0
CONNECTIONS	0	0.500	0
TOTAL			0

ADVANCED PLANETARY PROBE (PARTS COUNT RELIABILITY ASSESSMENT)
SUBSYSTEM 4 POWER SUBSYSTEM
UNIT 16 SPRING RETAINER (ANALOG)

COMPONENT PART	QTY	FAILURE RATE	EXTENSION

UNIT INPUTED AS ENTITY...SEE UNIT SUMMARY.

ADVANCED PLANETARY PROBE (PARTS COUNT RELIABILITY ASSESSMENT)
SUBSYSTEM 4 POWER SUBSYSTEM
UNIT 17 INS STRIPS (ANALOG)

COMPONENT PART	QTY	FAILURE RATE	EXTENSION

UNIT INPUTED AS ENTITY...SEE UNIT SUMMARY.

ADVANCED PLANETARY PROBE (PARTS COUNT RELIABILITY ASSESSMENT)
SUBSYSTEM 4 POWER SUBSYSTEM
UNIT 18 THERMOPILE ASSEMBLY (ANALOG)

COMPONENT PART	QTY	FAILURE RATE	EXTENSION

UNIT INPUTED AS ENTITY...SEE UNIT SUMMARY.

ADVANCED PLANETARY PROBE (PARTS COUNT RELIABILITY ASSESSMENT)
SUBSYSTEM 4 POWER SUBSYSTEM
UNIT 19 OUTER CASE (ANALOG)

COMPONENT PART	QTY	FAILURE RATE	EXTENSION

UNIT INPUTED AS ENTITY...SEE UNIT SUMMARY.

ADVANCED PLANETARY PROBE (PARTS COUNT RELIABILITY ASSESSMENT)
SUBSYSTEM 4 POWER SUBSYSTEM
UNIT 20 FINS (ANALOG)

COMPONENT PART	QTY	FAILURE RATE	EXTENSION

UNIT INPUTED AS ENTITY...SEE UNIT SUMMARY.

ADVANCED PLANETARY PROBE (PARTS COUNT RELIABILITY ASSESSMENT)
SUBSYSTEM 4 POWER SUBSYSTEM
UNIT 21 HOT FRAME (ANALOG)

COMPONENT PART	QTY	FAILURE RATE	EXTENSION

UNIT INPUTED AS ENTITY...SEE UNIT SUMMARY.

ADVANCED PLANETARY PROBE (PARTS COUNT RELIABILITY ASSESSMENT)
SUBSYSTEM 4 POWER SUBSYSTEM
UNIT 22 COLD FRAME (ANALOG)

COMPONENT PART	QTY	FAILURE RATE	EXTENSION

UNIT INPUTED AS ENTITY...SEE UNIT SUMMARY.

ADVANCED PLANETARY PROBE (PARTS COUNT RELIABILITY ASSESSMENT)
SUBSYSTEM 4 POWER SUBSYSTEM
UNIT 23 POWER CABLE (ANALOG)

COMPONENT PART	QTY	FAILURE RATE	EXTENSION

UNIT INPUTED AS ENTITY...SEE UNIT SUMMARY.

ADVANCED PLANETARY PROBE (PARTS COUNT RELIABILITY ASSESSMENT)
SUBSYSTEM 4 POWER SUBSYSTEM
UNIT 24 CONNECTOR (ANALOG)

COMPONENT PART	QTY	FAILURE RATE	EXTENSION

UNIT INPUTED AS ENTITY...SEE UNIT SUMMARY.

ADVANCED PLANETARY PROBE (PARTS COUNT RELIABILITY ASSESSMENT)
SUBSYSTEM 4 POWER SUBSYSTEM
UNIT 25 HERMETIC SEALS (ANALOG)

COMPONENT PART	QTY	FAILURE RATE	EXTENSION

UNIT INPUTED AS ENTITY...SEE UNIT SUMMARY.

ADVANCED PLANETARY PROBE (PARTS COUNT RELIABILITY ASSESSMENT)
SUBSYSTEM 4 POWER SUBSYSTEM
UNIT 26 HEADERS (ANALOG)

COMPONENT PART	QTY	FAILURE RATE	EXTENSION

UNIT INPUTED AS ENTITY...SEE UNIT SUMMARY.

ADVANCED PLANETARY PROBE (PARTS COUNT RELIABILITY ASSESSMENT)
SUBSYSTEM 4 POWER SUBSYSTEM
UNIT 27 FUEL CAPSULE ASSY (ANALOG)

COMPONENT PART	QTY	FAILURE RATE	EXTENSION

UNIT INPUTED AS ENTITY...SEE UNIT SUMMARY.

ADVANCED PLANETARY PROBE (PARTS COUNT RELIABILITY ASSESSMENT)
SUBSYSTEM 4 POWER SUBSYSTEM
UNIT 28 EQUIPMENT CONVERTER (ANALOG)

	COMPONENT PART	QTY	FAILURE RATE	EXTENSION
1	RES,CARBCOMP	19	3	57
2	RES,MET.FILM	8	3	24
8	DIO,SI,GENRL	33	5	165
10	DIO,SI,ZENER	4	13	52
11	DIO,SI,SWITC	6	2	12
18	CAP,FIX.CER.	12	5	60
21	CAP,MICA DIP	2	2	4
26	CAP,TANTFOIL	15	13	195
33	CONN,GEN/PIN	40	3	120
35	XIST,SI,LT1W	4	17	68
36	XIST,SI,GT1W	4	43	172
43	TRF,LT100V4T	2	30	60
45	TRF,LT100V6T	2	40	80
58	COILFILT,LOV	17	10	170
70	FUSE	1	100	100
	TOTAL	169		1339
	CONNECTIONS	276	0.500	138
	TOTAL			1477

ADVANCED PLANETARY PROBE (PARTS COUNT RELIABILITY ASSESSMENT)
SUBSYSTEM 4 POWER SUBSYSTEM
UNIT 29 TWT CONVERTER (ANALOG)

	COMPONENT PART	QTY	FAILURE RATE	EXTENSION
1	RES,CARBCOMP	15	3	45
2	RES,MET.FILM	11	3	33
8	DIO,SI,GENRL	42	5	210
10	DIO,SI,ZENER	3	13	39
11	DIO,SI,SWITC	6	2	12
18	CAP,FIX.CER.	8	5	40
22	CAP,MICABUTT	1	17	17
26	CAP,TANTFOIL	13	13	169
33	CONN,GEN/PIN	13	3	39
35	XIST,SI,LT1W	4	17	68
36	XIST,SI,GT1W	4	43	172
45	TRF,LT100V6T	2	40	80
46	TRF,GT100V4T	4	83	332
58	COILFILT,LOV	5	10	50
70	FUSE	1	100	100
	TOTAL	132		1406
	CONNECTIONS	260	0.500	130
	TOTAL			1536

ADVANCED PLANETARY PROBE (PARTS COUNT RELIABILITY ASSESSMENT)
SUBSYSTEM 4 POWER SUBSYSTEM
UNIT 30 CONTROL INVERTER-RECTIF (ANALOG)

COMPONENT PART	QTY	FAILURE RATE	EXTENSION
TOTAL	0		0
CONNECTIONS	0	0.500	0
TOTAL			0

ADVANCED PLANETARY PROBE (PARTS COUNT RELIABILITY ASSESSMENT)
SUBSYSTEM 4 POWER SUBSYSTEM
NO. OF COMPONENT PARTS= 1202 SUBSYSTEM FR= 29374

UNIT SUMMARY.....

NO	DESCRIPTION	PART USAGE	FAILURE RATE	SUM FR SQUARED	SUM FR CUBED	
1	SHUNT REGULATOR	ANALOG	495	0.12241E-13	0.48032E-21	
2	ENERGY STORAGE	ANALOG	10210	0.50003E-12	0.25000E-19	
3	CONTROL INVERTER-RECTIF	ANALOG	426	0.14430E-13	0.61105E-21	
4	1 CHANNEL SCIENCE DISTRI	ANALOG	543	0.57506E-13	0.11912E-19	
5	EQUIPMENT CONVERTER	ANALOG	1477	0.30223E-13	0.15859E-20	
6	TWT CONVERTER	ANALOG	1536	0.54426E-13	0.38052E-20	
7	SHUNT REG (NO SING FAIL)	ANALOG	495	0.12241E-13	0.48032E-21	(PLRD)
8	ENERGY STORAGE	ANALOG	10210	0.50003E-12	0.25000E-19	(PLRD)
9	CONTROL INVERTER	ANALOG	426	0.14430E-13	0.61105E-21	(PLRD)
10	1 CHANNEL SCIENCE	ANALOG	543	0.57506E-13	0.11912E-19	(PLRD)
11	THERMOELCTRC COUPLE ASY	ANALOG	98	0.	0.	
12	HOT JUNCTION ELECTRODE	ANALOG	1	0.	0.	
13	FOLLOWER	ANALOG	0	0.	0.	
14	FOLLOWER SPRING	ANALOG	10	0.	0.	
15	INSULATION SHIMS	ANALOG	0	0.	0.	
16	SPRING RETAINER	ANALOG	1	0.	0.	
17	INS STRIPS	ANALOG	10	0.	0.	
18	THERMOPILE ASSEMBLY	ANALOG	133	0.	0.	
19	OUTER CASE	ANALOG	1	0.	0.	
20	FINS	ANALOG	10	0.	0.	
21	HOT FRAME	ANALOG	1	0.	0.	
22	COLD FRAME	ANALOG	1	0.	0.	
23	POWER CABLE	ANALOG	20	0.	0.	
24	CONNECTOR	ANALOG	40	0.	0.	
25	HERMETIC SEALS	ANALOG	40	0.	0.	
26	HEADERS	ANALOG	40	0.	0.	
27	FUEL CAPSULE ASSY	ANALOG	30	0.	0.	
28	EQUIPMENT CONVERTER	ANALOG	1477	0.30223E-13	0.15859E-20	(PLRD)
29	TWT CONVERTER	ANALOG	1536	0.54426E-13	0.38052E-20	(PLRD)
30	CONTROL INVERTER-RECTIF	ANALOG	0	0.	0.	(PLRD)

MISSION RELIABILITIES....

BASIC ELEMENT SPECIFICATIONS

ELEMT NO.	REF. UNIT	REDUN. TYPE	NO. PRESENT	NO. NEEDED	OFF RATIO	PHASE L-FACTORS... 1	2	3	4	5	6
1	1	BINOM	1	1		1.000	1.000	1.000	1.000	1.000	1.000
2	2	BINOM	1	1		1.000	1.000	1.000	1.000	1.000	1.000
3	3	BINOM	1	1		1.000	1.000	1.000	1.000	1.000	1.000
4	4	BINOM	1	1		1.000	1.000	1.000	1.000	1.000	1.000
5	5	BINOM	1	1		1.000	1.000	1.000	1.000	1.000	1.000
6	6	BINOM	1	1		1.000	1.000	1.000	1.000	1.000	1.000
10	4	BINOM	10	10		1.000	1.000	1.000	1.000	1.000	1.000
11	4	BINOM	10	9		1.000	1.000	1.000	1.000	1.000	1.000
12	4	BINOM	10	8		1.000	1.000	1.000	1.000	1.000	1.000
13	4	BINOM	10	7		1.000	1.000	1.000	1.000	1.000	1.000
15	1	BINOM	2	1		1.000	1.000	1.000	1.000	1.000	1.000
16	2	BINOM	2	1		1.000	1.000	1.000	1.000	1.000	1.000
17	3	BINOM	2	1		1.000	1.000	1.000	1.000	1.000	1.000
18	5	BINOM	2	1		1.000	1.000	1.000	1.000	1.000	1.000
25	7	BINOM	1	1		1.000	1.000	1.000	1.000	1.000	1.000
26	8	BINOM	1	1		1.000	1.000	1.000	1.000	1.000	1.000
27	9	BINOM	1	1		1.000	1.000	1.000	1.000	1.000	1.000
28	10	BINOM	1	1		1.000	1.000	1.000	1.000	1.000	1.000
29	11	BINOM	1	1		1.000	1.000	1.000	1.000	1.000	1.000
48	18	BINOM	2	1		1.000	1.000	1.000	1.000	1.000	1.000
51	19	BINOM	1	1		1.000	1.000	1.000	1.000	1.000	1.000
52	20	BINOM	1	1		1.000	1.000	1.000	1.000	1.000	1.000
53	21	BINOM	1	1		1.000	1.000	1.000	1.000	1.000	1.000
54	22	BINOM	1	1		1.000	1.000	1.000	1.000	1.000	1.000
55	23	BINOM	1	1		1.000	1.000	1.000	1.000	1.000	1.000
56	24	BINOM	1	1		1.000	1.000	1.000	1.000	1.000	1.000
57	25	BINOM	1	1		1.000	1.000	1.000	1.000	1.000	1.000
58	26	BINOM	1	1		1.000	1.000	1.000	1.000	1.000	1.000
59	27	BINOM	1	1		1.000	1.000	1.000	1.000	1.000	1.000
70	28	BINOM	1	1		1.000	1.000	1.000	1.000	1.000	1.000
71	29	BINOM	1	1		1.000	1.000	1.000	1.000	1.000	1.000
72	30	BINOM	1	1		1.000	1.000	1.000	1.000	1.000	1.000
82	2	BINOM	4	3		1.000	1.000	1.000	1.000	1.000	1.000
83	22	BINOM	1	1		1.000	1.000	1.000	1.000	1.000	1.000
84	23	BINOM	1	1		1.000	1.000	1.000	1.000	1.000	1.000

LOGICAL EQUATIONS

L 14=1*2*3*5*10

```
L 19=15*16*17*18
L 20=19*10
L 21=19*11
L 22=19*12
L 23=19*13
L 24=15*2*17*12
L 30=25*26*27*29*12
L 31=25*2*17*29*12
L 49=046046048
L 50=49*49*49
L 60=51*52*53*54*55*56*57*58*59
L 61=60*60*60*50
L 62=58*58
L 63=001002062
L 64=021021063
L 65=64*64*64
L 66=65*50
L 67=14*61
L 68=1*82*3*5*12*61
L 73=1*82*72*70*12*61
L 74=001002068
L 75=1*82*3*70*12*61
L 85=47*83*84
```

MISSION PHASE RELIABILITIES

ELEMT	PHASE 1	2	3	4	5	6
1	0.9997624	0.9994062	0.9931333	0.9911296	0.9870170	0.9811715
2	0.9951112	0.9878227	0.8675144	0.8321188	0.7637277	0.6756609
3	0.9997955	0.9994889	0.9940876	0.9923613	0.9888166	0.9837747
4	0.9997394	0.9993486	0.9924699	0.9902736	0.9857671	0.9793647
5	0.9992913	0.9982292	0.9796501	0.9737643	0.9617576	0.9448616
6	0.9992630	0.9981585	0.9788458	0.9727307	0.9602608	0.9427234
10	0.9973970	0.9935052	0.9272004	0.9068847	0.8664490	0.8117913
11	0.9999969	0.9999810	0.9975489	0.9959582	0.9915508	0.9828366
12	1.0000000	1.0000000	0.9999508	0.9998951	0.9996790	0.9990543
13	1.0000000	1.0000000	0.9999993	0.9999982	0.9999920	0.9999655
15	0.9999999	0.9999996	0.9999528	0.9999213	0.9998314	0.9996455
16	0.9999761	0.9998517	0.9824476	0.9718159	0.9441754	0.8948041
17	1.0000000	0.9999997	0.9999650	0.9999416	0.9998749	0.9997367
18	0.9999995	0.9999969	0.9995859	0.9993117	0.9985375	0.9969598
25	1.0000000	0.9999998	0.9999775	0.9999625	0.9999196	0.9998305

26	0.9999881	0.9999259	0.9908503	0.9851131	0.9697190	0.9408124
27	1.0000000	0.9999999	0.9999839	0.9999731	0.9999422	0.9998781
28	1.0000000	0.9999998	0.9999771	0.9999618	0.9999180	0.9998272
29	0.9999530	0.9998824	0.9986368	0.9982376	0.9974161	0.9962439
48	1.0000000	1.0000000	0.9999966	0.9999943	0.9999877	0.9999740
51	0.9999995	0.9999988	0.9999861	0.9999820	0.9999736	0.9999616
52	0.9999952	0.9999880	0.9998608	0.9998200	0.9997360	0.9996161
53	0.9999995	0.9999988	0.9999861	0.9999820	0.9999736	0.9999616
54	0.9999995	0.9999988	0.9999861	0.9999820	0.9999736	0.9999616
55	0.9999904	0.9999760	0.9997216	0.9996401	0.9994721	0.9992323
56	0.9999808	0.9999520	0.9994434	0.9992803	0.9989446	0.9984652
57	0.9999808	0.9999520	0.9994434	0.9992803	0.9989446	0.9984652
58	0.9999808	0.9999520	0.9994434	0.9992803	0.9989446	0.9984652
59	0.9999856	0.9999640	0.9995825	0.9994601	0.9992083	0.9988487
70	0.9999997	0.9999985	0.9997944	0.9996576	0.9992694	0.9984722
71	0.9999997	0.9999983	0.9997798	0.9996333	0.9992179	0.9983653
72	1.0000000	1.0000000	1.0000000	1.0000000	1.0000000	1.0000000
82	0.9998575	0.9991247	0.9123647	0.8663651	0.7612217	0.6085794
83	0.9999995	0.9999988	0.9999861	0.9999820	0.9999736	0.9999616
84	0.9999904	0.9999760	0.9997216	0.9996401	0.9994721	0.9992323
14	0.9913791	0.9785870	0.7779532	0.7227557	0.6211373	0.5002440
19	0.9999755	0.9998480	0.9819601	0.9710139	0.9425177	0.8915327
20	0.9973726	0.9933541	0.9104737	0.8805976	0.8166436	0.7237385
21	0.9999724	0.9998289	0.9795532	0.9670893	0.9345542	0.8762309
22	0.9999755	0.9998479	0.9819117	0.9709121	0.9422152	0.8906896
23	0.9999755	0.9998480	0.9819594	0.9710122	0.9425102	0.8915020
24	0.9951111	0.9878221	0.8674004	0.8319175	0.7632584	0.6746050
30	0.9999410	0.9998080	0.9894127	0.9832104	0.9667693	0.9361194
31	0.9950643	0.9877061	0.8662394	0.8304855	0.7613533	0.6721954
49	0.9999998	0.9999988	0.9998426	0.9997370	0.9994350	0.9988070
50	0.9999994	0.9999965	0.9995280	0.9992113	0.9983061	0.9964252
60	0.9999122	0.9997804	0.9974559	0.9967114	0.9951805	0.9929974
61	0.9997360	0.9993379	0.9919186	0.9893857	0.9839413	0.9756388
62	0.9999616	0.9999040	0.9988870	0.9985610	0.9978902	0.9969327
63	1.0000000	1.0000000	0.9999988	0.9999979	0.9999955	0.9999906
64	1.0000000	0.9999998	0.9999740	0.9999565	0.9999065	0.9998024
65	0.9999999	0.9999994	0.9999220	0.9998696	0.9997196	0.9994074
66	0.9999993	0.9999959	0.9994500	0.9990809	0.9980261	0.9958347
67	0.9911174	0.9779391	0.7716662	0.7150842	0.6111626	0.4880575
68	0.9984436	0.9955941	0.8752382	0.8208714	0.7028246	0.5410086
73	0.9993558	0.9978687	0.8985481	0.8491858	0.7384960	0.5811340
74	0.9999976	0.9999806	0.9844345	0.9679129	0.9116868	0.7893269

75	0.9991515	0.9973587	0.8932356	0.8426991	0.7302371	0.5717049
85	0.7829521	0.7829403	0.7827312	0.7826641	0.7825261	0.7823289

ADVANCED PLANETARY PROBE (PARTS COUNT RELIABILITY ASSESSMENT)
TOTAL SYSTEM PARTS= 4466

COMPONENT PART USAGE

	PART TYPE	USAGE
1	RES,CARBCOMP	310
2	RES,MET.FILM	438
3	RES,CARBFILM	1
5	RES,WIRE,PWR	7
7	RES,VAR,CCOM	2
8	DIO,SI,GENRL	820
9	DIO,SI,RECT.	12
10	DIO,SI,ZENER	20
11	DIO,SI,SWITC	34
18	CAP,FIX.CER.	133
20	CAP,FIX,GLAS	58
21	CAP,MICA DIP	4
22	CAP,MICABUTT	2
26	CAP,TANTFOIL	58
27	CAP,TANT.SLD	14
28	CAP,TANT.WET	408
33	CONN,GEN/PIN	116
35	XIST,SI,LT1W	118
36	XIST,SI,GT1W	26
37	XIST,SI,SWIT	748
43	TRF,LT100V4T	4
45	TRF,LT100V6T	22
46	TRF,GT100V4T	8
48	MAGAMP3WNDGS	2
51	MEM.CR/HUND.	10
53	RELY.GEN.4CS	6
55	RLY,LG,2CS2W	152
58	COILFILT,LOV	46
61	COIL,ANALOG	4
62	IC,DIG.STOR	260
63	IC,DIG.GATES	609
64	IC,DIG.ISOL	6
65	IC,DIG.ANALG	2
70	FUSE	4

71 SOLAR CELL 2

ERROR TRACE. CALLS IN REVERSE ORDER.

CALLING ROUTINE	IFN OR LINE NO.	ABSOLUTE LOCATION
FCNV	00418	66377
FIOH	00078	71226
FRDD	00022	72611
PARKA3	00005	04127

ILLEGAL CHAR IN DATA BELOW OR BAD FORMAT

2 .96 5000GOBAD INTELSAT

EXECUTION TERMINATED.
AT 00353 XR1= 00004 XR2= 77775 XR4= 20210 XR3= 77671 XR5= 77340 XR6= 77560 XR7= 77777

ERROR TRACE. CALLS IN REVERSE ORDER.

CALLING ROUTINE	IFN OR LINE NO.	ABSOLUTE LOCATION
.LXCON	00112	57647
FCNV	00418	66377
FIOH	00078	71226
FRDD	00022	72611
PARKA3	00005	04127

APPENDIX K

NONGRAVITATIONAL TRAJECTORY PERTURBATIONS

1. SOLAR PRESSURE

1.1 Radial Component of Solar Pressure

For an antenna dish with ideal absorption ($\alpha_0 = 1$) the solar pressure acts purely in radial direction and produces in effect a reduction of solar gravity $g_\odot$ by the amount

$$a = \frac{F_r g_\oplus}{W} = \frac{P_o A g_\oplus}{r^2 W}$$

if the factor cos ξ in Section 2.4.4 of Volume 2 is approximated by 1. At r = 1 AU the value of a is

$$a_o = \frac{P_o A g_\oplus}{W} = 1.14 \times 10^{-6} \text{ ft/sec}^2$$

for an assumed spacecraft weight W = 550 lb* and antenna aperture area A = 200 ft^2. The magnitude of solar gravity at 1 AU is

$$g_{\odot o} = 1.943 \times 10^{-2} \text{ ft/sec}^2$$

The resulting relative gravity variation is thus given by

$$\epsilon = \frac{a_o}{g_{\odot o}} = \frac{\mu - \mu'}{\mu} = 0.587 \times 10^{-4}$$

where μ' designates the reduced gravitational constant corresponding to $g_{\odot o} - a_o$. Figure K-1 is a sketch of the trajectory perturbation

---

* The final design ended up slightly less than 500 pounds, increasing the effects computed here by the ratio 550/500, or a 10 percent increase.

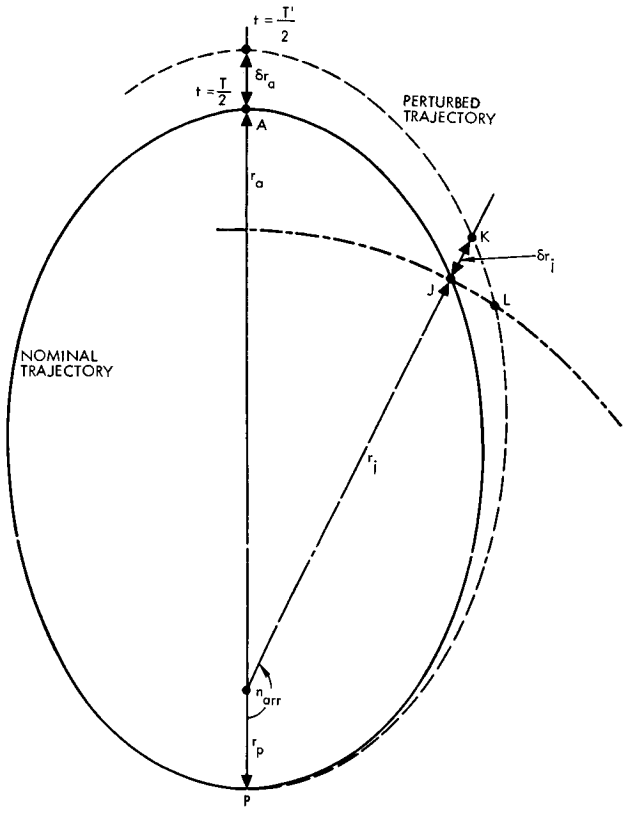

Figure K-1. Nominal and Perturbed Trajectory (Exaggerated) Resulting from Solar Pressure

resulting from the reduced value of μ' for identical launch conditions at periapsis. The perturbation effect at aphelion is expressed by

$$\delta = \delta(\epsilon) = \frac{r_a' - r_a}{r_a}$$

Since both trajectories have the same perihelion distance and velocity we obtain

$$V_p = \frac{2\mu}{r_p\left(\frac{r_p}{r_a} + 1\right)} = \frac{2\mu'}{r_p\left(\frac{r_p}{r_a'} + 1\right)}$$

or

$$\frac{\mu}{\frac{r_p}{r_a} + 1} = \frac{\mu(1-\epsilon)}{\frac{r_p}{r_a(1+\delta)} + 1}$$

from which follows, for small values of δ,

$$\delta \simeq \epsilon \left(1 + \frac{r_a}{r_p}\right) \simeq 7\,\epsilon$$

where $r_a \simeq 6$ AU and $r_p \simeq 1$ AU of the sample trajectory have been used. Hence the aphelion perturbation due to purely radial solar pressure is

$$\delta = 4.10 \times 10^{-4}$$

Thus

$$r_a' - r_a = \delta r_a = 2.46 \times 10^{-3}\ \text{AU} = 368 \times 10^3\ \text{km}$$

To the perturbation δr_a at aphelion corresponds a radial perturbation at the crossing of the orbit of Jupiter. This is illustrated in Figure K-1, which shows the nominal and perturbed spacecraft trajectory and the geometry of Jupiter encounter assuming a massless planet. In first approximation, the spacecraft distance at the true anomaly η_{arr} of the nominal encounter can be scaled in the ratio of the perturbed and unperturbed aphelion distances

$$r_j' = r_j(1 + \delta) = 5.1\,(1 + 4.1 \times 10^{-4})\ \text{AU}$$

Thus

$$\delta r_j = 2.09 \times 10^{-3}\ \text{AU} = 313 \times 10^3\ \text{km}$$

The spacecraft crosses the Jupiter orbit at a distance ΔS_1 from the nominal encounter, given by

$$\Delta S_1 \cong \frac{\delta r_j}{\tan \theta_j} = 2.67 \times 10^{-3} \text{ AU} = 400 \times 10^3 \text{ km}$$

A flight path angle $\theta_j = 38$ degrees at the nominal encounter is used in this approximation.

The time arrival t'_{arr} of the spacecraft at the true anomaly η_{arr} differs from the nominal encounter time, and is given approximately by

$$t'_{arr} \simeq \frac{T'}{T} t$$

where t_{arr}, t'_{arr} are the nominal and perturbed arrival times at η_{arr}; T, T' are orbital periods of the nominal and perturbed trajectory. The ratio of orbital periods is derived from the perturbation of aphelion distance,

$$\frac{T'}{T} = \sqrt{\frac{(a+\delta a)^3 \mu}{a^3 \mu (1-\epsilon)}} \simeq 1 + 1.5\delta = 1 + 6.15 \times 10^{-4}$$

Hence

$$t'_{arr} = 650 \, (1 + 6.15 \times 10^{-4}) \text{ day}$$

and

$$\Delta t_{arr} = t'_{arr} - t_{arr} = 0.40 \text{ day} = 9.6 \text{ hours}$$

after nominal encounter. During this time interval the spacecraft would be traveling a distance

$$\Delta S_o = V_{arr} \Delta t_{arr} = 335 \times 10^3 \text{ km}$$

where $V_{arr} = 31,800$ ft/sec is the nominal heliocentric arrival velocity of the spacecraft.

The distance of closest approach, or miss parameter, ΔB is found with the aid of Figure K-2, which shows the relative geometry of the

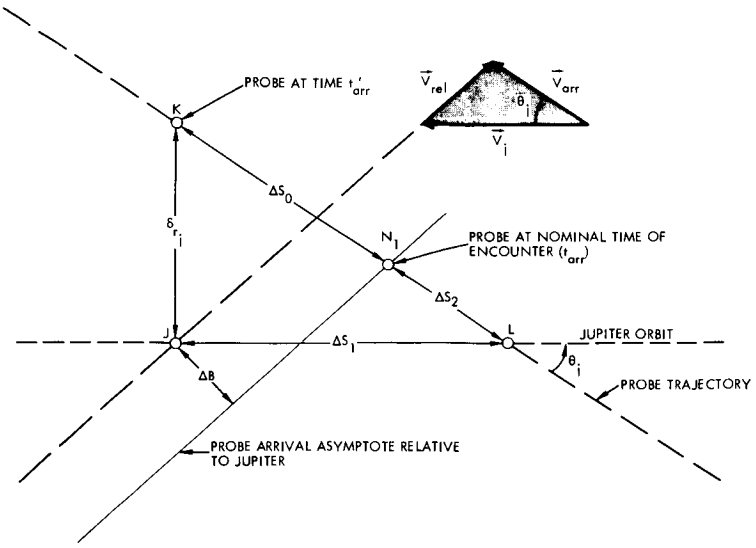

Figure K-2. Relative Geometry at Encounter

nominal and perturbed trajectory at Jupiter encounter, ignoring the effect of the planet's gravity field. The right triangle JLK in this diagram corresponds to the triangle JLK in Figure K-1. The sides of this triangle $\overline{JK} = \delta r_j$ and $\overline{JL} = \Delta S_1$ have been previously computed and yield

$$\overline{KL} = 508 \times 10^3 \text{ km}$$

At the nominal encounter time t_{arr} the spacecraft is at point N_1, a distance ΔS_o from K and a distance $\Delta S_2 = 173 \times 10^3$ km from L. ΔB is given by the relation

$$\Delta B = \left(\Delta S_1 - \Delta S_2 \frac{V_j}{V_{arr}} \right) \frac{V_{arr}}{V_{rel}} \sin \theta_j$$

which yields

$$\Delta B = 124 \times 10^3 \text{ km}$$

for the distances ΔS_1 and ΔS_2 obtained above, and the velocities

$$V_j = 42,800 \text{ ft/sec} = \text{Jupiter orbit velocity}$$

V_{arr} = 31,800 ft/sec = nominal heliocentric probe arrival velocity

V_{rel} = 26,400 ft/sec = relative probe velocity

This miss represents the effect of radial solar pressure, in the case of ideal absorption ($\alpha = 1$). It is seen that ΔB varies in proportion with the aphelion perturbation δr_a since the sides of the triangle JLK and hence ΔS_1 and ΔS_2 are proportional to this quantity, which in turn is proportional to ϵ.

The radial pressure perturbations resulting from nonideal absorption are obtained from the above results by varying the radial component F_r. This yields:

		Absorptivity		
Distances in 10^3 km		1.0	0.92	0.32
Predictable Deviations				
Aphelion perturbation	δr_a	368	388	535
Miss parameter	ΔB	124	131	180
Unpredictable Deviations (3σ)				
Uncertainty	$\Delta\alpha$	-	± 0.02	± 0.05
Aphelion perturbation	δr_a	-	± 4.8	± 12.3
Miss parameter	ΔB	-	± 1.6	± 4.2

1.2 Transverse Component of Solar Pressure

The nonideal absorption represented by the absorptivity values α_1 and α_2 gives rise to nonzero transverse components F_t of solar pressure. The resulting aphelion perturbations are obtained by first determining the velocity increments ΔV_{t_i} accumulated during time intervals in which positive or negative transverse components F_t are acting on the spacecraft These are found by integrating the acceleration term, i.e.,

$$\Delta V_{t_i} = \frac{g_\oplus}{W} \int_{t_1}^{t_2} F_t dt = \frac{1}{3}(1-\alpha) \frac{g_\oplus P_o A}{W} \int_{t_1}^{t_2} \frac{\sin \zeta}{r^2} dt$$

over intervals of $t_1 \leq t \leq t_2$ of positive or negative excursions of the quantity $\sin 2\xi/r^2$ and applying the resulting velocity increments at discrete trajectory points. The error sensitivity of the aphelion radius with respect to transverse velocity increments ΔV_{t_i} is given by

$$\frac{\partial r_a}{\partial V_{t_i}} = \frac{r_i V_a - r_a V_i \cos \theta_i}{V_a^2 - \frac{\mu}{r_a}}$$

where

V_a = velocity at aphelion

V_i = velocity at radius r_i

θ_i = flight path angle at radius r_i

The computation of the resulting transverse solar pressure effects is summarized below (distances in 10^3 km).

	Absorptivity	
	$\alpha_1 = 0.92 \pm 0.01$	$\alpha_2 = 0.32 \pm 0.05$
Predictable Deviations		
Aphelion	1.1	9.5
Miss parameter	0.4	3.2
Unpredictable Deviations (3σ)		
Aphelion	0.28	0.70
Miss parameter	0.10	0.24

The uncertainties in the above tabulations are those due to insufficient knowledge of the exact value of absorptivity α. Uncertainties resulting from unpredictable variations of the solar radiation constant P_0 during the transit of the spacecraft are listed in Section 7.4.4 of Volume 2.

2. UNBALANCED ATTITUDE CONTROL FORCES

To determine the cumulative effect of attitude control forces as a source of trajectory perturbations it is necessary to establish the magnitude and direction of these forces. This computation also provides an estimate of the required extra amount of attitude control propellant.

The asymmetrical solar pressure effect and its compensation by an attitude control torque is given by

$$T_1 = F_1 \ell_1$$

For the case of ideal absorption ($\alpha_0 = 1$) the solar pressure torque can be expressed by

$$T_1 = PA \ell_2 \sin \xi \cos \xi$$

Hence

$$F_1 = \frac{P_o A \ell_2}{2 \ell_1} \frac{\sin 2\xi}{r^2}$$

where

ℓ_1 = 6.25 feet = moment arm of attitude control jet measured from c.g.)

ℓ_2 = 2.25 feet = moment arm of center of solar pressure (measured from c.g.)

The propellant consumption for maintaining the equilibrium is given by

$$\Delta W_1 = \frac{1}{I_{sp}} \int_o^{T_F} |F_1| dt = \frac{P_o A \ell_2}{2 I_{sp} \ell_1} \int_o^{T_F} \frac{\sin 2\xi}{r^2} dt$$

Using the above stated values for A, ℓ_1, and ℓ_2, a specific impulse I_{sp} = 60 sec for the cold gas attitude control system, and the magnitude of the integral

$$J = \int_{o}^{T_F} \frac{1}{r^2} |\sin 2\xi| \, dt = 4.64 \times 10^6 \text{ sec},$$

we obtain for the total gas consumption

$$\Delta W_1 = 0.271 \text{ lb}$$

Actually, due to the increase in the radial solar pressure component F_r resulting from partial reflection of the incident radiation, this value would be increased by 45 percent in the case of $\alpha_2 = 0.32$. Hence

$$\Delta W_1' = 0.395 \text{ lb}$$

However, in this case the effect of the transverse pressure component F_t which opposes the radial pressure torque

$$T_2 = F_t \ell_1 \cos \xi = \frac{1}{3}(1-\alpha) P_o A \ell_1 \frac{\sin 2\xi}{r^2}$$

must also be taken into account. One half of the torque increment due to the term $2/3\,(1-\alpha)$ in the radial solar pressure component is balanced by the transverse pressure component and hence the total gas consumption

$$\Delta W_1'' = 0.333 \text{ lb}$$

is obtained.

The precession torque required to cause the spin axis to follow the relative motion ψ of the earth-line is given by

$$F_2 \ell_1 = I_1 \omega_1 \psi$$

where

F_2 = required precession force (lb), orthogonal to orbit plane, positive downward

I_1 = 200 slug ft^2, spin moment of inertia

ω_1 = 0.5 rad/sec = 5 rpm, spin rate

We can obtain the impulse required per degree of tracking motion

$$F_2 \frac{\Delta t}{\Delta \psi} = \frac{I_1 \omega_1}{\ell_1} = 0.278 \text{ lb sec per degree}$$

The velocity increment accruing from F_2 becomes

$$\Delta V = \frac{g_\oplus F_2}{W \Delta \psi} \Delta t \times 1.63 \times 10^{2} \text{ ft/sec per degree}$$

where W = 550 lb is the assumed spacecraft weight.

This ΔV corresponds to an expenditure of gas per degree of tracking motion

$$\Delta W_2 = \frac{I_1 \omega_1}{\ell_1 I_{sp}} = 4.65 \times 10^{-3} \text{ lb/deg}$$

assuming a specific impulse I_{sp} of 60 seconds for the cold gas attitude control jet.

The total cold gas consumption for the earth tracking task is obtained by integration of $|\dot{\psi}|$ during the entire mission. Thus

$$\Delta W_2 = \frac{1}{I_{sp}} \int_0^{T_F} |F_2| dt = \Delta W_2 \int_0^{T_F} |\dot{\psi}| dt = 0.56 \text{ lb}$$

where the value

$$\int_0^{T_F} |\dot{\psi}| dt = \sum |\Delta \psi| = 120 \text{ deg}$$

was obtained by summation of angle variations $|\Delta \psi|$ between maxima and minima of the $\psi(t)$ curve in Section 7.4.4, Volume 2, irrespective of sign.

Perturbations due to the unbalanced attitude control force applied to compensate for asymmetrical solar pressure was computed in the same manner as the effect of in-plane transverse solar pressure components, by applying discrete velocity increments in alternating directions. The resulting aphelion perturbation are

$$\delta r_{a0} = 10.3 \times 10^3 \text{ km} \qquad \text{for } \alpha = \alpha_0$$

$$\delta r_{a1} = 10.9 \times 10^3 \pm 0.14 \times 10^3 \text{ km} \qquad \text{for } \alpha = \alpha_1$$

$$\delta r_{a2} \times 15.0 \times 10^3 \pm 0.35 \times 10^3 \text{ km} \qquad \text{for } \alpha = \alpha_2$$

Perturbations due to the unbalanced attitude control force applied to achieve earth tracking are normal to the orbit plane. The orbit geometry diagram shown in Figure K-3 explains the effect of normal

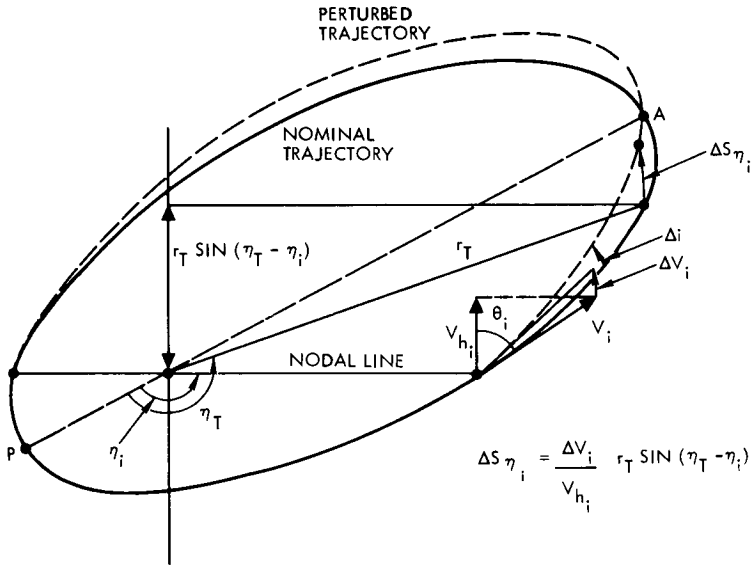

Figure K-3. Geometry of Out-of-Plane Perturbation

velocity increments ΔV_{n_i} on the inclination of the orbit plane, which is expressed by

$$\Delta_i = \frac{\Delta V_{n_i}}{V_{h_i}}$$

where $V_h = Vi \cos \theta_i$ is the horizontal velocity component at the point of application of ΔV_{ni}. The diagram also shows that the resulting out-of-plane deviation ΔS_{ni} at encounter of the target planet at distance r_T and true anomaly η_T is given by

$$\Delta S_{n_i} = \frac{\Delta V_{ni} \sin (\eta_T - \eta_i)}{V_i \cos \theta_i} r_T$$

The total effect of alternating intervals of positive and negative perturbing forces is approximated by applying the sequence of impulses ΔV_{ni} at points P_1, P_2, P_3 shown in the time history of the earth-line angle ψ.

The computation of the total out-of-plane perturbation at encounter yields

$$\Delta s_n = - 32.9 \times 10^3 \text{ km}$$

i.e., an excursion in downward direction.

The uncertainty in this value is essentially the uncertainty in the moment of inertia I_1 elsewhere estimated at 1 percent and the uncertainty in ℓ_1 which is believed negligible in comparison, leaving

$$\Delta s_n = -32.9 \times 10^3 \pm 0.33 \times 10^3 \text{ km}$$

3. MICROMETEOROID IMPINGEMENT

To determine a conservative estimate of perturbations due to micrometeoroid impingement a momentum multiplication factor $Q = 3$ is assumed, although all particles weighing in excess of 10^{-7} gram can be expected to penetrate the antenna dish structure entirely at impact speeds of 45,000 ft/sec and above. In these cases a multiplication factor $Q < 1$ would be a more realistic assumption. In view of the very small relative magnitude of the net perturbation effect contributed by this source, only the radial component of the momentum exchange will be considered here.

Figure K-4 shows three typical micrometeoroid flux densities designated C, D, and E which are applicable to various regions of the interplanetary space. A combination of fluxes C and D is assumed to apply in regions other than the asteroid belt. The combination of fluxes E

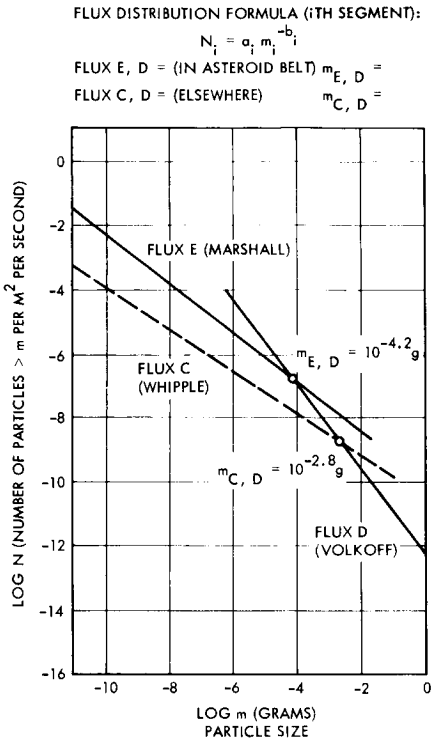

Figure K-4. Model of Micrometeoroid Flux Assumed in Trajectory

and D will be applied in the asteroid belt. The effective integrated mass of particles impinging per meter^2 per second is derived from*

$$M_i = \frac{a_i\, b_i}{b_i - 1}\left[\frac{1}{(m_i)_{min}^{b_i - 1}} - \frac{1}{(m_i)_{max}^{b_i - 1}}\right] \text{grams/m}^2 \text{ sec}$$

In a flux distribution composed of two straight segments as shown in Figure K-4 for the combinations C, D and E, D it can be shown that the integration process leading to this equation and the evaluation of the integrated mass uses the value $M_{C,D}$ or $M_{E,D}$ of particle mass at the

*G. J. Cloutier, "Attitude Perturbation of Space Vehicles by Meteoroid Impacts," J. Spacecraft, April 1966, p. 523.

intersection of the two line segments as the critical boundary value. The intersections occur at

$$M_{C,D} = 10^{-2.8} \text{ gram}$$

$$M_{E,D} = 10^{-4.2} \text{ gram}$$

Consequently, the effective integrated mass for the two flux densities C, D and E, D becomes, respectively,

$$M_{C,D} = 2.64 \times 10^{-11} \text{ gram/m}^2\text{/sec}$$

$$M_{E,D} = 8.5 \times 10^{-11} \text{ gram/m}^2\text{/sec}$$

Inserting these values of M and Q = 3 into the momentum exchange equation we obtain the following incremental velocities ΔV:

In the region from 1 to 2 AU	$\Delta V_1 = 4.02 \times 10^{-3}$ ft/sec
In the region from 2 to 4 AU (asteroid belt)	$\Delta V_2 = 12.25 \times 10^{-3}$ ft/sec
In the region from 4 to 5.1 AU	$\Delta V_3 = 3.44 \times 10^{-3}$ ft/sec

From these velocity increments the following contributions to the perturbation at aphelion are obtained by using the error sensitivity of aphelion distance with respect to radial velocity increments

$$\frac{\partial r_a}{\partial V_r} = \frac{r_a V_i \sin \theta_i}{\frac{\mu}{r_a} - V_a^2}$$

The resulting perturbations are

$$\Delta r_{a_1} = 168 \text{ km}$$

$$\Delta r_{a_2} = 411$$

$$\Delta r_{a_3} = 68$$

$$\Sigma \Delta r_a = 747 \text{ km}$$

A comparison of this result with the perturbation from radial solar pressure shows a ratio of approximately 1:400. This result can be verified approximately by a direct comparison of the average velocity increments accruing during the mission from micrometeoroid impingement and from solar radiation pressure.

For the velocity increment due to micrometeoroids we obtain

$$\Delta V_{mm} = \frac{1}{M_s} Q M_{m_{ave}} V_{m_{ave}} T_F A = 3.03 \times 10^{-2} \text{ ft/sec}$$

where

$$M_{m_{ave}} = 5.5 \times 10^{-11} \text{ gram/m}^2 \text{ sec}$$

$$V_{m_{ave}} = 45,000 \text{ ft/sec}$$

$$T_F = 650 \text{ days}$$

was assumed. The velocity increment due to radial solar pressure is given by

$$\Delta V_s = \frac{g_\oplus P_o A}{W} \int_o^{T_F} \frac{dt}{r^2} = \frac{g_\oplus P_o A}{WH} \Delta \eta$$

where

$H = 128 \times 10^3$ AU x ft/sec = angular momentum of nominal probe orbit

$\Delta \eta = 165$ deg = central angle to nominal intercept

The relation $H = \dot{\eta} r^2 =$ constant was introduced to simplify evaluation of the integral. The resulting velocity increment due to radial solar pressure is

$$\Delta V_s = 12.6 \text{ ft/sec}$$

The ratio $\Delta V_{mm}/\Delta V_s = 1:415$ approximates the ratio obtained above for the trajectory perturbations at aphelion and thus confirms the result

of the negligibly small effect of micrometeoroid pressure compared to solar pressure.

It is of interest to consider the potential effects of single impact events of micrometeoroids capable of causing the spacecraft to lose precise earth orientation and thereby to lose communication system lock-on. The momentum exchange resulting from single impacts (mass m_1) is expressed by the equation

$$\Delta H_m = Q\, m_1\, V_m\, r$$

where a realistic multiplication factor $Q \leq 1$ should be assumed for particles penetrating both skins of the antenna dish. It is assumed here that the most serious effect involves impacts at or near the rim of the antenna dish in a direction essentially parallel to the dish axis. In order to cause loss of lock-on this momentum change would have to be equal to

$$\Delta H_s = I_1\, w_1\, \Delta\xi$$

which is required to rotate the spin-stabilized spacecraft by an angle $\Delta\xi$ from its nominal earth-pointing orientation. Assuming the following parameters:

$$I_1 = 200 \text{ slug ft}^2$$

$$\Delta\xi = 12 \text{ deg}$$

the angular momentum increment will be

$$\Delta H_s = 40 \text{ ft-lb-sec} \quad \text{for } w_1 = 10 \text{ rpm}$$

$$20 \text{ ft-lb-sec} \qquad 5 \text{ rpm}$$

$$4 \text{ ft-lb-sec} \qquad 1 \text{ rpm}$$

Figure K-5 shows the number of impacts per mission and the change in angular momentum as a function of particle mass. As a conservative

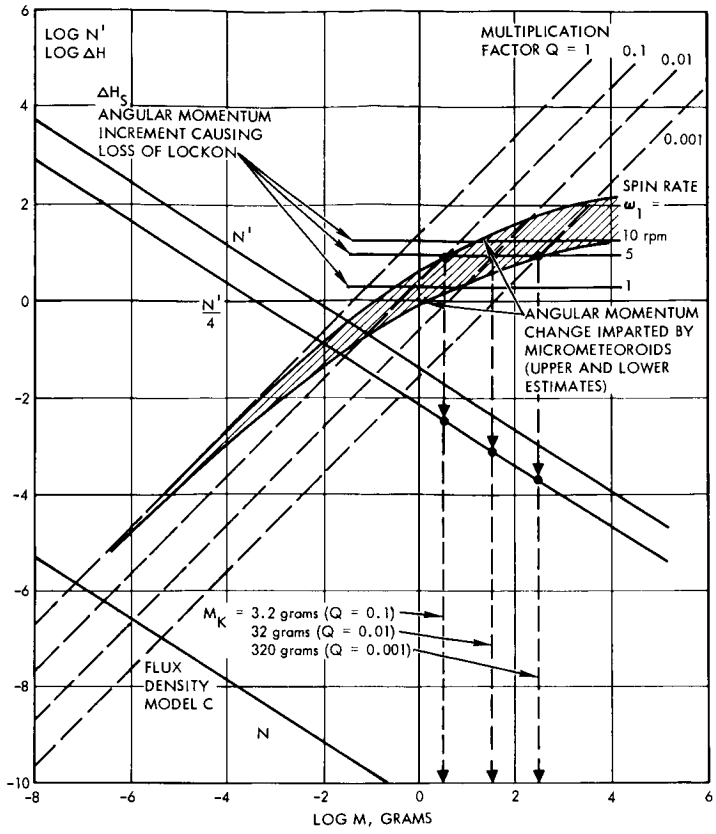

Figure K-5. Impact Conditions Resulting in Loss of Lock

assumption we assume that flux D, E which corresponds to micrometeoroid distributions in the asteroid region is encountered by the spacecraft during the entire mission. The diagram shows where the curve of angular momentum increment ΔH_m reaches the values required to cause loss of lock-on for the three spin rates ω_1 assumed. These intersections therefore determine the momentum of a particle of mass m_k sufficient to cause this attitude change. The diagram then shows how many impacts N' per mission can be expected of that particle size. Secondly, since only a fraction of the impinging particles of that size are near enough the rim of the dish to be of concern in this context, the diagram shows how many events per mission can be expected to be of this type. Assuming that the annular region near the rim comprises approximately one-quarter of the total dish area, this fraction of impacts is indicated by the curve labeled N'/4.

Actually as particle size increases the momentum multiplication factor decreases by orders of magnitude below the assumed value Q = 1. This factor is reflected in the diagram by a number of straight lines Q = 1, 0.1, 0.01, etc., and the intersection of these lines with the critical values of ΔH_s causing loss of lock-on. The resulting values of micrometeoroid mass m_k and the number of single events per mission are listed in Table K-1. Since the resulting micrometeoroid masses are in the neighborhood of 1 gram and above, it is obvious that the events considered here occur very rarely, in the order of 10^{-2} to 10^{-4} times per mission. Particles of this size would, of course, in many instances cause catastrophic damage to the spacecraft.

Table K-1. Impact Conditions Resulting in Loss of Lock-on (For Spin Rate of 5 rpm)

	Assumed Q Factor		
	0.1	0.01	0.001
Impacting particle mass m_k(g)	3.2	32	320
Number per mission N'/4	3×10^{-3}	10^{-3}	3×10^{-4}